Cellular Determinants of Reovirus Entry and Infection

A THESIS
SUBMITTED TO THE FACULTY OF THE GRADUATE SCHOOL
OF THE UNIVERSITY OF MINNESOTA
BY

Wade Loren Schulz

IN PARTIAL FULFILLMENT OF THE REQUIREMENTS
FOR THE DEGREE OF
DOCTOR OF PHILOSOPHY

Leslie A. Schiff, Ph.D., Advisor

October 2012

Acknowledgements

I would first like to thank my family. My parents have been a constant source of support and love. My wife, Laurie, has shown endless patience throughout medical and graduate school. I am also thankful for our new daughter. In just the few days we have known her, she has been a constant source of joy. My brother and sister, Chad and Kristen, have always provided their support and always welcome me when I go home.

I am also appreciative to all the friends and colleagues I have found in medical and graduate school. Jon and Brent have been excellent friends, are always enthusiastic, and have provided continuous support through my program. Aaron, who I met at the beginning of the MD/PhD program, has been a constant source of knowledge and assistance throughout my training. I would also like to thank my MD/PhD, graduate school, and medical school classmates who are too many to name, but have been the best group of physicians and scientists, present and future, to have learned and worked with. I would also like to thank Susan and Nick from the MD/PhD program, whose assistance has made life for everyone in the program easier. Without them, I cannot even imagine the number of hours that would have been spent on administrative tasks that they handle without hesitation.

I have also been thankful for the laboratory family. Linse, who has been one of the most dedicated laboratory scientists I have ever worked with. Her tireless devotion to our laboratory has truly made everyone's work and life easier.

Our undergraduate technicians, Oksana, Megan, and Lindsey have also been crucial for every experiment that we have completed. I would also like to thank Amelia, whose help and experiments have been vital to this thesis research. Each of these people has also become a friend during my time in graduate school. Finally, I would like to thank Leslie, who has made all of this work possible, and her husband, Steve. Leslie has been a fantastic mentor, always willing to offer advice and support. Her patience with the extra time necessary for my combined degree has made my transition between programs much easier. I look forward to knowing Leslie as a mentor for years to come, as her dedication to science and education makes her a true role model. I also extend my thanks to my thesis committee: Wade Bresnahan, Dana Davis, and David Masopust. Each of them has contributed to my success in graduate school and I appreciate their continued advice and support.

Abstract

Efficient entry is a critical determinant of reovirus oncolysis. While a model for the entry of reovirus virions has been described, the method by which partially uncoated intermediate subviral particles (ISVPs) enter host cells remains unknown. Biochemical studies have suggested that ISVPs can directly penetrate the plasma membrane since these particles can cause membrane damage and hemolysis at high multiplicities of infection. We used a combination of techniques to show that these particles can use endocytosis to enter and productively infect host cells. We found that uptake of reovirus virions and ISVPs was inhibited in cells treated with a small molecule inhibitor of dynasore. Analysis of reovirus replication in cells treated with genistein and in cells expressing dominant-negative caveolin-1 revealed that ISVPs use dynamin-dependent caveolar endocytosis to enter host cells. These studies also showed that reovirus virions were able to take advantage of caveolar endocytosis to infect cells. Because many viruses have recently been found to enter cells through dynamin-dependent and –independent endocytic pathways, we also assessed the role of cholesterol in reovirus infection. The growth of reovirus virions, but not ISVPs, was inhibited in cells treated with methyl-β-cyclodextrin, which extracts membrane cholesterol. We also wanted to learn whether reovirus entry had cell type-specific differences. Analysis of reovirus infection in a rat embryo fibroblast (CREF) and Ras-transformed CREF cell line suggested that reovirus particles lose the ability to use clathrin-mediated endocytosis in CREF cells following Ras

transformation. Reovirus can also infect cells that lack caveolae. To assess whether reovirus used different endocytic pathways to infect cells devoid of caveolae, we analyzed reovirus entry and infection in polarized Caco-2 cells. While reovirus infection of these cells was dynamin-independent, particle internalization occurred through both dynamin-dependent and –independent pathways. Visualization of particle uptake showed that particles internalized through dynamin-dependent endocytosis were transcytosed to the basolateral surface. These findings have demonstrated that reovirus can use a diverse set of endocytic pathways to enter and infect cells. The data presented in this thesis show that reovirus entry is a complex process that can vary in different cell types. In addition, it has revealed that particles internalized into various endocytic pathways are trafficked to different destinations in polarized epithelial cells.

Table of Contents

List of Tables

List of Figures

CHAPTER 1

Background and Literature Review

I. Introduction to viral entry and endocytosis

Viruses are obligate, intracellular microbes that carry only a fraction of the genes and proteins needed for replication. Viruses require a complex set of interactions with cellular proteins to successfully enter the host cell, replicate, and release progeny virions. A critical step in infection is gaining access to the cytoplasm, where viral components can take advantage of host cell replication machinery. While the cellular membrane presents a barrier to viral entry, viruses have evolved to take advantage of cellular endocytic and sorting machinery to access the cell interior. Although viral particles vary significantly in their structure, nearly all have been found to activate and undergo receptor-mediated endocytosis, including enveloped viruses that could fuse at the cellular membrane. Several endocytic pathways have been described and each of these pathways can be exploited for the internalization of viral particles (Figure 1.1) (97). These pathways can be grouped based on their dependence on the GTPase dynamin, which regulates scission of endocytic vesicles from the plasma membrane (92). Two well-described, dynamin-dependent pathways exist: clathrin-mediated and caveolar endocytosis (92). In addition, several dynamin-

Figure 1.1. Cellular endocytic pathways. This diagram illustrates many of the known endocytic pathways that can be used for viral entry. Vesicles and common sorting pathways are also indicated.

Figure 1.1

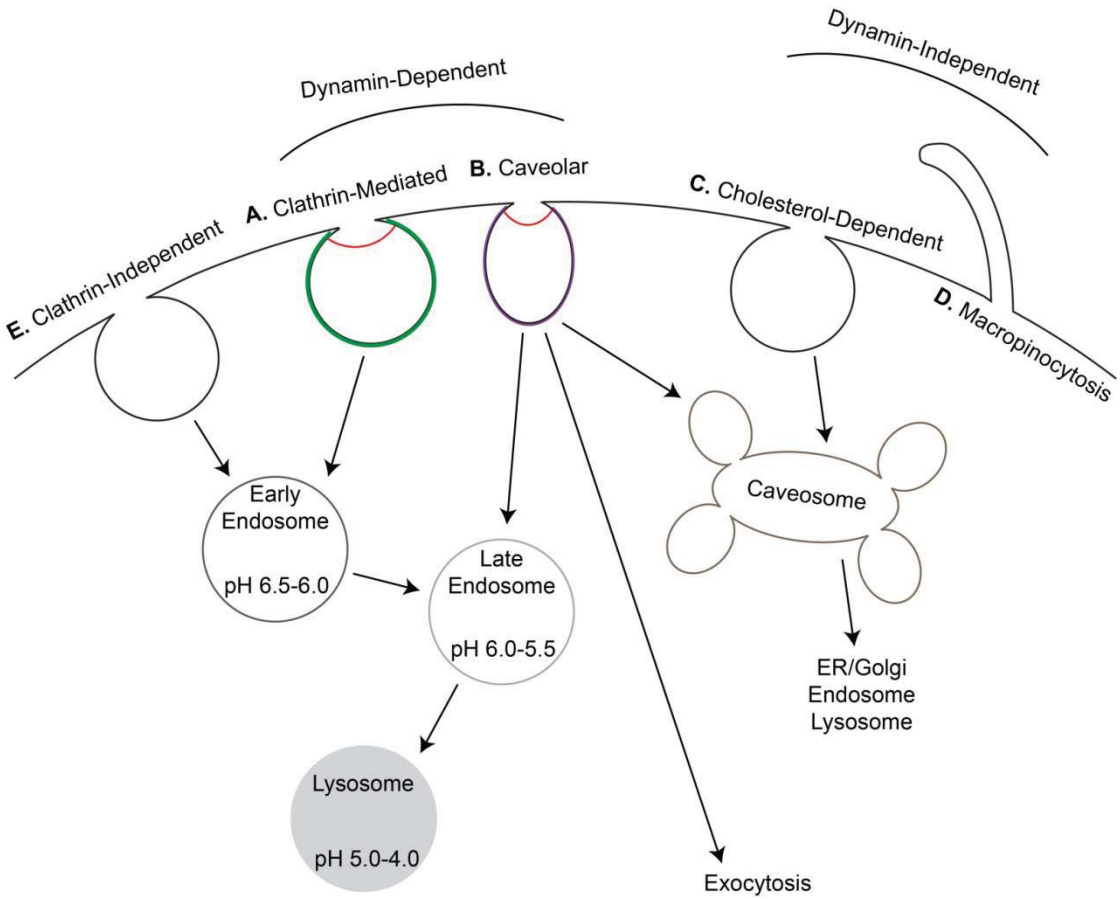
Dynamin-Dependent
Dynamin-Independent
E. Clathrin-Independent
A. Clathrin-Mediated
B. Caveolar
C. Cholesterol-Dependent
D. Macropinocytosis
Early Endosome
pH 6.5-6.0
Late Endosome
pH 6.0-5.5
Caveosome
ER/Golgi
Endosome
Lysosome
Lysosome
pH 5.0-4.0
Exocytosis

independent pathways, which are less well understood, can also be used for viral internalization and infection (86, 128, 149).

Clathrin-mediated endocytosis

Clathrin-mediated endocytosis (Figure 1.1A), is used for the uptake of intracellular microbes, bacterial toxins, and cellular metabolites (91). Clathrin-mediated endocytosis is characterized by the formation of a clathrin lattice that leads to an invagination of the plasma membrane (91). Interactions between clathrin and adaptor proteins, specifically AP-2, continue to deform the membrane until dynamin-mediated scission frees the vesicle from the surface (18). From the time of receptor activation, vesicles can be freed to the cytoplasm within one minute, making this one of the most active endocytic pathways within the cell (123). After scission, the GTPase Rab5 facilitates trafficking and fusion of clathrin-coated vesicles with the early endosome, a process that takes approximately five minutes and leads to acidification of the vesicle (132, 134). Cargo is sorted to the late endosome and lysosome within ten to fifteen minutes by a process that is mediated by the Rab7 GTPase (132, 134). Cargo can also be trafficked to other intracellular locations by clathrin-dependent endocytosis, including the trans-Golgi network through Rab9-positive vesicles, or the cell surface through Rab11-positive recycling endosomes (132, 134).

Caveolar endocytosis

A second dynamin-dependent pathway, caveolar endocytosis (Figure 1.1B), was discovered by Palade and Yamada in the 1950s (74, 163). Caveolae were first found to play a role in transcytosis in endothelial cells; however, they were later shown to have a more complex function in signal transduction and viral entry (109, 111). While the scission of caveolar vesicles from the plasma membrane requires dynamin, these vesicles lack the underlying scaffolding that can be seen as an electron-dense layer in high-resolution images of clathrin-coated pits (111). Following vesicle scission, caveolae can fuse to form a pH-neutral caveosome, from which cargo are trafficked to multiple intracellular locations (93, 109, 134). For example, SV40 is trafficked to the endoplasmic reticulum after internalization (93), and *Brucella* can be trafficked to a vesicle derived from ER components for replication and long-term survival within the host cell (93). Unlike vesicles internalized by clathrin-mediated endocytosis, many of these compartments remain pH-neutral, which allows pathogens to avoid degradation within the lysosome. However, some cargo can also be trafficked from caveolae to the endo/lysosomal pathway, which becomes acidified as the vesicles mature (86, 115). Interaction between endocytic pathways is common, as evidenced by the fact that cargo internalized by different pathways can end in the same intracellular compartment (86, 134).

Dynamin-independent endocytic pathways

More recently, many dynamin-independent pathways have also been identified. While the molecular details of these pathways are not as well understood, research has shown that they are important for the entry of many intracellular pathogens (86, 128). One such pathway is lipid raft-dependent endocytosis (86). This pathway results in trafficking to a pH-neutral caveosome (Figure 1.1C) and is used by adenovirus and coxsackievirus for cell entry (68, 86). A second dynamin-independent pathway that requires cholesterol and delivers cargo to pH-neutral vesicles is macropinocytosis (Figure 1.1D) (97, 134). It is not known if macropinocytosis requires the activation of receptors on the cell surface or if internalization of cargo occurs randomly after attachment to the cell surface, but inhibition of macropinocytosis can inhibit infection by influenza and adenovirus (5, 32). Finally, a clathrin- and dynamin-independent mechanism that delivers cargo to acidic compartments along the endo/lysosomal pathway has been described (Figure 1.1E) (86, 123, 134). This mechanism plays a role in the entry of influenza virus, which requires an acidic environment for successful fusion with the host cell membrane (86, 123). While the details of these pathways are still emerging, the study of viral entry has been vital for understanding the often subtle differences that define and regulate endocytic processes within the cell.

II. Viral penetration of the limiting membrane

Recent studies have shown that viruses can take advantage of many mechanisms to bypass the limiting membrane, which can be the plasma membrane at the cell surface, an endosomal or lysosomal membrane, the endoplasmic reticulum, or membrane components of the Golgi apparatus (52, 134). For example, influenza virus was first shown to enter cells through clathrin-mediated endocytosis, one of the most studied endocytic pathways (89). Once inside the endosomal pathway, acidification activates the viral fusion protein hemagglutinin (HA) and results in delivery of the nucleocapsid to the cytoplasm (55). However, later work based on single particle tracking showed that only 60% of influenza viral particles underwent clathrin-mediated endocytosis, while the remaining 40% took advantage of clathrin-independent pathways that deliver cargo to the endo/lysosomal pathway (123). This result not only showed that viruses can take advantage of multiple endocytic pathways for entry, but that multiple pathways can be responsible for entry within a single cell.

Entry of enveloped viruses

Enveloped viruses fuse with limiting membranes at various locations within the cell. While some enveloped viruses, such as HIV, were initially thought to fuse only at the cell surface, more recent studies have shown that these particles also take advantage of endocytosis to enter host cells (55, 113). Uptake

through these pathways can offer many benefits to viral infection. For example, viral particles within a vesicle can take advantage of cellular machinery for transport to distant sites of replication, avoid detection by the immune system, and take advantage of cellular cues, such as decreased pH and changes in calcium concentration, for initiating post-internalization steps of viral entry (86).

Entry of nonenveloped viruses

Nonenveloped viruses cannot breach cellular membranes by fusion. Instead, these viruses must either disrupt the integrity of cell membranes or form pores within membranes to gain cytoplasmic access (86, 150). This is typically achieved through one or more hydrophobic viral proteins that are exposed as the viral capsid is uncoated. Since large-scale disruption of cellular membranes would lead to cell death, penetration of the membrane is typically a regulated process and occurs after the virus is exposed to specific intracellular triggers (69, 150). For example, SV40 bypasses the ER membrane only after interacting with chaperone proteins within the ER lumen (103, 112), and adenovirus requires endosomal acidification to gain access to the cytosol (95). While details of nonenveloped viral entry are emerging, relatively little is known about the molecular signatures that enable viruses to traffic through specific intracellular compartments.

For my dissertation research, I investigated the mechanisms used by reovirus, a nonenveloped virus, to enter and infect host cells. This was

accomplished by using multiple approaches to inhibit endocytosis, including treatment with chemical inhibitors and the expression of dominant negative proteins. With these methods, I was able to identify a number of endocytic pathways that can be used by reovirus virions and uncoated viral particles to enter cells. During this process, I characterized the mechanisms used to productively infect several different cell types, including transformed and polarized cells. I also identified the endocytic pathway used to transport reovirus across polarized epithelial cells.

III. Reovirus biology

Reovirus is a nonenveloped, double-stranded (ds) RNA virus in the family *Reoviridae*. First isolated in 1951, reovirus has been recovered from both symptomatic and asymptomatic patients (125, 129). Because infection in humans is typically limited and is not associated with serious disease, these viruses were named respiratory enteric orphan (reo) viruses (125, 129). However, reovirus can cause severe neurologic infection in neonatal mice and acute respiratory disease has been reported in humans (129, 166). Reovirus consists of 10 dsRNA segments within two concentric protein shells. The genome is classified by size into three large (L1, L2, L3), three medium (M1, M2, M3), and four small (S1, S2, S3, S4) segments, which code for eight structural and four nonstructural viral proteins. While viral proteins are also classified by size as large (λ), medium (μ),

or small (σ), the viral protein and gene names do not always correlate—for example, the reovirus σ3 protein is encoded by the S4 gene (129). Viral proteins relevant to this thesis work include the σ3 protein, the outermost capsid protein which is removed during particle uncoating, the σ1 protein, which functions as the viral attachment protein, λ2, an inner capsid protein, and the membrane penetration protein μ1 (41, 45, 129, 168).

Four distinct reovirus particle types have been identified during infection, termed virions, intermediate subviral particles (ISVPs), ISVP*s, and core particles (129, 139, 168). The reovirus virion is environmentally stable and contains all eight structural proteins. The outermost capsid protein, σ3, prevents early exposure of the underlying protein, μ1, which can disrupt membranes (25, 168). During infection, proteases remove the σ3 protein and lead to extension of the attachment protein, σ1, to form an ISVP (45). Additional processing removes the σ1 protein and releases the amino-terminal myristoylated μ1 fragment, μ1N to form a particle known as the ISVP* (168, 169). This particle is believed to mediate membrane penetration which leads to the release of transcriptionally-active core particles into the cytoplasm (168, 169).

While reovirus is typically nonpathogenic in adults, it was found to preferentially replicate in and lyse transformed cells. This finding has led to ongoing studies of reovirus as an oncolytic therapy for several human cancers, including breast, colon, prostate, and lung cancer (58, 63, 104, 146, 147). Early studies linked reovirus oncolysis to Ras activation in transformed cells, as

otherwise nonpermissive cells transformed with the Ras oncogene could be infected with reovirus (29, 76, 133). While it was believed that Ras activation prevented the antiviral protein kinase R (PKR) response and promoted reovirus replication within cells, work from our lab and others demonstrated that reovirus can replicate in cells lacking constitutively active Ras (138). Additional work showed that reovirus could also productively infect NIH3T3 cells if viral particles were first uncoated to generate ISVPs *in vitro* (2). These findings led to a new hypothesis, that the oncolytic properties of reovirus are linked to efficient viral uncoating and entry (2).

IV. Reovirus attachment and entry

The molecular details of reovirus attachment and entry have been best studied in L929 murine fibroblasts. Based on relative affinities between cell surface receptors and viral attachment proteins, it has been proposed that reovirus infection begins when the cell attachment protein σ1 interacts with cell surface carbohydrates (Figure 1.2A) (9, 10). Carbohydrate binding occurs through the tail portion of the σ1 protein and these interactions vary depending on the viral strain (9, 27). The carbohydrate receptor for type 3 reovirus is sialic acid (9). While type 1 reovirus strains also contain a carbohydrate binding region in the σ1 tail, the receptor for this motif has not yet been identified (26, 59). Further, all strains have been found to bind to the proteinaceous receptor

Figure 1.2. Reovirus cell entry. This figure shows the pathways that may be used for entry by reovirus virions and ISVPs. A) Internalization of virions by clathrin-mediated endocytosis. Inset represents early steps of viral binding that lead to the activation of this pathway. B) Entry of reovirus ISVPs by two hypothesized pathways: endocytosis and direct membrane penetration.

Figure 1.2

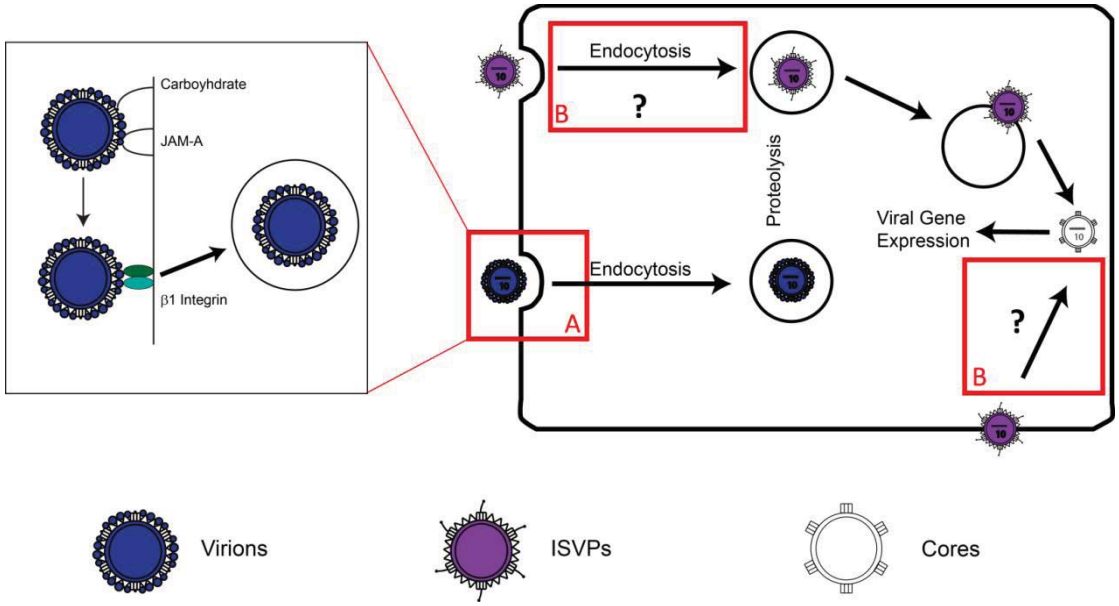
Carboyhdrate
JAM-A
β1 Integrin
Endocytosis
?
B
Proteolysis
Viral Gene
Expression
Endocytosis
A
?
B
Virions
ISVPs
Cores

junctional adhesion molecule A (JAM-A) through sequences that lie within the distal head region of σ1 (10, 64). The σ1 protein is responsible for a number of viral properties, including tissue tropism, apoptosis, and pathogenesis (14, 152).

After attachment, reovirus virions interact with β1 integrins. This interaction leads to the internalization of virions through clathrin-mediated endocytosis (34, 81). Once inside the endosomal pathway, proteases form ISVPs by removing the outermost capsid protein σ3, which exposes the membrane penetration protein μ1 (143). Several proteases have been implicated in reovirus uncoating. In murine L929 cells, the acid-dependent cysteine proteases cathepsin L and B can both mediate reovirus uncoating to form ISVPs (38). During infection of the gastrointestinal tract, pancreatic serine proteases such as trypsin and chymotrypsin can uncoat viral particles extracellularly (11, 41). A variety of other acid-dependent and –independent proteases also mediate infection of respiratory and immune cells (15, 47, 49). The molecular triggers that cause the uncoated particle to form membrane pores are not yet known. However, a series of biochemical experiments have revealed that increased particle concentration, higher temperatures, and the presence of K^+ and Cs^+ lead to the loss of the outer capsid protein σ1 and release of the μ1 cleavage products *in vitro* (16, 17, 99, 169). Interestingly, the μ1 cleavage product, μ1N, is capable of forming size-selective pores in a model membrane. The modified ISVPs, which have lost σ1 and the μ1 cleavage fragments, have been referred to as ISVP*s (129). These particles are believed to be similar to infection intermediates that

mediate membrane penetration. Once the endo/lysosomal membrane has been perforated, reovirus particles are thought to gain access to the cytoplasm and undergo a final conversion to become transcriptionally-active core particles (129).

While the mechanism by which reovirus virions attach to and enter cultured cells has been well studied, less is known about how extracellularly uncoated particles enter cells. Infection of the intestinal and respiratory tracts results in the extracellular uncoating of reovirus particles (11, 41). As the tumor microenvironment is also enriched in proteases (137, 159), ISVPs are likely the particles that enter transformed cells when used as an oncolytic therapy. Studies from several laboratories have demonstrated that ISVPs and the μ1N protein cause membrane damage, chromium release, and hemolysis (71, 79). These particles can also infect host cells in the presence of bafilomycin A1, which inhibits endosomal acidification, and chlorpromazine, which blocks clathrin-mediated endocytosis (47, 81). Together, these findings led to the hypothesis that ISVPs could gain cytoplasmic access directly from the plasma membrane (Figure 1.2B). However, EM analysis revealed that ISVPs could be found within endocytic vesicles (4, 143); leaving open the possibility that endocytic uptake might be important for reovirus infection.

V. Reovirus infection of intestinal epithelial cells

Reovirus infection of the gastrointestinal tract *in vivo* is significantly different from infection in non-polarized cell culture. During intestinal infection, reovirus virions are uncoated extracellularly by pancreatic serine proteases (11, 41). While reovirus virions can attach to cells grown in culture, conversion to ISVPs and extension of the σ1 protein is required for efficient binding and infection of the intestinal epithelium *in vivo* (13, 162). Even in cultured cells, polarization affects the binding of reovirus virions (3, 11). This suggests that studies using nonpolarized cells in culture may not always reflect infection *in vivo*.

In a mouse model of reovirus infection, ISVPs attach to microfold (M) cells of the mucosa-associated lymphatic tissue (MALT) (162). Since the cellular receptor JAM-A is isolated to tight junctions and localized to the sub-apical membrane of polarized epithelial cells, uptake through adjacent M cells is required for the transport of viral particles to the basolateral membrane (59, 162). While type 3 reovirus strains are able to bind to the apical surface of polarized enterocytes of the murine intestinal mucosa, type 1 strains can only bind to M cells in this model (155). Since reovirus type 3 can bind to sialic acid while type 1 strains cannot (9, 155), this suggests that σ1 interactions with sialic acid mediate attachment to polarized enterocytes. Later work showed that reovirus binding in the human intestinal tract may differ from the murine model described above.

Research by Ambler and Mackay demonstrated that reovirus type 1 could bind to polarized Caco-2 cells grown in culture (3). When polarized, these cells express a well-developed brush border and form tight junctions, resembling mature distal ileal cells (3). They also have many functional processes which resemble the human intestinal mucosa, such as receptor-mediated transcytosis of cobalamin and transport of low molecular weight compounds across the membrane (7, 36). Additional studies by Helander and colleagues found that reovirus type 1 could adhere to Caco-2 cells through α2,3-linked sialic acid (59). However, it was unknown whether reovirus could productively infect polarized human enterocytes or use them as a pathway for penetration of the intestinal mucosa following attachment at the apical surface.

VI. Goals

An ongoing area of research in the Schiff laboratory is to learn how reovirus enters host cells and bypasses the limiting membrane to initiate infection. Prior to the work described within this thesis, it was understood that virions entered cells through clathrin-mediated endocytosis (34, 81), and uncoated reovirus particles (ISVPs) were hypothesized to directly penetrate the plasma membrane at the cell surface (129). The main focus of this thesis was to determine if other endocytic pathways play a role in the entry of reovirus virions and whether ISVPs also take advantage of endocytosis to establish productive

infection. Since entry is critical for reovirus oncolysis (2), we also assessed whether reovirus uses different mechanisms to enter transformed and polarized cell lines. Our studies have revealed that ISVPs use endocytosis to establish productive infection, and that reovirus virions use a diverse set of cellular mechanisms to enter host cells. Finally, we showed that reovirus can enter and infect polarized human enterocytes from the apical surface and that reovirus may use these cells as a pathway for penetration of the intestinal mucosa. These findings have implications for ongoing clinical trials, as reovirus may be a less effective therapy in transformed cells that downregulate these endocytic pathways.

CHAPTER 2

Materials and Methods

Mammalian cells. Murine L929 fibroblasts were maintained as suspension cultures in SMEM supplemented to contain 5% heat-inactivated fetal calf serum (FCS) (Sigma-Aldrich, St. Louis, MO), 2 mM glutamine, 50 units/ml penicillin G, and 50 µg/ml streptomycin sulfate. Suspension cultures were grown in flasks kept in a non-humidified and non-CO_2 enriched 37°C incubator. Human A549 respiratory epithelial cells, 293 human embryonic kidney (HEK-293) cells and HEK-293T cells were maintained as monolayer cultures in RPMI supplemented to contain 10% heat-inactivated FCS, 2 mM glutamine, 50 units/ml penicillin G, and 50 µg/ml streptomycin sulfate. Caco-2 intestinal epithelial cells and Calu-3 respiratory epithelial cells were maintained as monolayer cultures in DMEM supplemented to contain 15% heat-inactivated FCS, 2 mM glutamine, 50 units/ml penicillin G, and 50 µg/ml streptomycin sulfate.

Viruses. Reovirus strain Lang (T1L) is a prototypic laboratory strain. Viral stocks were generated as described below and titers were determined by plaque assay on L929 cells.

Chemical inhibitors of endocytosis. Chlorpromazine (CPZ, Sigma-Aldrich, St. Louis, MO) was diluted in water at a stock concentration of 5 mg/mL

and used at a working concentration of 5 μg/mL to inhibit clathrin-mediated endocytosis. Dynasore (Dyn, Sigma-Aldrich, St. Louis, MO), a small molecule inhibitor of dynamin, was diluted to a stock concentration of 100 mM in dimethyl sulfoxide (DMSO), stored at -20°C, and was used at a working concentration of 100 μM. Genistein (Gen, Sigma-Aldrich, St. Louis, MO), a receptor tyrosine kinase inhibitor used to inhibit caveolar endocytosis, was kept at a stock concentration of 200 mM in DMSO, used at a working concentration of 200 μM, and stored at -20°C. Methyl-β-cyclodextrin (MβCD, Sigma-Aldrich, St. Louis, MO), which was used to extract membrane cholesterol, was kept at a stock concentration of 250 mM in water and used at a working concentration of 5 mM. Stock solutions of CPZ and MβCD were stored at room temperature.

Passage and generation of reovirus stocks. Reovirus stocks were prepared in L929 cells. Generally, 0.5 ml of passage 1 stock was used to infect L929 cells plated the previous day. Samples were incubated at 37^{o}C for 1 h with gentle agitation every 15 min to allow particles to adsorb. Warm SMEM medium was then added and samples were incubated at 37^{o}C until $\geq$ 90% of the cells demonstrated cytopathic effect (CPE). The samples were subjected to three cycles of freeze-thawing and the lysates were placed into sterile dram vials and stored at 4^{o}C. Second passage stocks were titered by standard plaque assay to quantify the number of plaque forming units (PFU)/ml. Passage 3 stocks were generated by infecting L929 cells with a sufficient quantity of passage 2 stock to

result in a multiplicity of infection (MOI) of 0.5 PFU/cell. Virus was adsorbed and collected as described above. Third passage stocks were titered by standard plaque assay and the genotype was confirmed by sodium dodecyl sulfate (SDS)-polyacrylamide gel electrophoresis (PAGE) and silver staining of the double stranded (ds) RNA.

Purification of reovirus virions. Purified virions were generated by pelleting 2 x 10^8 L929 cells by low speed centrifugation (145 g for 10 min). Cells were infected at a MOI of 2 PFU/cell in a final volume of 10 ml with third passage cell-lysate stocks. The samples were incubated in a 35^{o}C H_2O bath for 1.5 h with gentle swirling every 15 min to allow particles to adsorb. After adsorption, warm SMEM was added to bring the cells to a final concentration of 5 x 10^5 cells/ml. The infected cells were then incubated in a 35^{o}C H_2O bath with constant agitation until viability dropped to 70% – determined by 0.4% trypan blue exclusion. Cells were pelleted by low speed centrifugation and frozen overnight at -80^{o}C. Pellets were resuspended in 7 ml HO buffer (250 mM NaCl, 10 mM Tris [pH 7.4]) and then transferred to a 30 ml Corex tube. Two 30 second sonication pulses at 30% power with a Sonifier cell disrupter were used to disrupt cells on ice, followed by the addition of 1/100th the volume of 10% deoxycholic acid. The mixture was incubated on ice for 30 min, with gentle swirling every 10 min. One half of the total volume of trichlorotrifluoroethane (Freon) was added to the sample and it was sonicated until emulsified. Another half volume of Freon was added and the

sonication step was repeated. The sample was centrifuged at 7,000 x g for 25 min at 4°C. The aqueous phase, which contains the virions, was removed with a sterile plastic pipet and placed in a sterile corex tube. The Freon emulsification and centrifugation steps were repeated. The second aqueous phase was layered onto a 1.25-1.45 g/cc CsCl gradient and centrifuged overnight at 88700 x g and 4°C using a SW41 rotor (Beckman, Fullerton, CA). After centrifugation, the centrifugation tube was punctured and the drops corresponding to the visible band of virions was collected in a sterile dram vial. Purified virions were dialyzed at 4°C for 2 days in 2 L of 1x virion dialysis buffer (VDB) (0.15 M NaCl, 10 mM $MgCl_2$, 10 mM Tris at a pH of 7.5) in Spectra/Por molecularporous membrane tubing with a molecular weight cut off of 12,000-14,000 daltons (Spectrum Laboratories, Inc., Rancho Dominguez, CA). Purified virions were tittered by standard plaque assay and particle concentration was determined using a spectrophotometer on the assumption that 1 OD_{260} = 2.1 x 10^{12} particles/ml.

Generation of intermediate subviral particles. Intermediate subviral particles (ISVPs) were prepared by diluting purified virions in 1x VDB to a concentration of 1 x 10^{13} particles/ml and treating with 200 µg/ml chymotrypsin (CHT). T1L virions were incubated in a 32°C H_2O bath for 30 min. Tubes were removed from the H_2O bath, placed on ice and phenylmethanesulfonyl fluoride (PMSF) was added to a final concentration of 1 mM. ISVPS were stored at 4°C. Titers were determined by standard reovirus plaque assay and particles were

analyzed by SDS-PAGE and coomassie blue staining (gel fix [1:3:6 glacial acetic acid:isopropanol:H_2O] containing 0.5% coomassie blue) to ensure that ISVPs had been generated.

Standard reovirus plaque assay. L929 cells were plated in 6-well plates at a concentration of 1 x 10^6 cells/well in 3 ml total volume of SMEM and incubated overnight at 37^{o}C. The following day, medium was removed from the wells and cells were infected with 0.1 ml dilutions of virus in cold gel saline. Plates were rocked every 15 min for 1.5 h at room temperature or 1 h at 37^{o}C, after which a 3 ml overlay (1% agar, 1X199, 2.5% heat-inactivated fetal calf serum, 2 mM glutamine, 100 units/ml penicillin G sodium, 100 µg/ml streptomycin sulfate, 0.25 µg/ml amphotericin B) was added to each well. The overlay was allowed to solidify for approximately 15 min at room temperature and plates were returned to a 37^{o}C incubator. Four days postinfection, 2 ml of overlay was added to each well as described above. Seven days postinfection, 2 ml of overlay was added to each well, except that 2.5% fetal calf serum was omitted from the overlay and neutral red was included at a final concentration of 0.05%. Plaques were counted the following day and viral titers determined.

Chymotrypsin reovirus plaque assay. Chymotrypsin plaque assays were occasionally used to determine viral titer prior to an experiment. Day 1 of the CHT plaque assay is identical to the standard plaque assay described above.

After medium was removed from the wells on day 2, each well was rinsed with 2 ml phosphate buffered saline (PBS) + 2 mM $MgCl_2$ and cells were infected as described above. After adsorption, the inoculum was removed by aspiration and cells were overlaid with 3 ml of 1% agar, 1X199, 2 mM glutamine, 100 units/ml penicillin G sodium, 100 µg/ml streptomycin sulfate, 0.25 µg/ml amphotericin B and 10 µg/ml CHT. The plates were incubated at 37^{o}C for 2 to 5 days until plaques were visible. At that time, 2 ml of overlay was added to each well, except that 2.5% fetal calf serum was omitted from the overlay and neutral red was included at a final concentration of 0.05%. Plaques were counted the same day and viral titers determined.

Flow cytometric analysis of reovirus binding. L929 cells were incubated at a concentration of 2 x 10^6 cells/ml with vehicle (DMSO) or 100 µM dynasore in SMEM for 1 hour at 37°C. Reovirus particles were adsorbed at a concentration of 1 x 10^5 particles/cell at 4°C. Unbound viral particles were removed by centrifugation and the cells were fixed in 1.6% formaldehyde for thirty minutes then washed twice with PBS. Cells were stained with rabbit antiserum raised against reovirus T1L and diluted 1:5,000 (Dr. Barbara Sherry, North Carolina State University, Raleigh, NC) for 90 minutes, washed twice with PBS, and counterstained with allophycocyanin (APC)-conjugated anti-rabbit antibodies diluted 1:200 (Jackson ImmunoResearch, West Grove, PA) for 90 minutes. Cells were washed and resuspended in 1 mL of PBS and viral binding

was assessed by flow cytometry using an LSR II flow cytometer (BD Biosciences, San Jose, CA). Data were analyzed with the FlowJo analysis software (Treestar, Ashland, OR).

Visualization of reovirus uptake and infection. A549 cells were plated at a density of 7 x 10^4 cells/well in 8-well CultureSlides (BD Falcon, Bedford, MA). Twenty-four hours after plating, the cells were treated with vehicle or inhibitor for 1.5 hours then equilibrated at 4°C for 30 minutes. Reovirus virions or ISVPs were diluted in gel saline to a concentration of 1.0 x 10^5 particles/cell and allowed to adsorb at 4°C for 1 hour. Cells were washed with ice cold PBS to remove unbound particles and warm medium with or without inhibitor was added back and the cultures were allowed to incubate at 37°C. At 10 minutes postinfection (mpi), cells were fixed in ice cold 1.6% formaldehyde at 4°C for 30 minutes then washed three times with PBS. Cells were then permeabilized with 0.2% Triton X-100 at room temperature for 3 minutes and washed once with PBS. Texas Red-labeled phalloidin (Life Technologies, Grand Island, NY) in 0.1% Triton X-100 was added for 20 minutes at room temperature to label actin. The cells were washed three times with PBS followed by staining with either anti-T1L (1:5,000) or a combination of anti-T1L (1:5,000) and anti-T3D (1:5,000) antibody in 0.1% Triton X-100 for 90 minutes at 37°C, then washed three times with PBS. DyLight 488-labelled donkey anti-rabbit antibody diluted 1:200 (Jackson ImmunoResearch, West Grove, PA) was added and allowed to

incubate for 90 minutes at 37°C. Slides were washed three times in PBS and coverslips mounted using VECTASHIELD® HardSet with DAPI (Vector Laboratories, Burlingame, CA). Cells were imaged with an Olympus FluoView 1000 upright confocal microscope and images processed with the Olympus FV10-ASW software.

Visualization of pathway-specific ligand uptake. A549 cells were plated and treated with inhibitor as described above. Alexa Fluor® 488-labelled transferrin (10 μg/ml, Life Technologies, Grand Island, NY) or FITC-labeled cholera toxin subunit B (10 μg/ml, Sigma-Aldrich, St. Louis, MO) in gelatin saline were adsorbed to cells at 4°C. After 1 hour, cells were washed with PBS, warm medium with vehicle or inhibitor was added to the cells, and cultures were placed in a 37°C incubator. Cells were fixed 30 minutes later with 1.6% formaldehyde then washed three times with PBS. Coverslips were mounted using VECTASHIELD® HardSet with DAPI. Cells were imaged with an Olympus FluoView 1000 upright confocal microscope and images processed with the Olympus FV10-ASW software.

Transfection of 293 cells with dominant negative expression plasmids. A plasmid expressing dominant negative caveolin-1 (DN-cav1*)* containing the Y14F mutation and an empty control vector (pEGFP-N1) were obtained from Dr. Mark McNiven (Mayo Institute, Rochester, MN). 293 cells were

plated in 6 well trays and transfected with pEGFP-N1 control vector or DN-cav1 using Lipofectamine™ 2000 (Invitrogen) at a DNA (μg) to Lipofectamine™ 2000 (μl) ratio of 1:2.5. Twenty four hours post-transfection, cells were infected with reovirus T1L at an MOI of 20. Infection was quantified by flow cytometry at 24 hpi.

Flow cytometric analysis of reovirus infection. Monolayers were detached with Cellstripper (cellgro, Manassas, VA) at 24 hours postinfection (hpi) and cell suspensions were fixed with 1.6% formaldehyde. Fixed cells were washed twice with PBS, permeabilized with 0.2% Triton X-100 at room temperature for 3 minutes, then washed again with PBS. Cells were stained with rabbit antibody to the reovirus non-structural protein μNS diluted 1:2,500 (Dr. Max Nibert, Harvard, Boston, MA) for 90 minutes with constant agitation at 37°C followed by two washes with PBS. Cells were then counterstained with APC-conjugated secondary antibody (diluted 1:200) for 90 minutes at 37°C. Cells were then washed and resuspended in 1 mL PBS. Reovirus-infected cells were quantified by flow cytometry on an LSR II flow cytometer and analyzed with the FlowJo analysis software.

Immunoblot analysis of reovirus infection. Cells were harvested from 6 well trays with manual disruption then collected by low speed centrifugation. Medium was discarded and cells resuspended in 150 μL of Tris lysis buffer (10

mM Tris pH 7.5, 2.5 mM $MgCl_2$ 100 mM NaCl, 0.5% Triton X-100) for 30 minutes at 4°C. Cell debris was removed by centrifugation and the supernatant sheared using a 1 mL syringe. Supernatant was diluted 1:1 in 2X sample buffer (0.6 M sucrose, 250 mM Tris pH 8, 2% SDS, 10% 2-mercaptoethanol) and samples were boiled for 4 minutes. Proteins were separated on a 10% SDS-polyacrylamide gel then transferred to a nitrocellulose membrane. The membrane was washed in TBST then cut below the Kaleidoscope (Bio-Rad) band representing 79 kDa. The larger molecular weight proteins were probed with rabbit antibody for the reovirus non-structural protein μNS (diluted 1:12,500) for 1 hour at room temperature, while the smaller molecular weight proteins were probed for the β-actin housekeeping gene with a mouse anti-β-actin antibody (Abcam, Cambridge, MA). The membrane was washed three times in TBST and the larger molecular weight portion stained with horseradish peroxidase (HRP) conjugated anti-rabbit antibody diluted 1:7,500 (GE Healthcare, Waukesha, WI) and the smaller molecular weight portion stained with HRP conjugated anti-mouse antibody diluted 1:5,000 (GE Healthcare, Waukesha, WI) at room temperature for 1 hour. The membranes were washed three times with TBST and secondary antibodies reacted with Amersham ECL Western Blotting Reagent (GE Healthcare, Waukesha, WI) for 1 minute at room temperature. Autoradiograph film was exposed to the membrane for 20 seconds and 3 minutes and developed with a Konica Minolta SRX-101A developing system.

Assessment of cell viability. L929 cells were seeded in six well trays at a density of 2 x 10^6 cells/well. Four hours after plating, inhibitors were added at various concentrations and the cultures were incubated at 37°C for twenty-four hours. Cells were removed from the plates with Cellstripper, pelleted by centrifugation, and stained with the TACS Annexin V-FITC kit (Trevigen, Gaithersburg, MD) per the manufacturer's protocol. Briefly, the samples were then washed with PBS and stained in 100 µL incubation reagent (1X binding buffer, 10% propidium iodide, 10% Annexin V-FITC) at room temperature for 15 minutes. Single stain and unstained controls were generated using 1X binding buffer to replace propidium iodide or Annexin V-FITC. After staining, 400 µL of 1X binding buffer was added and the samples placed on ice. Viability was assessed using an LSR II flow cytometer and data were analyzed with the FlowJo analysis software.

Growth and polarization of cells on transwell plates. Caco-2 cells were plated at a density of 2 x 10^4 cells/well into 6.5 mM diameter, 0.4 µM pore, clear polyester transwell supports (Corning, Manassas, VA). Medium was changed every 3 days and resistance readings were taken at twenty-one days after plating to assure that cells were polarized by finding a transepithelial resistance greater than 650 Ω with a MilliCell-ERS (Millipore).

Analysis of horseradish peroxidase transcytosis. Transcytosis of horseradish peroxidase (HRP) was analyzed by adding 200 µL of HRP (25 µg/mL, Life Technologies) to polarized Caco-2 cells that had been treated with 100 µM dynasore for 1 hour at 37°C. Sterile PBS (500 µL) was placed into the basolateral chamber of the transwell culture and cells were incubated at 37°C for 30 minutes. Transwells were removed from the tray and 100 µL of the basolateral medium was removed for analysis in triplicate. An HRP standard (0.025 ng) and experimental samples were serially diluted and 100 µL 3,3', 5,5"-tetramethylbenzidine (TMB) substrate (Cell Signaling Technology) was added to the apical surface. Reactions were incubated at room temperature for 5 minutes then terminated by the addition of 250 mM hydrochloric acid. The analyte level was then quantified by obtaining absorbance readings (450 nm) within 5 minutes of reaction termination.

Generation of shRNA expressing plasmids. *Escherichia coli* containing shRNA plasmids were obtained from the University of Minnesota shRNA core facility. Bacteria were streaked on LB agar plates containing 0.05 mg/ml carbenicillin and incubated at 37°C for 18 hours. Single colonies were used to inoculate 150 mL LB agar cultures containing 0.05 mg/ml carbenicillin that were grown at 37°C for 18 hours. Plasmids were collected with a Plasmid MiniPrep kit (Qiagen) or PureYield Midiprep kit (Promega, Madison, WI).

Generation of shRNA lentiviral stocks. 293T cells were seeded in a 10 cm plate at a density of 5.5 x 10^6 cells/plate and incubated at 37°C for 24 hours. DNA/Arrest-In complexes were formed by diluting 37.5 µg of DNA (9 µg transfer vector containing shRNA, 28.5 µg packaging mix, Fisher Scientific, Chicago, IL) into 1 ml of serum-free medium. Separately, 187.5 µL of Arrest-In (Fisher Scientific, Chicago, IL) was diluted to a total volume of 1 ml in serum-free medium. Diluted DNA and Arrest-In were combined and incubated for 20 minutes at room temperature. Three milliliters of serum-free medium was added to the reaction and then overlaid to 293T cultures for 4 hours at 37°C. The transfection mixture was then aspirated and replaced with 12 ml completed culture medium. Cells were returned to 37°C and incubated for 48 hours followed by collection of virus-containing supernatant into 1 ml aliquots which were stored at -80°C. Titers were determined as described below.

Determination of lentivirus titers. 293T cells were seeded in a 24-well plate at a density of 2 x 10^5 cells/well. Twenty-four hours after plating, cells were infected with serial 5-fold dilutions of shRNA-expressing lentivirus at 37°C for five hours. Fresh medium was added and the cells were incubated for 48 hours at 37°C. For constructs in the pGIPZ library, the number of GFP-expressing colonies was counted in each well to determine the initial titer. For constructs in the pLKO.1 library, 1 µg/ml puromycin was added and the cultures incubated

until all cells in the negative control were lysed. Viable colonies in each well were counted to determine the viral titer.

Transduction of 293 cells with shRNA expressing lentivirus. 293 cells were seeded in 6 well trays at a density of 1 x 10^6 cells/well. Twenty-four hours after plating, cells were infected with lentivirus at an MOI of 3 and incubated at 37°C for 1 hour. The inoculum was then removed and fresh medium added. Cultures were incubated at 37°C for 48 hours followed by the addition of medium containing 1 mg/ml puromycin for selection of shRNA-expressing colonies.

Transduction of 293 cells with pooled shRNA expressing lentivirus. 293 cells were seeded in 10 cm dishes at a density of 1 x 10^6 cells/well. Twenty-four hours after plating, cells were infected with lentivirus at an MOI of 0.3 and incubated at 37°C for 1 hour. The inoculum was then removed and fresh medium added. Cultures were incubated at 37°C for 48 hours followed by the addition of medium containing 1 mg/ml puromycin.

Statistical analysis. Mean values for triplicate samples are shown from representative growth experiments; error bars indicate the standard error of the mean. For ligand uptake and dominant negative caveolin-1 experiments, mean values for at least triplicate samples were compared using a paired (normalized)

or unpaired (non-normalized) Student's *t* tests. *P* values < 0.05 were considered statistically significant.

CHAPTER 3

Reovirus Uses Multiple Endocytic Pathways for Cell Entry

I. Introduction

To establish infection, viruses must bypass the limiting membrane either at the cell surface or through an intracellular compartment, such as the endosome. Enveloped viruses achieve this through membrane fusion, mediated by envelope glycoproteins (51). Viral membrane fusion can be triggered by receptor interactions at the plasma membrane or specific conditions within the endosome (55). For example, the fusogenic activity of some envelope glycoproteins, such as the dengue virus glycoprotein E and the influenza hemagglutinin (HA) protein, is triggered by acid-dependent conformational changes (55). Nonenveloped viruses are unable to take advantage of membrane fusion to enter cells and instead must disrupt or form pores in the limiting membrane. These processes may also be triggered by exposure to specific stimuli such as low vesicular pH, proteases, or receptor interactions (150).

Reovirus is a nonenveloped, double-stranded RNA virus in the family *Reoviridae* that commonly infects humans but is rarely pathogenic in adults (145). The observation that reovirus replicates preferentially in transformed cells has led to its development as a human cancer therapy (2, 29). It is likely that a number of virus and host determinants contribute to reovirus' oncolytic potential.

Early studies proposed a model in which mutations in Ras inhibit antiviral PKR signaling and activate other signal transduction pathways to promote viral protein synthesis and apoptosis in reovirus-infected transformed cells (142). More recent work from our laboratory and others revealed that efficient cell entry of reovirus particles into transformed cells is a major determinant of its oncolytic potential (2, 84, 133).

The molecular details of reovirus entry have been best characterized in L929 mouse fibroblasts. In this cell line, entry is initiated by interactions between virions and the cellular receptor junctional adhesion molecule-A (JAM-A), followed by the activation of β1 integrins and uptake of viral particles through clathrin-mediated endocytosis (8, 34, 75, 81). Within vesicles of the endocytic compartment, the outermost capsid protein, σ3, is removed by proteolysis and the membrane penetration protein μ1 is exposed, generating an intermediate subviral particle (ISVP) (15, 72, 144). During intestinal infection *in vivo*, secreted pancreatic serine proteases in the intestinal tract remove σ3 extracellularly to form ISVPs (11, 13). ISVPs may also be formed extracellularly during oncolytic therapy, as tumor microenvironments are often characterized by a high concentration of secreted proteases (88, 137, 164).

Virions and ISVPs have distinct protein compositions and structures that may impact the mechanism used to enter host cells. Although clathrin-mediated endocytosis plays a role during infection by virions, studies have shown that this pathway is dispensable for infection by ISVPs (81). In addition, μ1, which is

exposed on ISVPs, can cause membrane damage and chromium release when cells are infected at high multiplicities of infection (MOIs) (79, 169). This has led to the suggestion that ISVPs may enter cells by direct membrane penetration. However, ISVPs have been detected within endocytic vesicles of infected cells (4, 144), leaving open the possibility that ISVPs require endocytosis to establish productive infection. In addition, many viruses are now known to take advantage of multiple endocytic pathways to enter cells (30, 86, 110). While it has been established that reovirus virions use clathrin-mediated endocytosis for cell entry (81), the importance of other pathways, such as caveolar and lipid raft-mediated endocytosis, is currently unknown (23, 35, 44, 94, 121). This led us to investigate the role of clathrin-independent endocytosis during infection by reovirus virions and ISVPs.

We found that two different chemical agents which disrupt caveolar endocytosis inhibited particle uptake and replication of both virions and ISVPs. Experiments using dominant negative caveolin-1 confirmed the role of caveolar endocytosis in infection by virions and ISVPs, and delayed-addition experiments revealed that inhibition of this pathway impacted an early step of the viral life cycle. We also discovered that infection by virions was inhibited when cells were depleted of membrane cholesterol, but this effect was not observed when infections were initiated with ISVPs. These results provide some of the first evidence that reovirus ISVPs use endocytosis to productively infect host cells

and that virions take advantage of multiple endocytic pathways to initiate infection.

II. Results

Reovirus ISVPs are internalized by dynamin-dependent endocytosis. While it is well established that reovirus virions take advantage of clathrin-mediated endocytosis to enter cells, ISVPs do not appear to use this pathway (81). Clathrin-independent endocytic pathways have been described, including caveolar endocytosis and macropinocytosis, and these are now known to play a role in the entry of some viruses (86, 134). To investigate the possibility that reovirus ISVPs enter cells through clathrin-independent endocytosis, we first examined the role of dynamin during internalization of reovirus virions and ISVPs. Dynamin, which is involved in the scission of clathrin-coated vesicles and caveolae from the plasma membrane, can be inhibited with the small-molecule inhibitor dynasore (42, 80, 148, 165). We used confocal microscopy to visualize reovirus particle uptake in A549 respiratory epithelial cells that had been pretreated with either vehicle (DMSO) or 100 μM dynasore and then synchronously infected with either T1L virions or ISVPs. A549 cells were selected because it is permissive to infection by both virions and ISVPs (48) and it has properties in adherent cell culture that made it easy to visualize particle uptake. Whereas vehicle-treated cells showed significant uptake of virions and

ISVPs into the cytoplasm at 10 mpi, we found that particles were concentrated at the periphery of dynasore-treated cells (Figure 3.1). The effect of dynasore on virion uptake is consistent with the role of dynamin in clathrin-mediated endocytosis, but the effect on ISVP internalization suggested that these uncoated particles also use a dynamin-dependent endocytic pathway to gain access to the cytoplasm.

Dynasore inhibits infection by ISVPs. The imaging experiments described above suggest that dynamin is required for the entry of ISVPs. However this approach does not distinguish between infectious and non-infectious particles. To determine if dynamin is important for productive infection, we assessed the growth of ISVPs in the presence of dynasore. L929 cells treated with either vehicle (DMSO) or dynasore were infected with virions or ISVPs at an MOI of 3. Infections were terminated at various times and viral yields were quantified by plaque assay on L929 cells. We found that dynasore treatment inhibited the growth of both virions (Figure 3.2A) and ISVPs (Figure 3.2B). Similar results were obtained in human A549 respiratory epithelial cells (Figure 3.2C) and human embryonic kidney (HEK) 293 cells (Figure 3.2D). These data suggest that ISVPs take advantage of a dynamin-dependent endocytic pathway to infect L929 mouse fibroblasts and transformed human cell lines.

The results of our imaging experiments suggest that dynasore inhibits replication by inhibiting viral uptake; however, they do not rule out another effect on later

Figure 3.1. Virions and ISVPs are internalized by dynamin-mediated endocytosis. Reovirus virions and ISVPs undergo dynamin-mediated endocytosis. Reovirus T1L virions or ISVPs were adsorbed at a concentration of 1 x 10^5 particles/cell to adherent A549 cells that had been pre-treated with vehicle (DMSO) or dynasore. The monolayers were fixed at 10 minutes post-infection and labeled with anti-reovirus T1L antiserum (green), phalloidin (red), and DAPI (blue). Scale bars represent 20 μM.

Figure 3.1

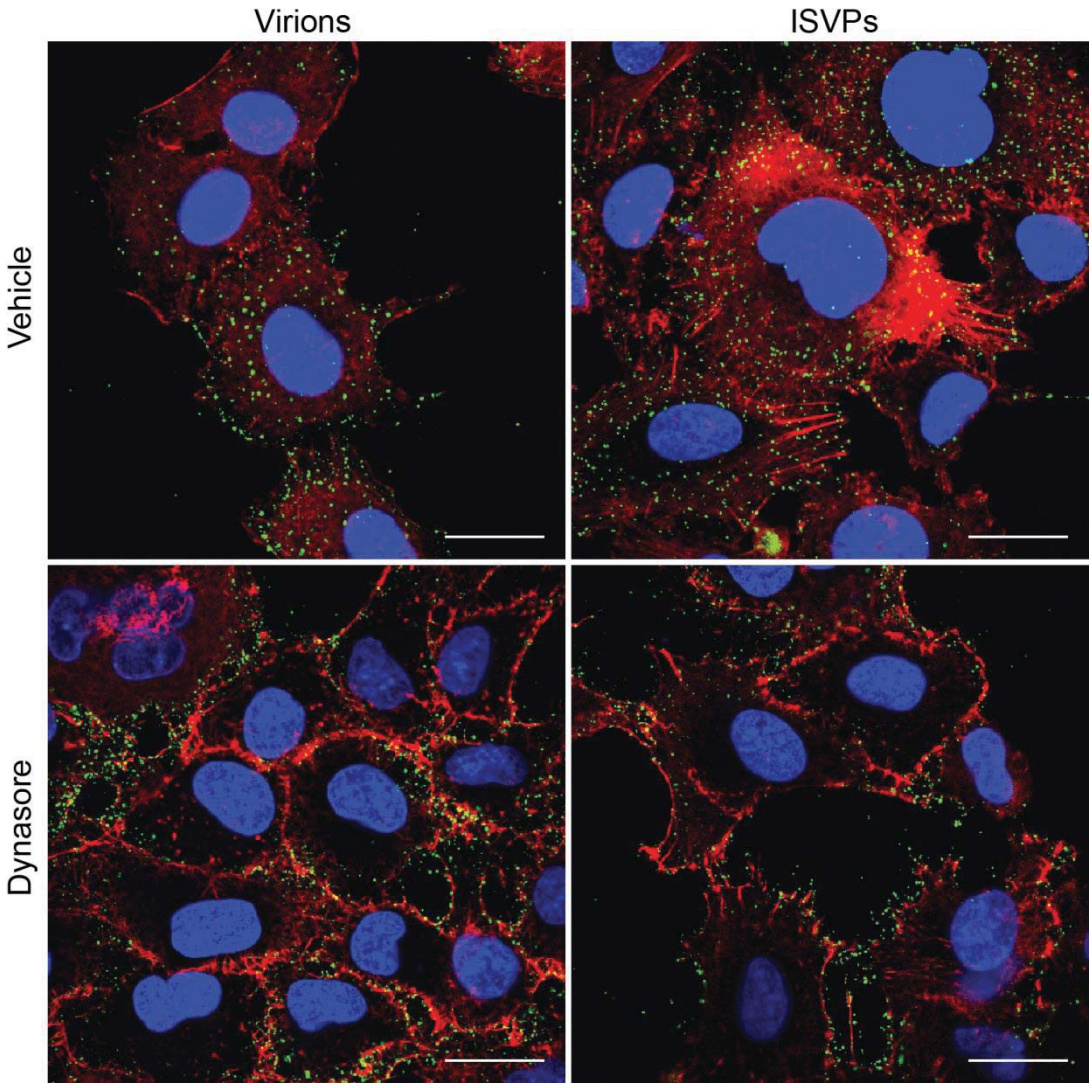

Figure 3.2. Reovirus infection is dynamin-dependent. A-B) L929 cells were pre-treated with vehicle (DMSO) or dynasore and infected with reovirus T1L virions (A) or ISVPs (B) at an MOI of 3. After adsorption, fresh medium with vehicle or inhibitor was added to the cultures and samples were collected at the indicated times post-infection. Viral yields were quantified by plaque assay on L929 cells. A549 (C) and 293 cells (D) were pre-treated with DMSO or dynasore and infected at an MOI of 3. Samples were harvested at 24 hpi and viral yields were quantified by plaque assay on L929 cells.

Figure 3.2

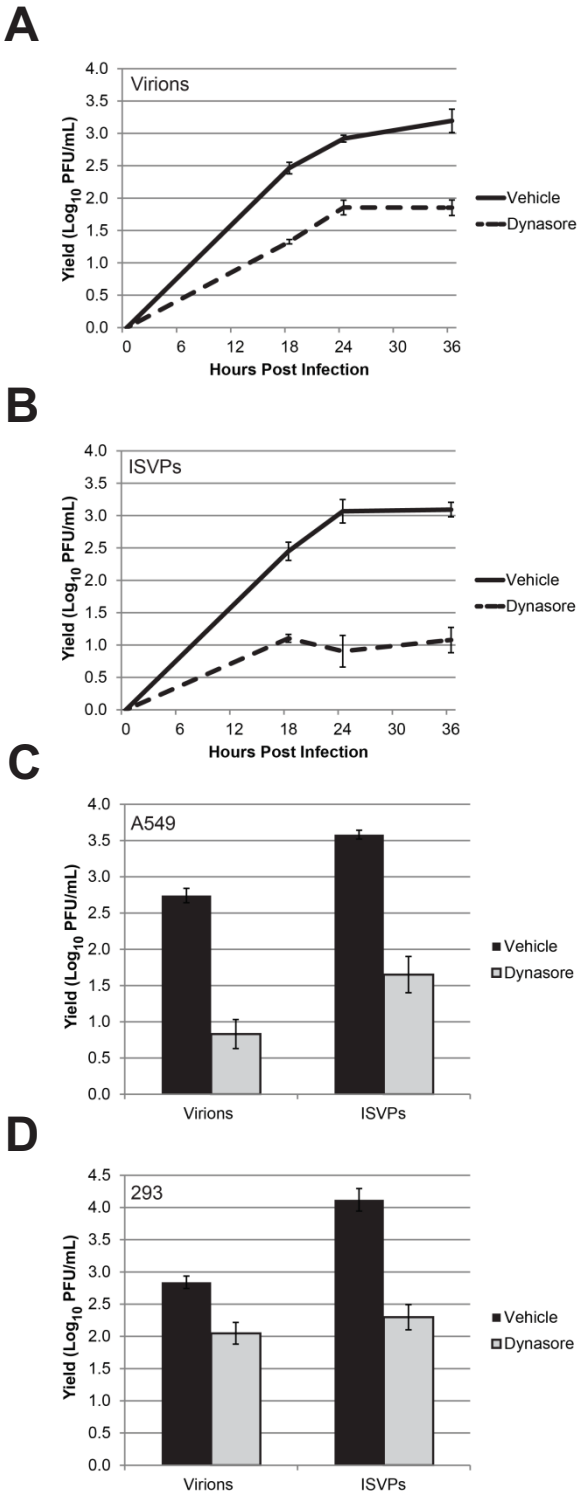
A
Virions
Yield (Log10 PFU/mL)
Hours Post Infection
Vehicle
Dynasore
B
ISVPs
Yield (Log10 PFU/mL)
Hours Post Infection
Vehicle
Dynasore
C
A549
Yield (Log10 PFU/mL)
Virions
ISVPs
Vehicle
Dynasore
D
293
Yield (Log10 PFU/mL)
Virions
ISVPs
Vehicle
Dynasore

steps in the replication cycle. To address this possibility, we performed a delayed-addition experiment in which dynasore was added at various times prior to or after adsorption. Cells were harvested at 24 hpi and infection was analyzed by immunoblotting for the reovirus non-structural protein μNS. In cultures pretreated with dynasore, infection was inhibited by 90% (Figure 3.3). In contrast, addition of dynasore after adsorption had a minimal effect on viral replication. This finding supports the conclusion drawn from our imaging studies—that dynasore inhibits reovirus replication at an early step of the viral life cycle.

Agents that disrupt vesicular transport can alter receptor recycling to the cell surface (37). To determine if the inhibitory effect of dynasore on reovirus infection was due to effects on virion attachment, we directly assessed the consequences of treatment on reovirus binding to L929 cells. Cells were pretreated with DMSO or dynasore, and virions were adsorbed for one hour. The samples were then fixed, stained for reovirus, and binding was analyzed by flow cytometry. We found that vehicle- and dynasore-treated cells had similar fluorescence profiles after reovirus adsorption (Figure 3.4), demonstrating that dynasore treatment does not result in reduced viral binding at the cell surface.

Our results suggested that, like virions, ISVPs enter cells through a dynamin-dependent pathway. To confirm that our working concentration of dynasore inhibited both of the known dynamin-dependent pathways, we used the pathway-specific ligands transferrin and cholera toxin subunit B (CTB), which are taken up by clathrin-mediated and caveolar endocytosis, respectively (61, 118). Following

Figure 3.3. Dynamin inhibits reovirus infection early in the viral lifecycle. Dynasore was added to L929 cells at the indicated times prior to or after adsorption with reovirus virions. Infected cell lysates were analyzed at 24 hpi for μNS expression by immunoblotting. Band intensities of μNS and β-actin were quantified to determine the relative μNS expression level of each sample. The top panel is a representative immunoblot and the bottom panel is a quantification of band intensities. Values in the graph represent the relative μNS expression level compared to vehicle-treated cells from a representative experiment.

Figure 3.3

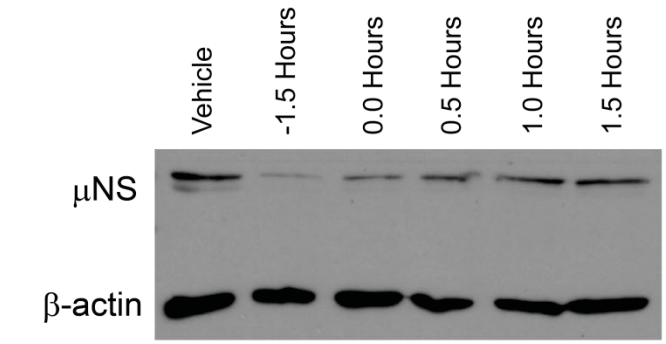
Vehicle
-1.5 Hours
0.0 Hours
0.5 Hours
1.0 Hours
1.5 Hours
μNS
β-actin

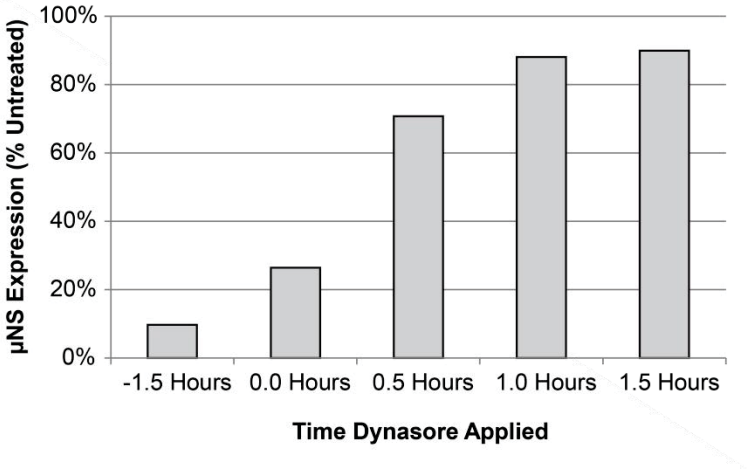
μNS Expression (% Untreated)
100%
80%
60%
40%
20%
0%
-1.5 Hours
0.0 Hours
0.5 Hours
1.0 Hours
1.5 Hours
Time Dynasore Applied

Figure 3.4. Dynamin inhibition does not decrease reovirus binding. L929 cells in suspension culture were pre-treated with vehicle (DMSO) or dynasore and adsorbed with reovirus virions at a concentration of 1 x 10^5 particles/cell (white peaks) or an equivalent volume of gel saline (gray peaks). After adsorption, cells were fixed and stained with an anti-reovirus T1L antibody. Reovirus binding was quantified by flow cytometry.

Figure 3.4

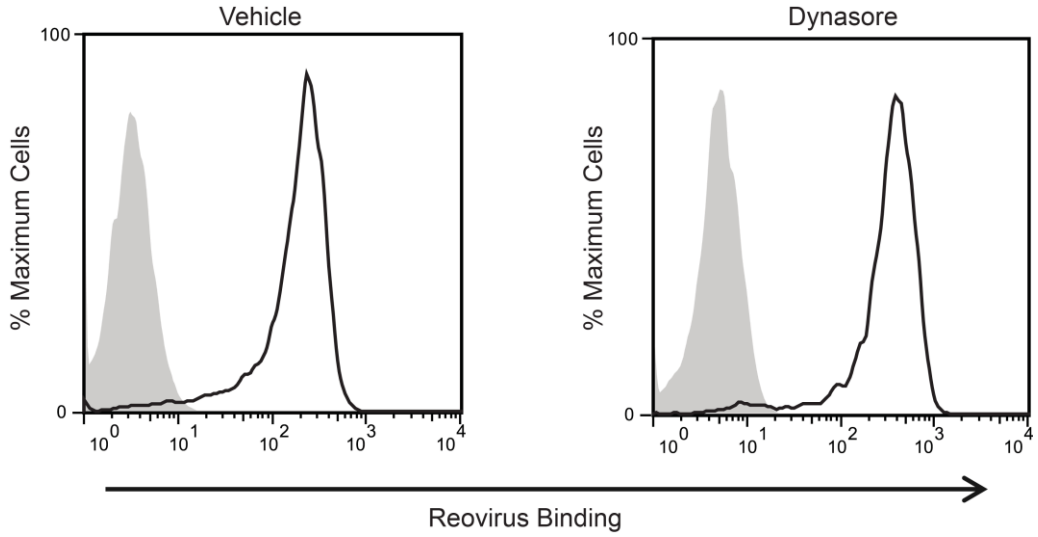
Vehicle
Dynasore
100
0
% Maximum Cells
10^0
10^1
10^2
10^3
10^4
Reovirus Binding

dynasore treatment, A549 cells were incubated with pre-labeled ligands, fixed at 10 mpi, and the transferrin- and CTB-positive cells were quantified by immunofluorescence. We found that the number of transferrin and CTB-positive cells was significantly reduced in treated samples (Figure 3.5A), demonstrating that dynasore effectively inhibits both clathrin-mediated and caveolar endocytosis. To confirm that dynasore did not affect reovirus growth as a consequence of cytotoxicity, we determined viral yields in cells that were treated with increasing concentrations of the inhibitor. This analysis revealed that dynasore inhibition of reovirus infection was dose-dependent, with a maximum effect that plateaued at a concentration of 100 μM, our working concentration for particle uptake and growth experiments (Figure 3.5B). Annexin V and propidium iodide staining revealed that dynasore had only minimal effects on cell viability, with cells remaining over 80% viable at all concentrations tested (Figure 3.5B). Together, these results argue that the effect of dynasore on reovirus replication is a consequence of the inhibition of dynamin-dependent pathways rather than a non-specific, cytotoxic effect of the inhibitor.

Virions and ISVPs can utilize caveolar endocytosis for cell entry. While ISVPs had reduced viral yields in dynasore-treated cells, they can infect cells treated with chlorpromazine, which inhibits clathrin-mediated endocytosis (81). These results led us to predict that ISVPs would enter cells through dynamin-dependent, caveolar endocytosis, which has recently been implicated in

Figure 3.5. Dynasore inhibits dynamin-dependent endocytosis without affecting cell viability. A) A549 cells were pre-treated as described above and then incubated with Alexa 488-transferrin or FITC-CTB. After 1 h at 4°C, warm medium was added to the cultures and the cells were fixed after 10 minutes. The percentage of transferrin- or CTB-positive cells was determined by counting three similarly confluent fields in three independent experiments. Between 450 and 750 cells were counted in each experiment. Error bars represent standard error of the mean for the three independent experiments. B) L929 cells were treated with dynasore at the indicated concentrations and incubated for 24 hours at 37°C. Cells were stained with annexin V/PI and viability was assessed by flow cytometry. A parallel set of samples was pre-treated with dynasore, infected with T1L virions or ISVPs at an MOI of 3 and assayed for viral yield at 24 hpi.

Figure 3.5

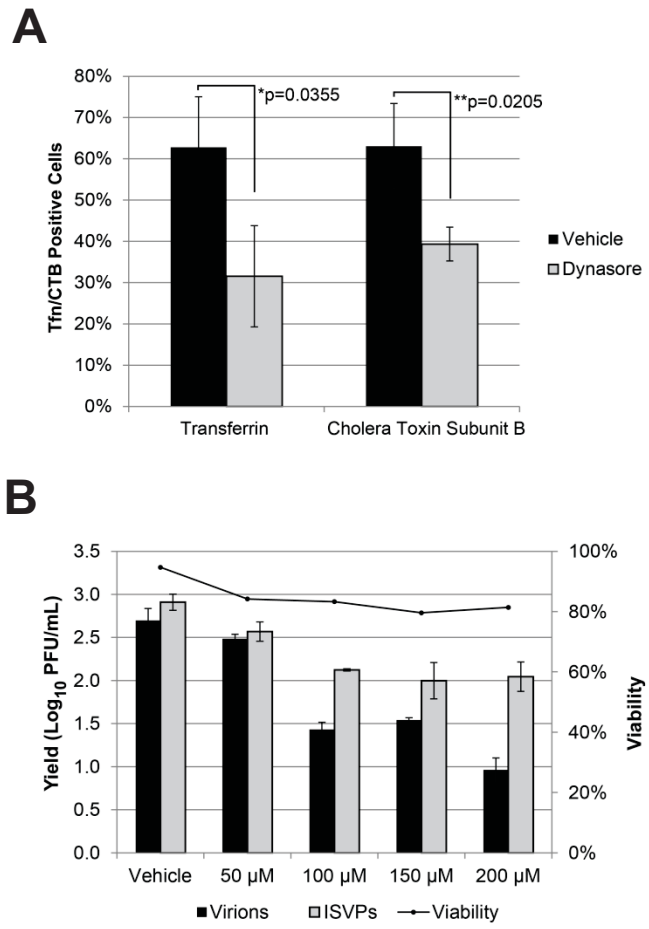
A
80%
70%
60%
50%
40%
30%
20%
10%
0%
Tfn/CTB Positive Cells
*p=0.0355
**p=0.0205
Vehicle
Dynasore
Transferrin
Cholera Toxin Subunit B
B
3.5
3.0
2.5
2.0
1.5
1.0
0.5
0.0
Yield (Log10 PFU/mL)
100%
80%
60%
40%
20%
0%
Viability
Vehicle
50 µM
100 µM
150 µM
200 µM
Virions
ISVPs
Viability

the entry of avian reovirus (66). To investigate this possibility, we treated L929 cells with 200 μM genistein to inhibit the caveolar pathway and assessed the effect on viral growth. Consistent with our hypothesis, replication of ISVPs was inhibited by genistein (Figure 3.6A). This agent also inhibited the growth of reovirus virions (Figure 3.6B), suggesting that these particles are capable of accessing multiple endocytic pathways. Genistein inhibited the replication of both virions and ISVPs in A549 and HEK-293 cells (Figure 3.6C), and immunofluorescence analysis revealed that it inhibited particle uptake in A549 cells (W.S. Schulz and L.A. Schiff, unpublished observations). Consistent with published data (82), it inhibited infection by virions, but not ISVPs in HeLa cells (Figure 3.7).

Genistein blocks caveolar endocytosis by inhibiting the Src kinase-dependent phosphorylation of caveolin-1, preventing vesicle fusion (6, 107). However, this tyrosine kinase inhibitor can impact other intracellular signal transduction pathways, including those involved in cell cycle progression and apoptosis (70, 106, 117). We assessed the viability of genistein-treated L929 cells to determine if cell death was a factor in reducing viral yields. We found that after 24 h of treatment, genistein did not significantly affect L929 cell viability at any of the concentrations tested, but did significantly reduce viral yield (Figure 3.8A), arguing against an apoptotic mechanism. We also confirmed that genistein selectively inhibited caveolar endocytosis by analyzing transferrin and CTB uptake in A549 cells. Whereas genistein inhibited CTB internalization, which is

Figure 3.6. Reovirus virions and ISVPs use caveolar endocytosis in multiple cell lines. A-B) L929 cells were pre-treated with vehicle (DMSO) or 200 μM genistein and infected with reovirus T1L ISVPs (A) or virions (B) at an MOI of 3. Viral yields were determined at the indicated times post-infection by plaque assay on L929 cells. C) A549 and 293 cells were pre-treated and infected as described above and viral yields were determined at 24 hpi.

Figure 3.6

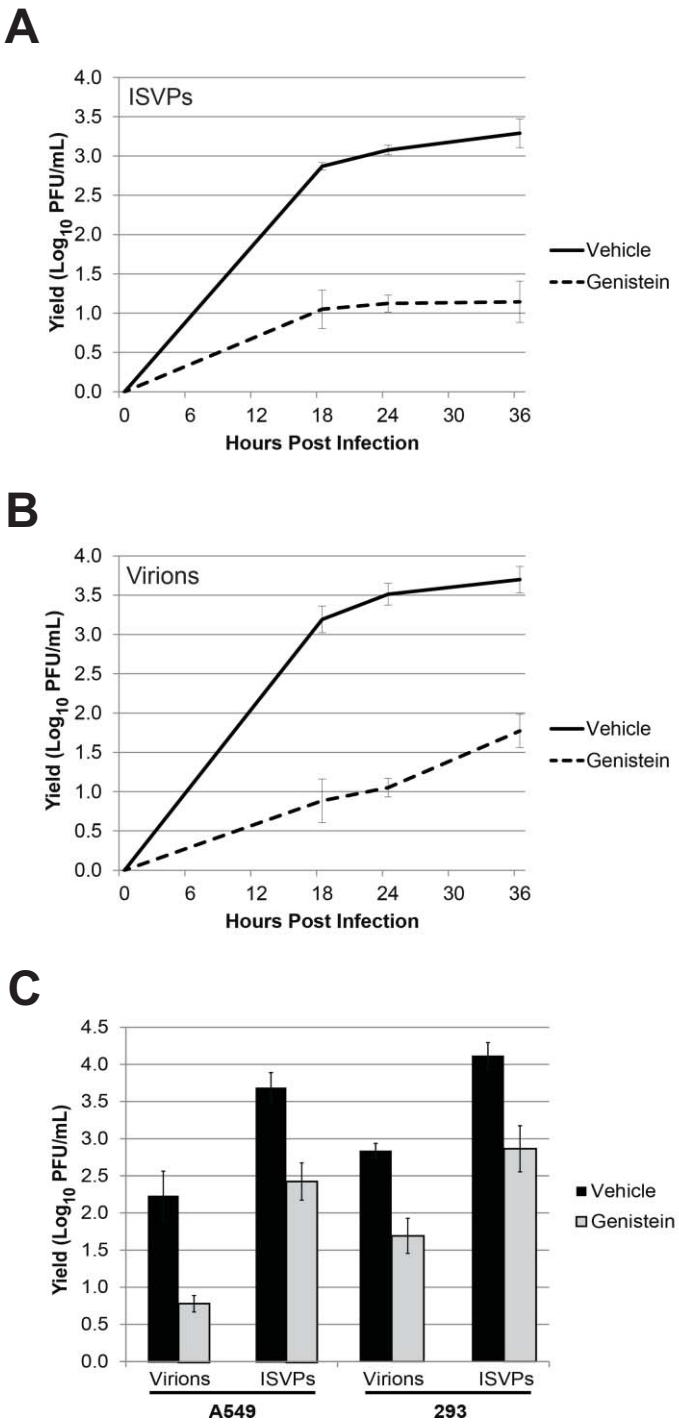
A
ISVPs
Yield (Log10 PFU/mL)
4.0
3.5
3.0
2.5
2.0
1.5
1.0
0.5
0.0
0
6
12
18
24
30
36
Hours Post Infection
Vehicle
Genistein
B
Virions
Yield (Log10 PFU/mL)
Hours Post Infection
Vehicle
Genistein
C
Yield (Log10 PFU/mL)
4.5
4.0
3.5
3.0
2.5
2.0
1.5
1.0
0.5
0.0
Virions
ISVPs
Virions
ISVPs
A549
293
Vehicle
Genistein

Figure 3.7. Genistein does not inhibit reovirus infection in HeLa cells. HeLa cells seeded in 8-well CultureSlides were pre-treated as described above and infected at an MOI of 15. At 24 hpi, cultures were fixed and stained with antiserum specific for reovirus T1L. Infection was analyzed by indirect immunofluorescence and the percentage of infected cells was determined from three equally confluent fields of view.

Figure 3.7

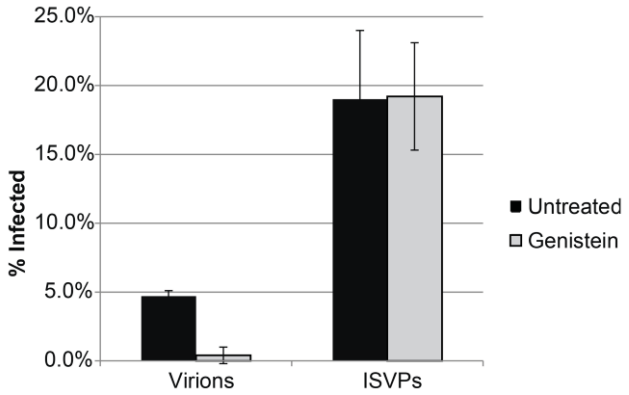
25.0%
20.0%
15.0%
10.0%
5.0%
0.0%
% Infected
Virions
ISVPs
Untreated
Genistein

caveolin-dependent, it had no effect on the clathrin-dependent uptake of transferrin (Figure 3.8B). To determine whether genistein targets an early stage in infection, we performed a delayed-addition experiment. In infected cells that were pretreated with genistein, μNS expression was decreased by over 60% (Figure 3.9). However, when genistein was added at or after adsorption, this effect was greatly diminished. This result is consistent with findings in HeLa cells (82) and suggests that genistein inhibits reovirus infection at an early step of the viral life cycle, most likely cell entry.

Caveolin-1 is important for infection by reovirus virions and ISVPs. Because genistein is a broad-spectrum receptor tyrosine kinase inhibitor, we used an independent approach to determine if reovirus particles enter cells through the caveolar pathway. Caveolin-1 is a scaffolding protein involved in caveolar morphogenesis (37). Expression of a dominant negative form of the protein with a Y14F mutation has been shown to inhibit caveolar endocytosis (6, 50, 111). We transfected HEK-293 cells with either empty vector (pEGFP-N1) or vector expressing dominant negative caveolin-1 (DN-cav1). Twenty-four hours after transfection, the cultures were infected with either virions or ISVPs. At 24 hpi, infected cultures were fixed and stained with an antiserum directed against the reovirus non-structural protein μNS, and reovirus-positive cells were quantified by flow cytometry. The percentage of GFP-positive (transfected) cells that were also μNS-positive (infected) was calculated for both DN-cav1 and

Figure 3.8. Genistein inhibits caveolar endocytosis without affecting cell viability. A) L929 cells were pre-treated with the indicated concentrations of genistein and viability was assessed by annexin V/PI staining at 24 hpi. A parallel set of samples was infected with T1L virions or ISVPs and assayed for viral yield at 24 hpi. B) A549 cells were pre-treated as described above and incubated with Alexa 488-transferrin or FITC-CTB. After 1 h at 4°C, warm medium was added to the cultures and the cells were fixed after 30 minutes. The percentage of transferrin- or CTB-positive cells was determined by counting three similarly confluent fields. Error bars represent the standard deviation for each sample.

Figure 3.8

A

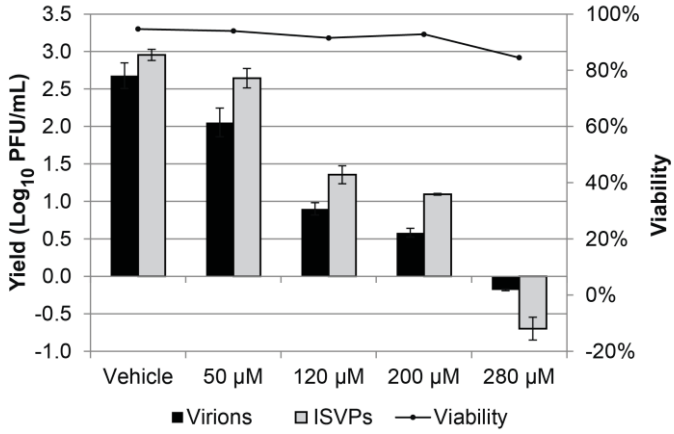
3.5
3.0
2.5
2.0
1.5
1.0
0.5
0.0
-0.5
-1.0
Yield (Log10 PFU/mL)
100%
80%
60%
40%
20%
0%
-20%
Viability
Vehicle
50 µM
120 µM
200 µM
280 µM
Virions
ISVPs
Viability

B

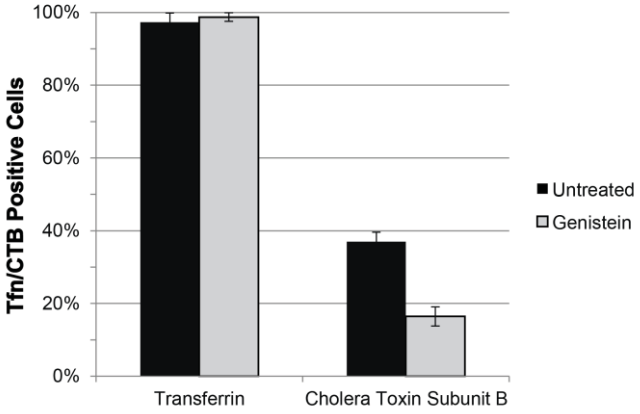
100%
80%
60%
40%
20%
0%
Tfn/CTB Positive Cells
Transferrin
Cholera Toxin Subunit B
Untreated
Genistein

Figure 3.9. Genistein inhibits reovirus infection early in the viral lifecycle. Genistein was added to L929 cells at the indicated times prior to or after adsorption with reovirus virions. Infected cell lysates were analyzed at 24 hpi for μNS expression by immunoblotting. The immunoblot (top panel) is from a representative experiment. Band intensities of μNS and β-actin were quantified to determine the relative μNS expression level of each sample. The values in the graph are derived from three independent experiments, and represent the relative μNS expression level compared to that in vehicle-treated cells (bottom panel).

Figure 3.9

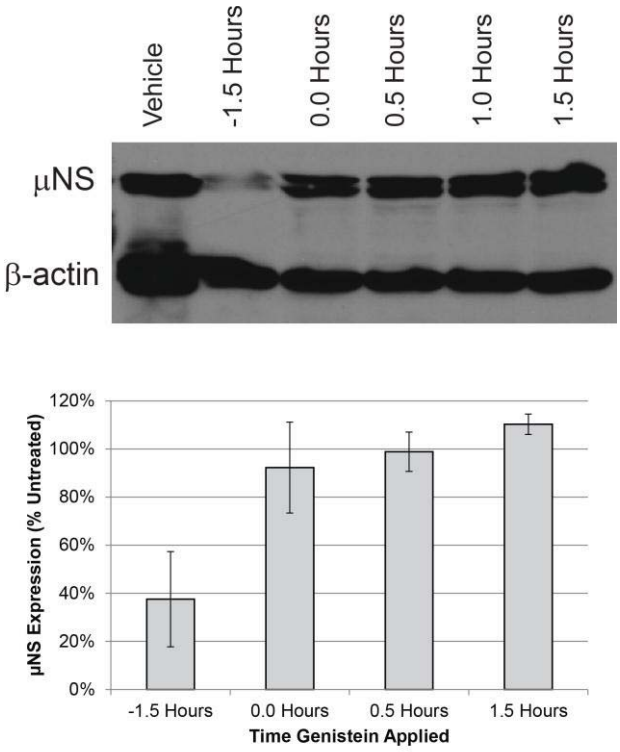
Vehicle
-1.5 Hours
0.0 Hours
0.5 Hours
1.0 Hours
1.5 Hours
μNS
β-actin
120%
100%
80%
60%
40%
20%
0%
μNS Expression (% Untreated)
-1.5 Hours
0.0 Hours
0.5 Hours
1.5 Hours
Time Genistein Applied

pEGFP-N1-transfected samples in three independent experiments (Figure 3.10). This analysis revealed that expression of DN-cav1 significantly reduced infection by reovirus virions and ISVPs relative to the vector-only control. This level of inhibition was similar to that seen with dominant negative Rab proteins (83). Together, these results support a role for caveolin-1 and caveolar endocytosis during infection by both virions and ISVPs.

Cholesterol is important for infection by reovirus virions. Recent work reveals that many viruses enter cells through specialized, detergent-resistant microdomains of the cell membrane, called lipid rafts (24, 44, 68, 94). To determine if lipid rafts play a role in reovirus infection, we used MβCD to extract membrane cholesterol, which is enriched in lipid rafts. Since MβCD can often be cytotoxic, we first assessed viability and viral growth in L929 cells treated with various concentrations of inhibitor. We found that MβCD was cytotoxic at concentrations above 5 mM (Figure 3.11A). While the growth of reovirus virions was inhibited at this concentration, the replication of ISVPs was unaffected (Figure 3.11A). To determine if the replication of ISVPs was inhibited at later times of infection in MβCD-treated cells, we performed a kinetic analysis. We found that the growth of ISVPs was similar in MβCD- and vehicle-treated cells at each time point tested, while the growth of virions was inhibited (Figure 3.11B, Figure 3.11C). We examined reovirus binding in the presence of MβCD to determine if cholesterol depletion had a differential effect on the capacity of

Figure 3.10. Caveolar endocytosis is important for reovirus infection. Caveolin-1 is important for infection by virions and ISVPs. 293 cells were transfected with empty vector or vector expressing dominant negative caveolin-1. Cells were infected with T1L virions or ISVPs 24 hours after transfection and then fixed and stained for μNS at 24hpi. The number of transfected cells that were also μNS-positive (infected) was determined by flow cytometry. The relative percentage of infected cell compared to empty vector (pEGFP-N1) transfected controls is displayed. Error bars represent the standard error of the mean for three independent experiments.

Figure 3.10

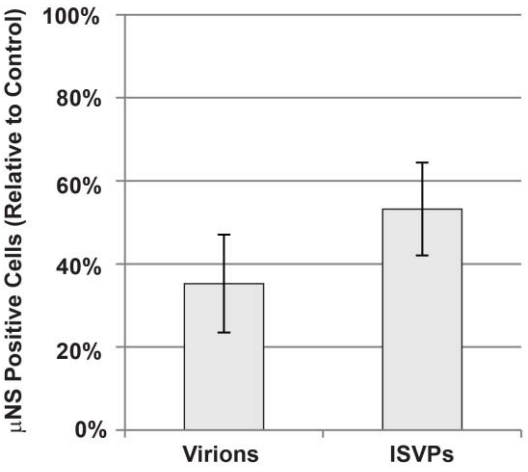
μNS Positive Cells (Relative to Control)
100%
80%
60%
40%
20%
0%
Virions
ISVPs

Figure 3.11. Cholesterol is important for infection by reovirus virions but not ISVPs. A) L929 cells were pre-treated with the indicated concentrations of MβCD and viability was assessed at 24 hpi. A parallel set of samples was infected with T1L virions or ISVPs at an MOI of 3 and assayed for viral yield at 24 hpi. B-C) L929 cells were pre-treated with vehicle (water) or 5mM MβCD, and infected with reovirus T1L virions (B) or ISVPs (C) at an MOI of 3. Viral yields were determined at the indicated times post-infection by plaque assay on L929 cells.

Figure 3.11

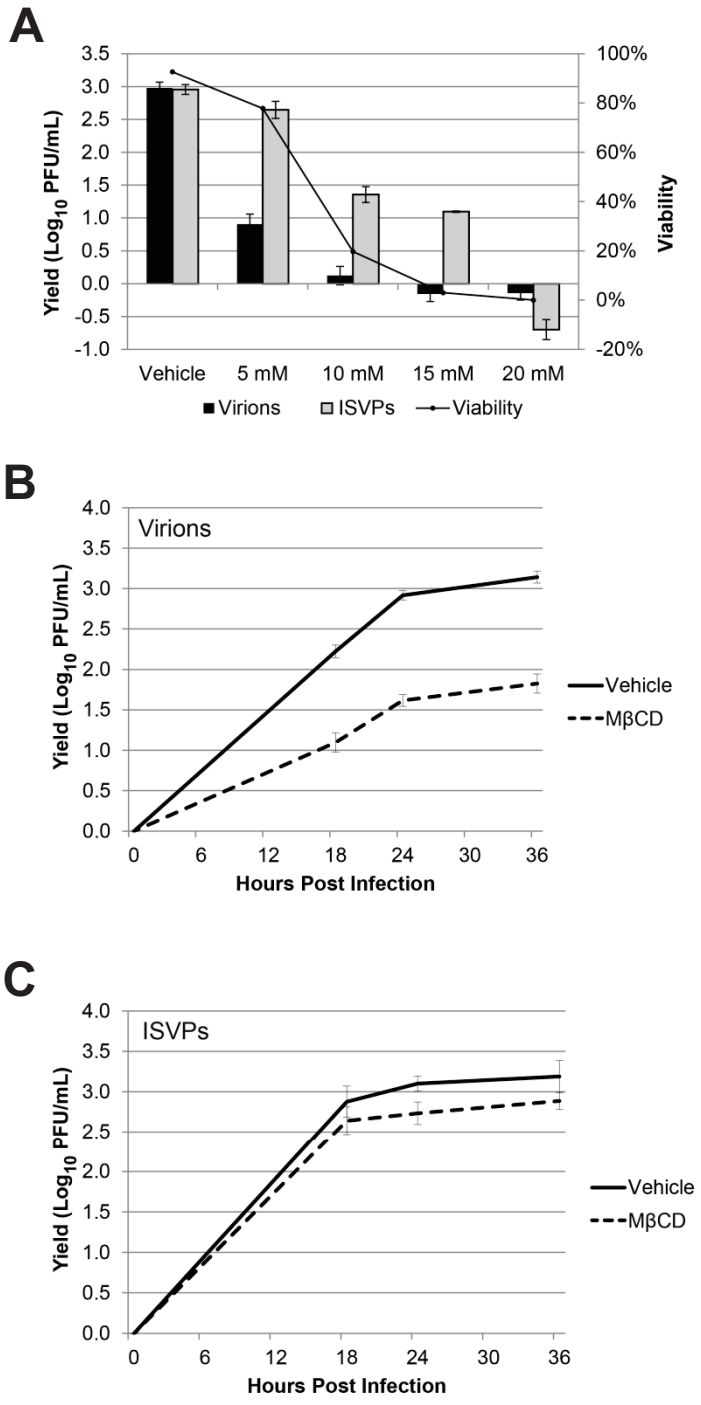
A
Yield (Log10 PFU/mL)
Viability
100%
80%
60%
40%
20%
0%
-20%
Vehicle
5 mM
10 mM
15 mM
20 mM
Virions
ISVPs
Viability
B
Virions
Yield (Log10 PFU/mL)
Hours Post Infection
Vehicle
MβCD
C
ISVPs
Yield (Log10 PFU/mL)
Hours Post Infection
Vehicle
MβCD

virions and ISVPs to interact with cells. Reovirus virions or ISVPs were adsorbed to L929 cells that had been pretreated with either vehicle (water) or MβCD, to deplete cholesterol. After adsorption, the samples were fixed and stained with anti-reovirus antiserum and binding was analyzed by flow cytometry. We found no difference in the capacity of virions or ISVPs to bind to MβCD-treated samples (Figure 3.12A). This finding argues that the growth defect seen after infection with virions is not due to decreased binding by these particles.

Cholesterol can play a critical role in viral assembly as well as viral entry (57). To determine if MβCD impacts an early or late event in reovirus infection, we took advantage of the fact that its effect can be reversed by replenishing cholesterol after extraction (105). L929 cells were pretreated with vehicle or MβCD for 1.5 h prior to virus adsorption and cholesterol was added to selected samples, either at the time of adsorption or 30 minutes prior to adsorption. Viral protein expression was assessed at 24 hpi (Figure 3.12B). As expected, viral protein expression was significantly inhibited in MβCD-treated cells that did not receive additional cholesterol. When cholesterol was added to the cultures at the time of virus adsorption, we saw a similarly low level of viral gene expression, but the inhibitory effect of MβCD was diminished when cholesterol was added to the cultures 30 minutes prior to adsorption, consistent with an effect on early events of infection. Cholesterol depletion has been reported to affect multiple endocytic pathways (90, 120). To better understand the role of cholesterol in reovirus replication, we tested whether MβCD inhibited either of the classical dynamin-

Figure 3.12. Cholesterol is important for an early, post-binding step of reovirus infection. A) L929 cells in suspension culture were pre-treated with vehicle (water) or MβCD and adsorbed with reovirus virions (gray lines) or ISVPs (black lines) at a concentration of 1 x 10^5 particles/cell or an equivalent volume of gel saline (shaded peaks). After adsorption, cells were fixed and stained with an anti-reovirus T1L antibody. Reovirus binding was quantified by flow cytometry. B) Cells were treated with MβCD for one hour and 0.1 mM water-soluble cholesterol was added prior to or at the time of adsorption. Infection was analyzed by immunoblotting for μNS at 24 hpi. The top panel shows band intensities relative to β-actin and the bottom panel is a representative immunoblot.

Figure 3.12

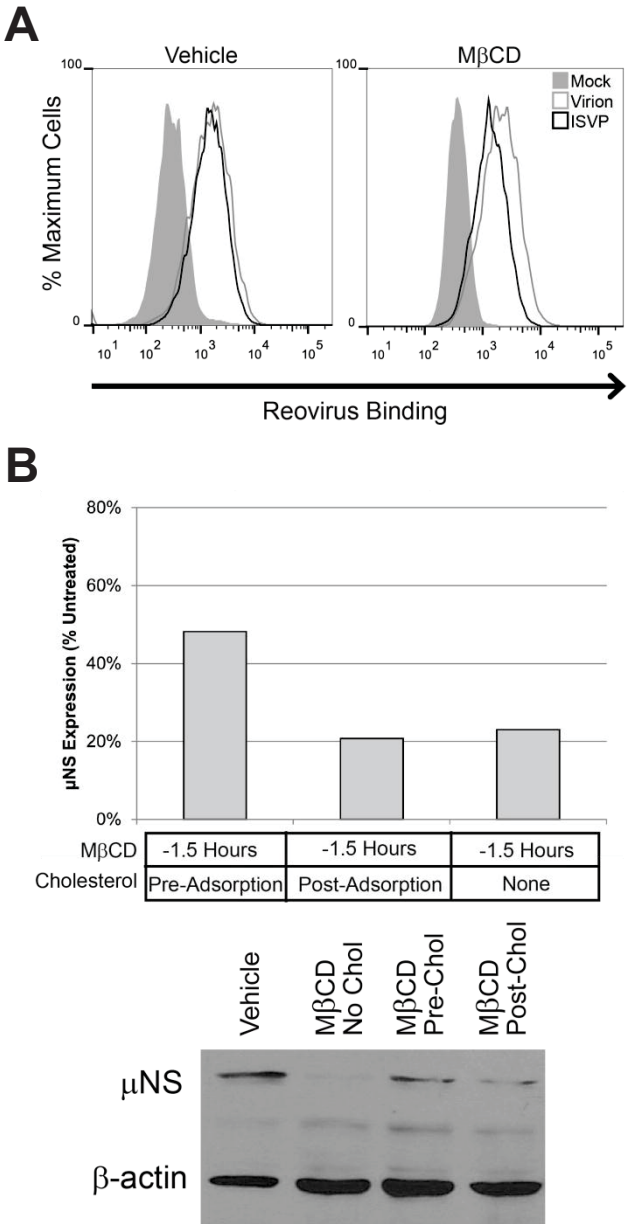
A
Vehicle
MβCD
Mock
Virion
ISVP
% Maximum Cells
100
0
10^1 10^2 10^3 10^4 10^5
Reovirus Binding
B
μNS Expression (% Untreated)
80%
60%
40%
20%
0%
MβCD
Cholesterol
-1.5 Hours
Pre-Adsorption
-1.5 Hours
Post-Adsorption
-1.5 Hours
None
Vehicle
MβCD No Chol
MβCD Pre-Chol
MβCD Post-Chol
μNS
β-actin

dependent pathways under our infection conditions. We found that MβCD treatment did not affect the uptake of either transferrin or CTB (Figure 3.13) in A549 cells, suggesting that it inhibits the replication of reovirus virions by affecting a cholesterol-dependent, dynamin-independent pathway.

We considered the possibility that cholesterol might be more important for infections by virions than ISVPs because it plays a direct role in the conversion of virions to ISVPs. To determine if cholesterol promotes ISVP formation, reovirus virions were incubated with cholesterol, chymotrypsin, or both at 32°C. At the indicated times, PMSF was added to inhibit chymotrypsin and particles were visualized by SDS-PAGE. We found that cholesterol had no impact on the formation of ISVPs *in vitro*, as proteolytic cleavage of the μ1c protein to the δ fragment was not altered in the presence of cholesterol, and cholesterol alone did not promote ISVP formation (Figure 3.14). Together these results are consistent with a model in which cholesterol is important for an early, post-binding step in the reovirus life cycle.

III. Discussion

Early work on reovirus cell entry showed that virion uncoating by endosomal proteases is an essential step of the viral life cycle (144). This same study demonstrated the presence of both virions and ISVPs within endocytic vesicles at early times of infection. Although these particles appeared to be taken

Figure 3.13. MβCD inhibits reovirus infection independent of clathrin and caveolin. A549 cells were pre-treated with vehicle (water) or MβCD for 1 hour. Treated cells were incubated with pre-labeled transferrin or CTB. Warm medium was added to the cultures and after 15 minutes, cells were fixed and ligand uptake was visualized by confocal microscopy. Scale bars represent 50 μM.

Figure 3.13

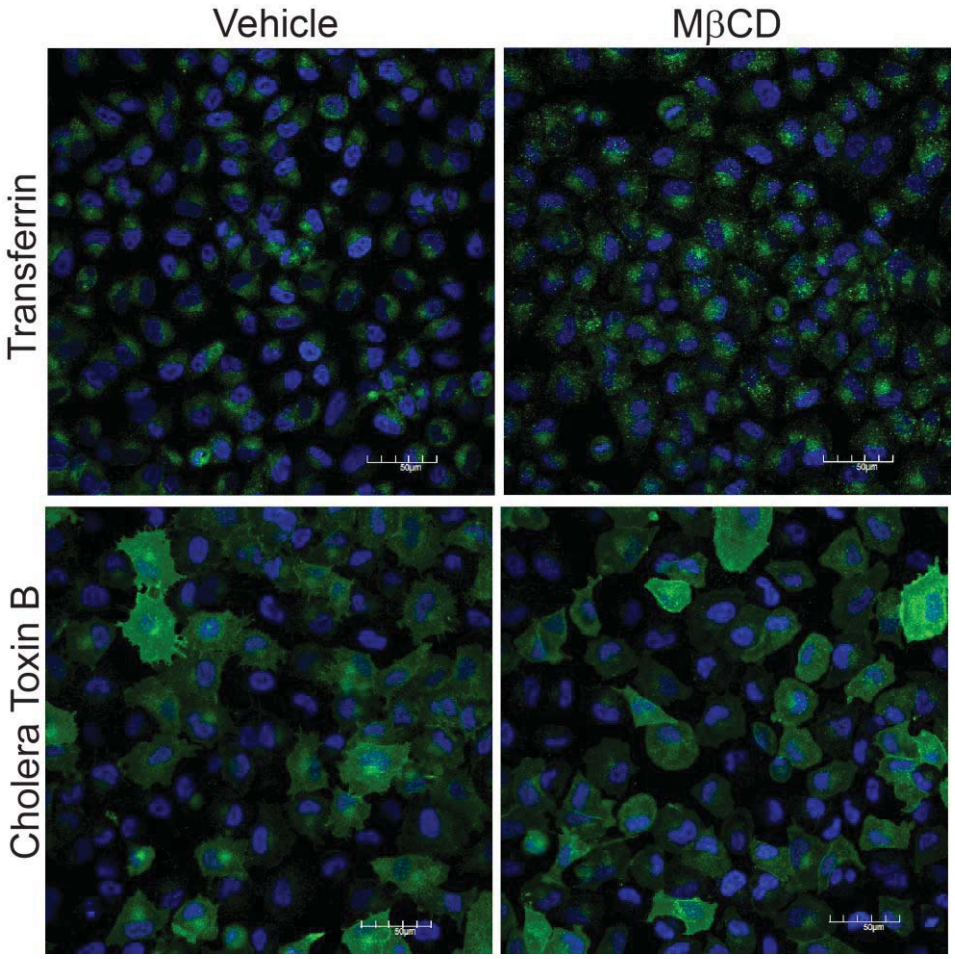

Figure 3.14. Cholesterol does not promote ISVP formation *in vitro.* 5 x 10^{10} reovirus virions were incubated with chymotrypsin, cholesterol, or both in virion dialysis buffer at 32°C. At the indicated times, digestions were terminated with PMSF and the particles were visualized by SDS-PAGE and Coomassie blue staining.

Figure 3.14

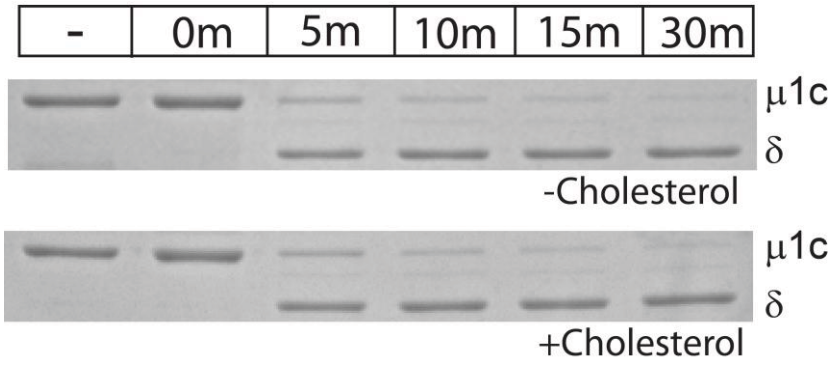

up by endocytosis with equivalent efficiency, it was not clear if endocytosis was a productive pathway for infection by ISVPs. Later studies showed that infection by reovirus virions, but not ISVPs, occurred by uptake through clathrin-mediated endocytosis (81) and that ISVPs could cause direct membrane damage (25, 79). These data suggested that ISVPs may be capable of entering the cytoplasm directly at the cell membrane. In this study, we used two independent chemical inhibitors of caveolar endocytosis as well as dominant-negative caveolin to show that inhibition of the dynamin-dependent caveolar pathway significantly reduces yields when infections are initiated with ISVPs.

We found that genistein treatment, which inhibits caveolar endocytosis by preventing vesicle fusion (6, 107), inhibited infection by ISVPs in a number of different cell lines, including L929 mouse fibroblasts, A549 human lung epithelial cells and 293 human embryonic kidney cells. Dynasore, which inhibits the scission of caveolae, also inhibited ISVP infection in these cells. However, we and others (82) have found that ISVPs are not sensitive to genistein treatment in HeLa cells. Since HeLa cells express very low levels of caveolin (136), this result is not surprising. Reovirus can clearly infect cells that are devoid of caveolae, such as polarized intestinal epithelial cells (10, 102). Because virions are converted to ISVPs in the intestinal tract (11, 13), these data suggest that ISVPs enter intestinal tissue and cells with low levels of caveolar endocytosis through one or more alternative pathways such as direct membrane penetration or

dynamin-independent macropinocytosis, described recently as an entry pathway for Ebola virus (126).

While we have not ruled out direct membrane penetration as an entry mechanism for ISVPs, we have demonstrated that caveolar endocytosis is a route for productive infection by these particles. The function of endocytosis during infection by virions is clear, as uncoating, an essential step in the reovirus life cycle, occurs within the endocytic compartment (144). However, endocytic transport may provide other advantages to reovirus particles during infection, including transport to specific intracellular locations and removal of particles from the cell surface to avoid activation of the immune system (60, 85, 86). Reovirus replication takes place within viral factories located in the perinuclear region of the infected cell (19, 100, 101). Transport of ISVPs to this region is likely important, whether the infection is initiated by uncoated particles or virions that become uncoated in the endocytic pathway. Recent work has shown that reovirus virions need to traffic to late endosomes and that some particles are eventually delivered to lysosomes (83). We detected particles in lysosomes when infections were initiated with either virions or ISVPs (Figure 3.15). This result is consistent with data showing that both clathrin-mediated and caveolar pathways can traffic cargo to lysosomes (51, 56, 108).

Our work suggests that reovirus virions, like adenovirus (5, 156) and influenza virus (33, 121, 135), can enter cells by both dynamin-dependent and dynamin-independent endocytic pathways. Our experiments with pathway-

Figure 3.15. Reovirus virions and ISVPs can traffic to the lysosome. Virions or ISVPs were allowed to adsorb to adherent A549 cells at a concentration of 1 x 10^5 particles/cell for 1 hour at 4°C. Warm medium was added and cells were incubated at 37°C for 15 minutes. The infected monolayers were fixed and stained with an anti-T1L antiserum (green), an anti-LAMP1 antibody (red) and DAPI (blue), and cells were visualized by confocal microscopy. The boxed region is magnified in the inset. Arrows indicate colocalization between reovirus and LAMP1.

Figure 3.15

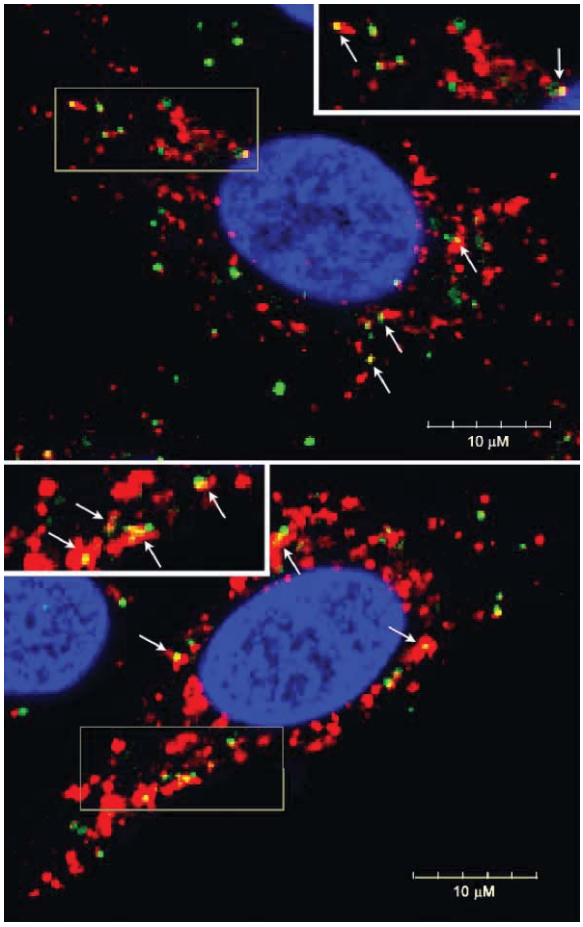

specific ligands argue that multiple dynamin-dependent endocytic pathways and a dynamin-independent pathway function to promote reovirus infection in L929 and A549 cells. In these cell lines, one can demonstrate an effect on viral replication by inhibiting a single pathway; similar results have been reported in other viral systems (46, 78). We showed that MβCD, which extracts membrane cholesterol, inhibits the growth of reovirus virions. Because cholesterol has been implicated in caveolar endocytosis and agents such as MβCD can also affect clathrin-mediated endocytosis at high concentrations (120), we analyzed the uptake of transferrin and cholera toxin subunit B, which depend on the clathrin- and caveolar dynamin-dependent endocytic pathways, respectively. Uptake of these ligands was unaffected by MβCD, which demonstrates that both clathrin-mediated and caveolar pathways are functional and that the requirement for cholesterol in virion entry is not due to effects on clathrin-mediated or caveolar endocytosis. We also found that MβCD treatment had no effect on the binding of reovirus virions or ISVPs to cells and that cholesterol did not promote ISVP formation *in vitro*. These results argue that differences in binding are not responsible for the growth defect seen after virion infection of MβCD-treated cells and that cholesterol is not required for the conversion of virions to ISVPs. Together, these findings suggest that reovirus virions can access a lipid-dependent, dynamin-independent endocytic pathway to establish productive infection. Several such pathways have been described, including

macropinocytosis (96) and the clathrin-independent carrier/GPI-anchored-protein-enriched endosomal compartment (CLIC/GEEC) pathway (73, 124).

Our data demonstrate that reovirus virions and ISVPs use different endocytic pathways for entry. ISVPs enter cells through the caveolar pathway, whereas virions can access clathrin-dependent, caveolar- and dynamin-independent/lipid raft-dependent pathways. These differences may be the consequence of differential exposure of protein motifs on the surface of the two particle types. It has been suggested that exposed Arg-Gly-Asp (RGD) and Lys-Gly-Glu (KGE) motifs on the λ2 protein may enable reovirus to recognize β1 integrins (34). Because they are found on a vertex-associated core protein, these motifs would be present on both virions and ISVPs and their presence cannot explain the differences we found in the entry of virions and ISVPs. Rotavirus, another member of the family *Reoviridae*, engages several integrins for attachment and internalization, including α2β1 and α4β1 (62). We analyzed reovirus capsid sequences for the presence of other potential integrin binding motifs. Our analysis revealed the presence of one such motif (IDSS) in the σ3 protein, which matches the α4β1 binding consensus L/I-D/E-V/S/T-P/S (67, 122). Virion uncoating would lead to the removal of σ3 and the loss of this motif from incoming particles, explaining how virions might activate the clathrin-dependent pathway through integrin binding, while ISVPs would not.

Reovirus is currently undergoing clinical trials as an oncolytic therapy (84, 142, 146, 147, 157). Many recent trials have examined the efficacy of reovirus as

a combination therapy with radiation and chemotherapeutic agents (147). Understanding the cellular pathways used by virions and ISVPs for cell entry is critical to the rational design of combination therapies, because agents that affect critical entry pathways may reduce the efficiency of reovirus as an oncolytic agent. For example, the epidermal growth factor receptor (EGFR) is a target of several chemotherapeutics (114). Inhibition of this receptor reduces caveolin-1 expression (1) and, interestingly, EGFR inhibition can also negatively impact reovirus replication in cell culture (141). Thus, chemotherapeutic agents that target the EGFR might inhibit reovirus entry and infection in patients undergoing combination therapy. As entry is a critical determinant of reovirus oncolysis (2), learning how virions and ISVPs gain access to the cytoplasm is important for the continued development of reovirus as a human cancer treatment.

CHAPTER 4

Cellular Determinants of Reovirus Entry and Infection

I. Introduction

Many viruses, including poxvirus, adenovirus, measles, and reovirus, are being investigated as potential oncolytic therapies (12, 28, 147, 167). To be a safe and effective oncolytic therapy, a virus must preferentially kill tumor cells without affecting normal cells. In several oncolytic models, this is achieved by engineering viral particles that lack genes or proteins needed for replication in primary cells (167) or by integrating chemotherapeutic agents into the viral particle (159). While many viruses have been shown to be effective oncolytic therapies, the use of otherwise pathogenic viruses can cause significant safety concerns, especially in immunocompromised individuals (154). Reovirus is therefore an attractive oncolytic agent, as it has a natural preference for replication in transformed cells and does not cause significant human disease (133, 145, 147).

Early studies linked reovirus infection efficiency and Ras activation (29, 76, 133). However, many cell lines highly susceptible to reovirus infection express low levels of activated Ras (2). It was therefore hypothesized that other mechanisms may play a role in the selectivity of reovirus infection. Later evidence showed that reovirus uncoating and entry was a critical determinant of

infection (2). These studies demonstrated that uncoated reovirus particles could readily infect restrictive cell lines and led to the development of a new model for reovirus oncolysis, in which transformed cells with increased levels of protease expression lead to more efficient reovirus uncoating and infection (2).

While entry is recognized to be a critical step of reovirus infection and a major determinant of oncolysis, many of the cellular proteins that regulate this process remain unknown. Host factors known to regulate reovirus infection have been identified through the use of various chemical inhibitors, knockout cell lines, and dominant negative proteins. However, the interactions between host and viral components are often complex and identifying proteins that impact viral replication with a single gene approach is difficult and time consuming. Several high-throughput methods, including yeast two-hybrid assays and RNA interference (RNAi) screens, have been developed to identify genes involved in virus-host protein interactions. In this chapter, we describe the use of an shRNA screen for high-throughput identification of cellular genes that are involved in lytic reovirus infection. With this method, we identified several host genes that may be involved in reovirus infection and confirmed the importance of one of them, RhoA. This chapter also describes experiments aimed at exploring the role of transformation and other cell type-specific differences in reovirus cell entry.

II. Results

RNAi screening can identify host genes involved in reovirus infection. Since reovirus is being investigated as an oncolytic therapy, we sought to identify cellular determinants that confer susceptibility to reovirus infection. RNAi screening is one approach to identify host determinants that regulate infection, and it has been performed in several viral systems, including influenza and HIV (20, 116, 130). To identify cellular genes that promote reovirus infection, we used a lentiviral shRNA library to knock down cellular gene expression, and we then infected the transduced cells with reovirus. By sequencing the shRNA construct in surviving cells we hoped to identify genes that are normally required for lytic infection by reovirus. To perform this assay (Figure 4.1), 293 cells were infected at an MOI of 0.3 to ensure that each cell was transduced with a single shRNA construct that also expressed a puromycin resistance gene. Forty-eight hours after transduction, cultures were treated with puromycin and surviving cells were infected with reovirus. Individual colonies were cloned after ten days and total cellular DNA was harvested and sequenced to identify the shRNA construct that was expressed.

Since this screen looks for transduced cells that survive lytic reovirus infection, we first determined the amount of reovirus needed to lyse 293 cells in culture. To assess reovirus-induced lysis, 293 cells were transduced with a non-silencing shRNA construct and cells expressing this construct were selected with puromycin. Cultures were infected with reovirus T1L virions at various MOIs and lysis was assessed at various days postinfection. We found that an MOI of

Figure 4.1. Strategy for shRNA screen to identify genes involved in lytic reovirus infection. This figure illustrates the approach to identify shRNA constructs that inhibit reovirus infection. Briefly, 293 cells grown to 30% confluency were infected with lentivirus at a low MOI (0.3) to ensure that each cell was not transduced with more than a single shRNA construct. After transduction, shRNA-expressing cells were selected with puromycin and infected with reovirus T1L virions at an MOI of 10. Surviving colonies were cloned and total DNA was harvested and sequenced to determine which shRNA construct was expressed.

Figure 4.1

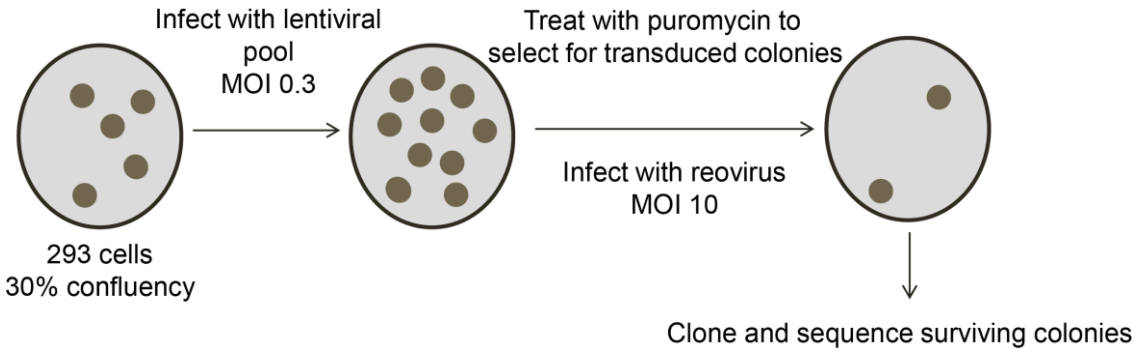
Infect with lentiviral
pool
MOI 0.3
Treat with puromycin to
select for transduced colonies
Infect with reovirus
MOI 10
293 cells
30% confluency
Clone and sequence surviving colonies

greater than 5 could successfully lyse all cells in the culture, with the rate of lysis plateauing at an MOI of 10 (Table 4.1A). This result shows that reovirus can successfully lyse lentivirus-transduced cells for use in screening.

We next wanted to use this screen to identify a set of host genes involved in reovirus infection. We transduced 293 cells with pooled lentiviral stock containing approximately 6,000 gene targets per pool. After puromycin selection, shRNA-expressing cells were infected with reovirus T1L virions at an MOI of 10. Colonies that survived infection were cloned and total DNA was harvested and sequenced to identify the shRNA that was expressed in the surviving 293 cells. In this preliminary screen, we screened approximately 2,400 different genes and identified six shRNA constructs that inhibited reovirus-induced lysis (Table 4.1B). Four of these genes are known to be involved in cellular transformation (MCF2L2, EP300, TOM1, CCND1) and one gene is involved in cell metabolism and antiviral drug resistance (DCK) based on their descriptions in the GeneCards database (127). The final gene identified in the screen, RhoA, is known to be important for endocytosis (39). Because cell entry is only one step of the viral life cycle, it is likely that this screen identifies a larger number of genes involved in other steps of viral replication. However, the identification of a gene involved in endocytosis in this preliminary assay suggests that shRNA-based screening can also identify host genes that promote reovirus entry.

RhoA is important for infection by reovirus virions and ISVPs. Because of our interest in viral entry, we performed additional experiments to

Table 4.1. Reovirus T1L can lyse 293 cells in culture. 293 cells seeded in 10 cm culture trays were infected with reovirus T1L virions at the indicated MOIs. Cultures were checked daily for the indication of cytopathic effects and medium was changed every three days. The table indicates the number of days post-infection that no viable cells were noted.

Table 4.2. shRNA constructs that inhibit reovirus infection. 293 cells were transduced with pooled shRNA-expressing lentivirus. Transduced cells were selected with puromycin and infected with reovirus T1L virions at an MOI of 10. Colonies that survived infection were cloned and total DNA was harvested and sequenced. shRNA constructs identified by sequencing along with their function as indicated by the GeneCards database are listed.

Table 4.1

MOI	Date of Plate Clearing
3	> Day 20
5	Day 16
10	Day 9
15	Day 9

Table 4.2

Gene	Function
RhoA	GTPase involved in clathrin-independent endocytosis
MCF2L2	Regulator of Rho-dependent signal transduction
Deoxycitidine Kinase (DCK)	Deficiency associated with resistance to antiviral agents
EP300	E1A binding protein
TOM1	Target of v-myb oncogene
CCND1	Cyclin D1

confirm the role of RhoA in reovirus infection. RhoA is a GTPase that interacts with Rac1 and Cdc42 to promote clathrin-independent endocytosis (39). Studies have shown that RhoA is important for infection by avian reovirus (66), but its role in mammalian reovirus infection is unknown. To assess the effect of RhoA on reovirus infection, 293 cells were transduced with one of several shRNA constructs directed against RhoA. After puromycin selection, transduced cells were infected with reovirus T1L virions at an MOI of 15 and infection was analyzed by immunoblotting for the reovirus non-structural protein μNS. At 24 hpi (96 hours post-transduction), we found that both RhoA expression and reovirus viral protein expression were reduced in hairpin-expressing cells relative to cells expressing a nonsilencing control plasmid (Figure 4.2). These data confirm that RhoA is important for reovirus infection and are consistent with findings described in Chapter 3, which reveal that that reovirus virions and ISVPs can use clathrin-independent endocytosis for infection.

Reovirus uses different endocytic pathways to infect transformed cells. Since viral entry is an important determinant of reovirus oncolysis, we asked if specific endocytic pathways promote reovirus infection in transformed cell lines. To explore this question, we analyzed reovirus infection in rat embryo fibroblasts (CREF) and a paired cell line that expresses constitutively-activated Ras (Ras-CREF). Cells were treated with various inhibitors of endocytosis and infected with reovirus T1L virions. At 18 hpi, the cells were fixed and stained with antiserum specific for reovirus and infection was quantified by indirect

Figure 4.2. RhoA is important for reovirus infection. 293 cells were transduced with lentivirus containing shRNA constructs specific for human RhoA. Forty-eight hours after transduction, cells expressing shRNA constructs were selected with puromycin and forty-eight hours later were infected with reovirus T1L virions at an MOI of 15. Infected cell lysates were analyzed at 24 hpi for μNS and RhoA expression by immunoblotting. Band intensities of μNS, RhoA and β-actin were quantified to determine the relative μNS expression level of each sample. The values in the graph represent the relative μNS or RhoA expression level compared to vehicle-treated cells. The shRNA 2 sample is the construct initially identified by the shRNA screen.

Figure 4.2

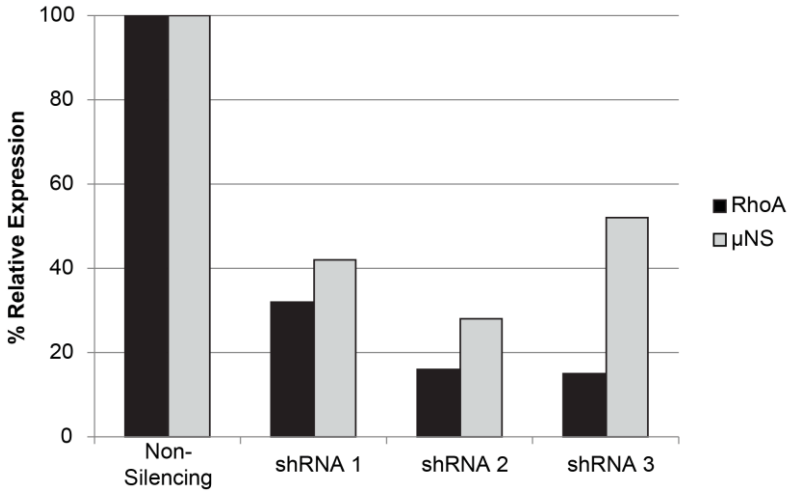
100
80
60
40
20
0
% Relative Expression
Non-Silencing
shRNA 1
shRNA 2
shRNA 3
RhoA
µNS

immunofluorescence. Our results revealed that chlorpromazine, which inhibits clathrin-mediated endocytosis, and genistein, which inhibits caveolar endocytosis, both decreased viral infectivity in the non-transformed cell line (Figure 4.3). As expected, dynasore, which inhibits both of these pathways, also reduced viral infection in the non-transformed CREF cells. We also analyzed the effect of MβCD, which inhibits lipid-dependent entry pathways, and found that this agent inhibited infection by reovirus virions in non-transformed CREF cells. These results parallel those in murine L929 cells. Interestingly, chlorpromazine had no effect on reovirus infection in transformed Ras-CREF cells and the effect of dynasore was reduced (Figure 4.3). Taken together, these data suggest that reovirus does not use clathrin-mediated endocytosis to infect transformed CREF cells, but can take advantage of caveolar and lipid raft-mediated endocytosis to infect these cells.

Many transformed cells are known to express high levels of proteases, some of which can be secreted and lead to extracellular virion uncoating (137). Since ISVPs are not internalized by clathrin-mediated endocytosis, extracellular conversion of virions to ISVPs would result in a chlorpromazine-resistant phenotype. To determine if ISVPs are generated extracellularly in Ras-CREF cells, reovirus virions were adsorbed to CREF and Ras-CREF cells, the infections were incubated at 37°C for 10 minutes, and the cultures were then subjected to three freeze/thaw cycles to release virus. Total virus was used as inoculum in a single cycle growth experiment in L929 cells treated with the

Figure 4.3. Reovirus infects transformed and non-transformed rat embryo fibroblasts through different endocytic pathways. CREF and Ras-CREF cells seeded in 8-well CultureSlides were treated with dynasore, chlorpromazine, genistein, or MβCD for 1 h and then incubated at 4°C for 20 m. Reovirus T1L virions were adsorbed at an MOI of 20 and fresh medium with or without inhibitor was added back to the cultures. After 24 hours, cells were fixed and stained with an antiserum specific for the reovirus non-structural protein μNS and infected cells enumerated by indirect immunofluorescence. The graph represents the percentage of infected cells compared to an untreated control in three similarly confluent fields of view.

Figure 4.3

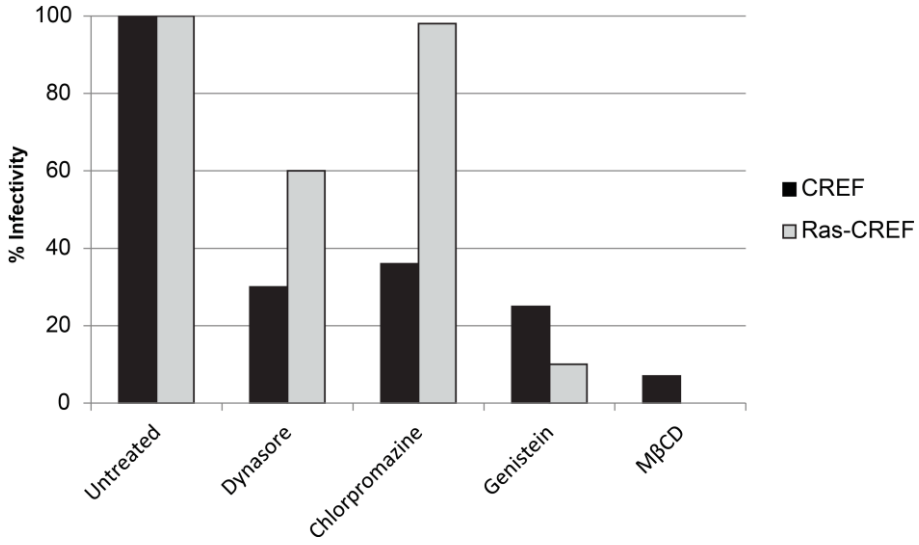
100
80
60
40
20
0
% Infectivity
Untreated
Dynasore
Chlorpromazine
Genistein
MβCD
CREF
Ras-CREF

cysteine protease inhibitor E-64 which blocks uncoating and inhibits the growth of reovirus virions (Figure 4.4). If ISVPs were generated extracellularly in Ras-CREF cells, we would expect these particles to replicate in E-64-treated L929 cells. When we analyzed viral yields at 24 hpi, we found that the growth of reovirus particles adsorbed to CREF and Ras-CREF cells was equivalent in E-64-treated and untreated cells (Figure 4.5). This demonstrates that ISVPs are not generated in the Ras-transformed CREF cells and supports our hypothesis that reovirus enters transformed and nontransformed cells through different endocytic pathways.

Reovirus infection of transformed colorectal cells is dynamin-independent. Reovirus is currently being investigated as a therapy for several human cancers, including those of the colon, breast, lung, and prostate (58, 63, 104). While our work demonstrates that reovirus virions and ISVPs can both infect murine L929 cells through dynamin-dependent endocytosis, we wanted to investigate whether reovirus is internalized by dynamin-dependent pathways in a more clinically relevant human cell line. For these experiments, we chose Caco-2, a polarizable cell line isolated from human colorectal cancer (43). To assess the importance of dynamin-dependent endocytosis, Caco-2 cells were grown on glass CultureSlides, treated with dynasore, and infected with reovirus T1L ISVPs at an MOI of 100. At 20 hpi, cells were fixed and stained with antiserum specific for reovirus T1L and infection was quantified by indirect immunofluorescence. We found that dynasore had no effect on reovirus infection in Caco-2 cells

Figure 4.4. Experimental approach used to determine if Ras-CREF cells generate ISVPs extracellularly. Reovirus T1L virions were adsorbed to CREF or Ras-CREF cells seeded in a 60mm dish for 1 hr at 4°C. The cultures were washed to remove unbound virus, warm medium was added back, and the cultures were incubated at 37°C for 10 min. Cultures were subjected to three freeze/thaw cycles, total virus was collected, and used as inoculum for a growth experiment in L929 cells pre-treated with E64. Viral yields were quantified by plaque assay in L929 cells.

Figure 4.4

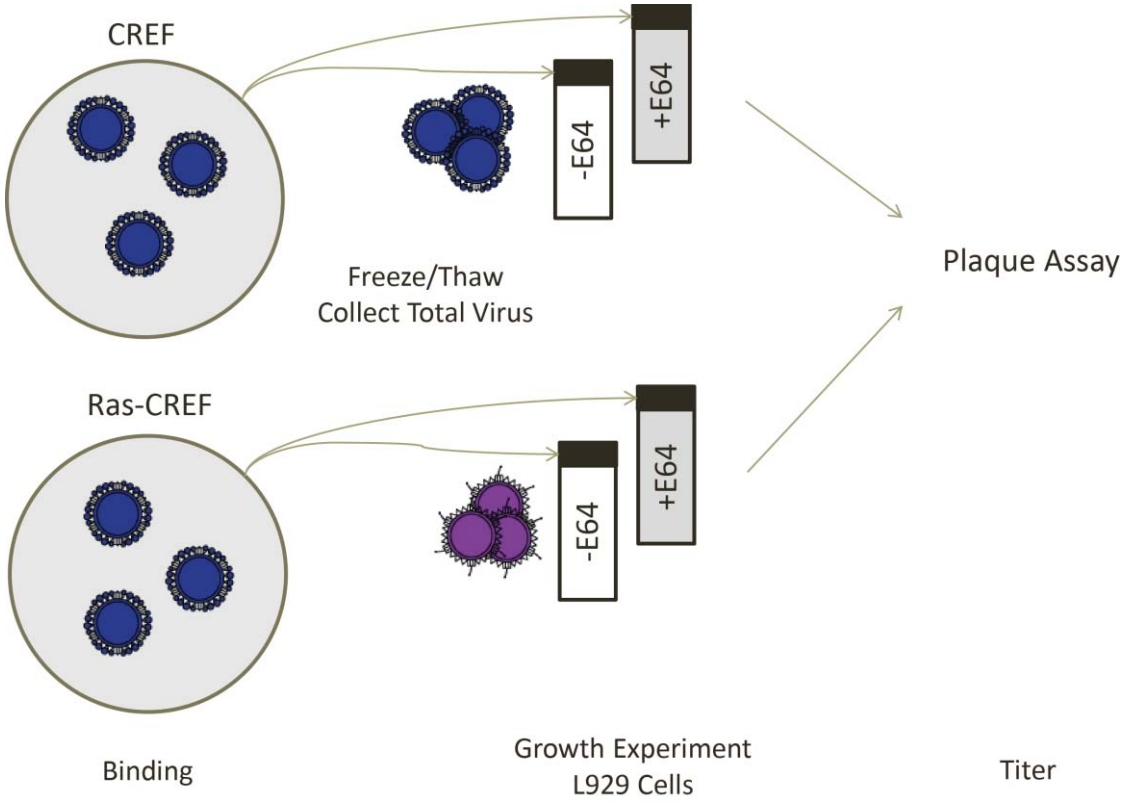
CREF
+E64
-E64
Freeze/Thaw
Collect Total Virus
Plaque Assay
Ras-CREF
+E64
-E64
Binding
Growth Experiment
L929 Cells
Titer

Figure 4.5. Reovirus binding to Ras-CREF cells does not convert virions to E-64-resistant particles. L929 cells pre-treated with E-64 were infected with inoculum collected from CREF and Ras-CREF cells adsorbed with reovirus virions as described previously. At 24 hpi, total virus was collected and viral yields determined by plaque assay on L929 cells.

Figure 4.5

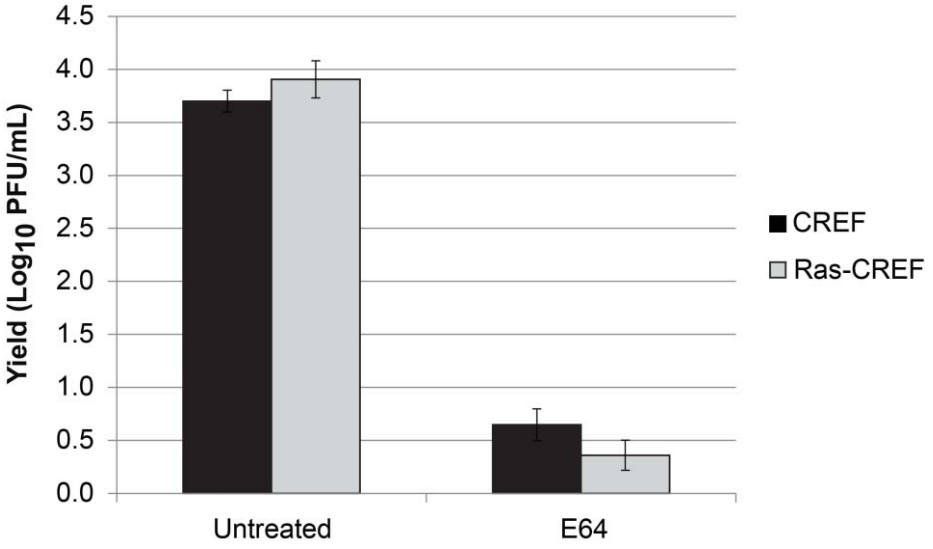
4.5
4.0
3.5
3.0
2.5
2.0
1.5
1.0
0.5
0.0
Yield (Log10 PFU/mL)
Untreated
E64
CREF
Ras-CREF

(Figure 4.6). This finding suggests that reovirus infection of cells derived from human colorectal adenocarcinoma is dynamin-independent.

III. Discussion

Unlike many other oncolytic viruses, reovirus is naturally oncolytic, requires no engineering to target tumor cells, and is otherwise nonpathogenic (147). Therefore, determining which host factors promote reovirus replication in transformed cells is important for maximizing the potential of reovirus therapy. For example, tumor tissue could be screened for the upregulation of genes that promote reovirus infection to select cancers that are most susceptible to reovirus infection. While single-gene approaches have traditionally been used to learn about virus-host interactions, these methods are unable to quickly identify a large number of target genes. Our pilot study suggests that shRNA-based screening can be used to identify host genes that are important for lytic infection by reovirus. While this method is not specific for any particular stage of the viral life cycle, we identified genes that encode proteins predicted to affect several steps of the viral life cycle, including entry and protein synthesis. Follow-up experiments were done to confirm that RhoA promotes reovirus infection. RhoA regulates signal transduction related to clathrin-independent endocytosis (39) and a recent report has shown that it is involved in the redistribution of the reovirus cellular receptor JAM-A from tight junctions (140). RhoA silencing

Figure 4.6. Dynasore does not inhibit reovirus infection of Caco-2 cells. Caco-2 cells seeded in 8-well CultureSlides were treated with vehicle (DMSO) or dynasore for 1 h and then incubated at 4°C for 20 m. Reovirus T1L virions were adsorbed at an MOI of 20 and fresh medium with or without inhibitor was added back to the cultures. After 24 hours, cells were fixed and stained with an antiserum specific for the reovirus non-structural protein μNS and infected cells enumerated by indirect immunofluorescence. The graph represents the number of infected cells compared to an untreated control in three similarly confluent fields of view.

Figure 4.6

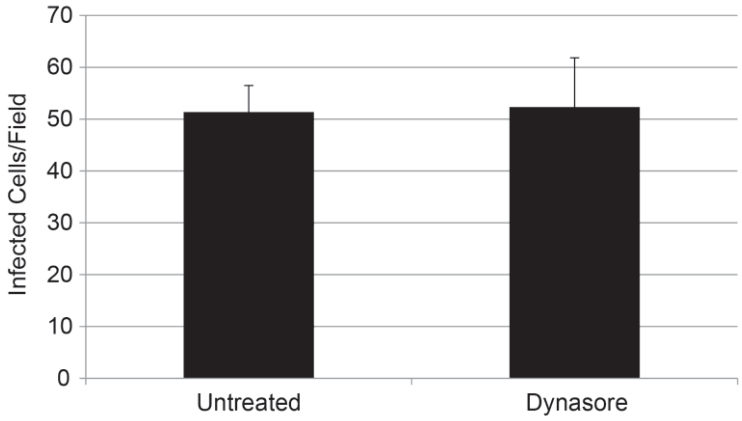
70
60
50
40
30
20
10
0
Infected Cells/Field
Untreated
Dynasore

inhibited infection by both virions and ISVPs. This result is consistent with our finding that both intact virions and ISVPS particles are internalized by clathrin-independent endocytosis. In the future, our laboratory intends to use this shRNA screening approach to identify other genes involved in reovirus infection.

We were interested in the effects of transformation on reovirus cell entry, and over the course of our studies, analyzed the importance of particular endocytic pathways in a variety of cell lines. In experiments described in Chapter 3, we demonstrated that reovirus ISVPs can use caveolar endocytosis, which is dynamin-dependent, to enter and infect host cells. Previous studies demonstrated that reovirus can infect Caco-2 cells, which are derived from human adenocarcinoma and express low levels of caveolin (43, 102). We therefore wanted to learn whether ISVPs used a different mechanism to enter these cells. We found that ISVPs could infect Caco-2 cells through a dynamin-independent mechanism. Our results do not distinguish between the possibility that ISVPs infect by a dynamin-independent endocytic pathway such as macropinocytosis or instead enter Caco-2 cells by direct membrane penetration.

Transformation is known to alter the activity of endocytic pathways within cells. Single changes in endocytic activity may alter the effectiveness of reovirus oncolysis, we also assessed whether reovirus entry into non-transformed and Ras-transformed cells differed. We found that reovirus uses different endocytic pathways to infect Ras-transformed CREF and non-transformed CREF cells. Clathrin-mediated endocytosis is important for the infection of non-transformed

CREF cells, but inhibition of this pathway had no effect on reovirus infection in the Ras-transformed cell line. Due to the diversity of cell types that can be infected by reovirus (48), it is likely that different pathways are used to enter and infect cells in different tissues. These findings highlight the importance of using multiple cell types in the study of reovirus infection.

CHAPTER 5

Reovirus Infection and Transcytosis from the Apical Membrane of Polarized Epithelial Cells

I. Introduction

Reovirus is a nonenveloped, double-stranded RNA virus that commonly infects humans, but is rarely pathogenic in adults (145). In cell culture, infection is initiated by interactions between the cell attachment protein σ1 and the cellular receptor, junctional adhesion molecule A (JAM-A) (10, 75). Virions then interact with β-integrins and are internalized by dynamin-dependent and –independent endocytic pathways (34, 81). Once inside the endosomal compartment, proteases remove the outer capsid protein σ3 to form intermediate subviral particles (ISVPs), which gain access to the cytoplasm (15, 72, 144). When reovirus infects hosts through the enteric tract, secreted pancreatic serine proteases form ISVPs extracellularly (11, 13).

Experiments in mouse and rabbit models of reovirus infection have shown that within the intestinal epithelium, reovirus binds to microfold (M) cells, which endocytose reovirus particles from the luminal surface and deliver them to the basolateral membrane (59, 160, 162). However, studies using polarized human Caco-2 cells, which resemble distal ileal enterocytes, revealed that reovirus T1L particles bind and are internalized at the apical surface of human absorptive

enterocytes (3). Attachment of ISVPs to polarized intestinal epithelial cells is believed to involve recognition of α2-3-linked sialic acids, as JAM-A is localized to tight junctions (59). In addition, neuraminidase treatment of these cells, which cleaves sialic acid, inhibits reovirus attachment (59). While it was previously known that reovirus could attach to polarized human enterocytes, it was unknown whether these cells could be productively infected from the apical surface. In this study, we investigated whether absorptive enterocytes can be productively infected as a pathway for penetration of the mucosal membrane.

II. Results

Reovirus infection of polarized Caco-2 cells does not require JAM-A. To understand the molecular mechanisms that promote reovirus infection of intestinal tissue, we used polarized Caco-2 cells grown on transwell supports. Although reovirus T1L can bind to the apical surface of polarized Caco-2 cells (3), the reovirus receptor JAM-A is believed to be inaccessible from the apical surface of polarized epithelial cells (40, 59). To determine if JAM-A is important for reovirus infection of polarized enterocytes, we first asked whether it co-localizes with reovirus during attachment. Polarized Caco-2 cells were adsorbed with reovirus virions at the apical surface for 1 hour (h) and the cultures were immediately fixed and stained with an antibody directed against JAM-A and anti-reovirus antiserum to detect reovirus particles. When viewed from the top (Figure

5.1A, left panel), JAM-A could be found localized to the intracellular junctions, while viral particles were localized on the cell surface. Single image slices from the vertical and transverse planes (Figure 5.1A, right panel) revealed that JAM-A is primarily distributed to the sub-apical membrane and intracellular junctions in the polarized Caco-2 cultures. While a small amount of JAM-A was found at the apical surface of the cultures, there was little colocalization of JAM-A and reovirus immediately after adsorption.

To determine if JAM-A is functionally important for reovirus infection of enterocytes, polarized Caco-2 cells were incubated with the JAM-A antibody for 45 minutes prior to infection. At 18 hours postinfection (hpi), we stained the cultures with an antiserum directed against the reovirus non-structural protein μNS and quantified infection by indirect immunofluorescence. This analysis revealed that reovirus was capable of productively infecting polarized Caco-2 cells when adsorbed to the apical membrane; however, pretreatment of the polarized culture with JAM-A antibody had no effect on the number of infected cells in each field ($p > 0.66$) (Figure 5.1B). Consistent with published work (10), pretreatment of non-polarized Caco-2 cells with anti-JAM-A antibody significantly reduced the number of reovirus-infected cells in the culture ($p < 0.015$) (Figure 5.1C). These data suggest that reovirus engages a receptor other than JAM-A for attachment and infection of polarized Caco-2 cell cultures.

Reovirus infection of polarized intestinal epithelial cells is dynamin-independent. Recent work from our lab revealed that both intact virions and

Figure 5.1. Reovirus does not bind to JAM-A in polarized Caco-2 cells. A) Polarized Caco-2 cells grown on transwell supports were adsorbed with reovirus T1L at a concentration of 1 x 10^5 particles/cell 21 days after seeding. Cells were fixed immediately after adsorption, stained with T1L-specific antiserum (green) and anti-JAM-A antibody (red), and imaged by confocal microscopy. The left panel represents an axial, maximum intensity projection. The right panel is an axial and transverse slice from the same set of confocal images. Scale bars represent 10 μM (left) and 15 μM (right). B) Polarized Caco-2 cells were pre-incubated with a JAM-A specific antibody on the apical membrane for 45 min at room temperature and infected with reovirus T1L at an MOI of 100. At 24 hpi, the cells were stained with antiserum directed against the reovirus nonstructural protein μNS and visualized by indirect immunofluorescence. Infection was scored by counting the number of infected cells in three similarly confluent fields of view. C) Non-polarized Caco-2 cells were treated with a JAM-A specific antibody, infected, and stained as described above. The graph represents the percentage of infected cells in three independent fields of view.

Figure 5.1

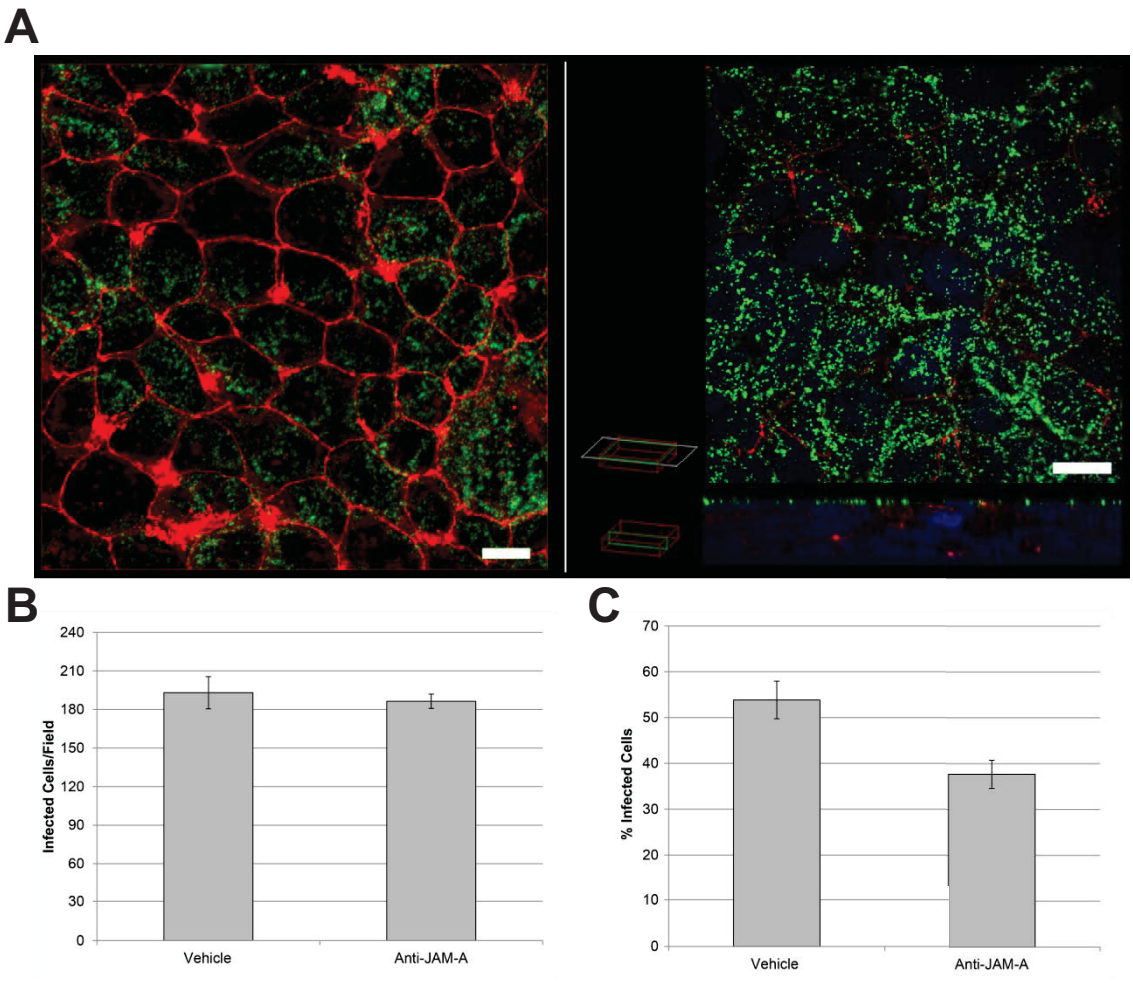
A
B
Infected Cells/Field
240
210
180
150
120
90
60
30
0
Vehicle
Anti-JAM-A
C
% Infected Cells
70
60
50
40
30
20
10
0
Vehicle
Anti-JAM-A

uncoated particles (ISVPs) can enter cultured cells through dynamin-dependent endocytic pathways (131). To assess whether reovirus infection of polarized epithelium is dynamin-dependent, Caco-2 cells were grown on transwell supports and treated apically with 100 μM dynasore to inhibit dynamin-dependent endocytosis (80, 148). Analysis of transferrin uptake revealed that the inhibitor effectively reduces clathrin-dependent endocytosis at this concentration (Figure 5.2A). Since reovirus virions are uncoated extracellularly within the lumen of the intestinal tract, dynasore-treated and control cultures were infected with T1L ISVPs at an MOI of 100. At 18 hpi, cultures were fixed and stained with anti-reovirus antiserum and visualized by confocal microscopy. Axial and transverse maximum intensity projections showed a similar number of cells with diffuse cytoplasmic staining localized to the apical surface of the culture in untreated and dynasore-treated cells (Figure 5.2B). Since these cells did not have contact with the transwell support, these data suggest that cells are infected from virus applied at the apical surface. We also assessed viral titers after infection of polarized Caco-2 cultures with either virions (Figure 5.3A) or ISVPs (Figure 5.3B), and observed similar titers in dynasore- and vehicle-treated cells. Together, these results reveal that reovirus can infect polarized enterocytes from the apical surface but that dynamin-dependent mechanisms are not required.

Reovirus is transported from the apical to basolateral membrane of Caco-2 cells. Evidence suggests that reovirus is transported across the intestinal epithelium by M cells in murine models of infection (161, 162), but

Figure 5.2. Reovirus infects apical cells in polarized cultures. A) Polarized Caco-2 cells were treated with vehicle or dynasore for 1 h and then incubated at 4°C for 20 m. Transferrin (green) was adsorbed to the apical membrane for 1 h and the cultures washed with ice cold PBS. Warm medium with or without inhibitor was added and the cultures were incubated at 37°C for 10 minutes. Cells were fixed, stained with Texas Red-conjugated phalloidin (red) to label actin and uptake was visualized by confocal microscopy. Scale bars represent 10 μM. B) Polarized Caco-2 cells were treated as described above and adsorbed with reovirus T1L ISVPs at an MOI of 100. Eighteen hpi, cells were fixed and stained with Texas Red-conjugated phalloidin (red) and antiserum specific for reovirus T1L (green), and infection was visualized by confocal microscopy. Scale bars represent 20 μM.

Figure 5.2

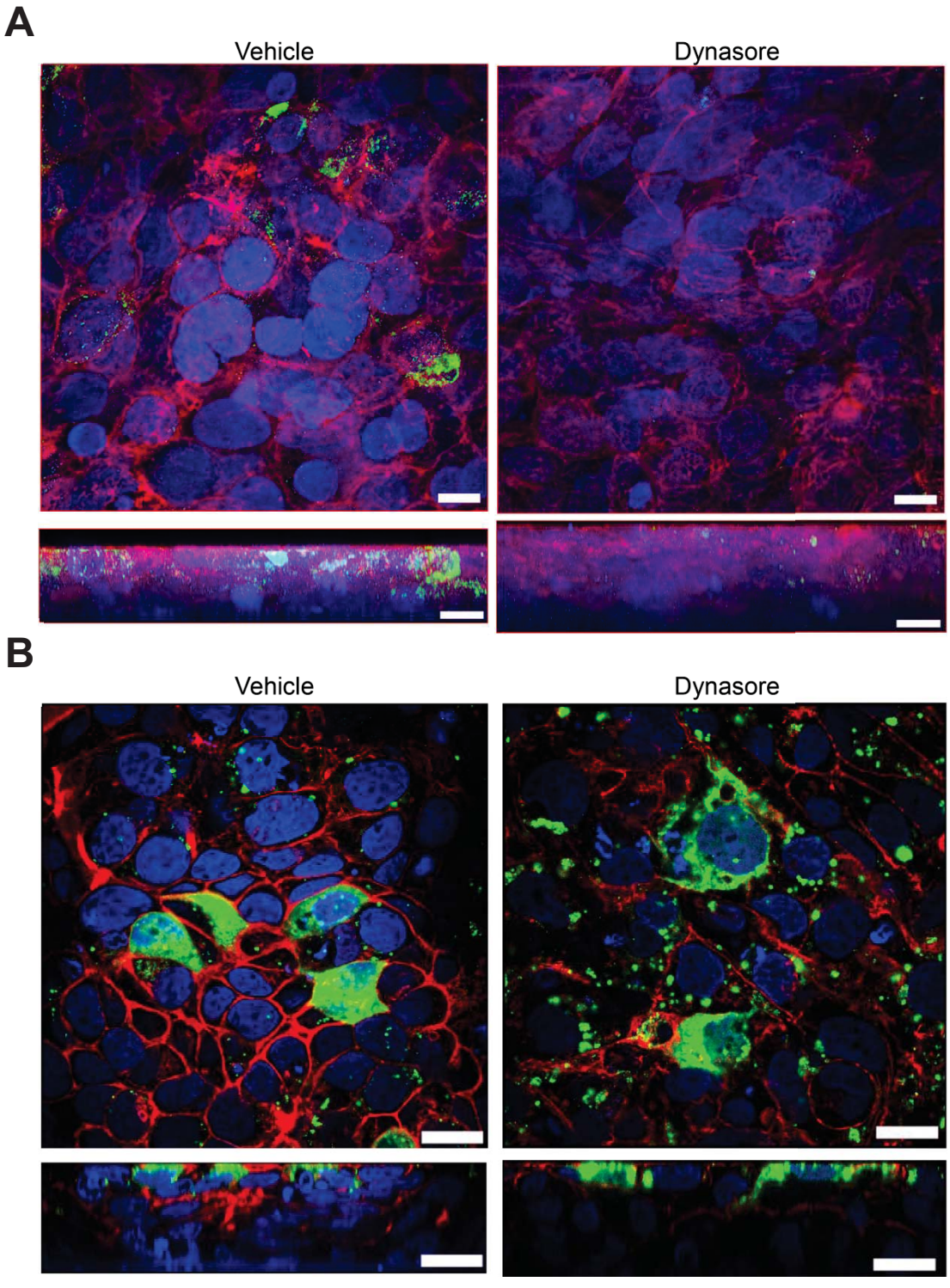

Figure 5.3. Reovirus infection of polarized Caco-2 cells is dynamin-independent. Polarized Caco-2 cells were treated and infected with T1L virions (A) or ISVPs (B) as described above, using an MOI of 100. At 18 hpi, cells were subjected to three cycles of freezing and thawing, and viral titers were determined by plaque assay on L929 cells. Values represent the mean (± SE) of triplicate samples.

Figure 5.3

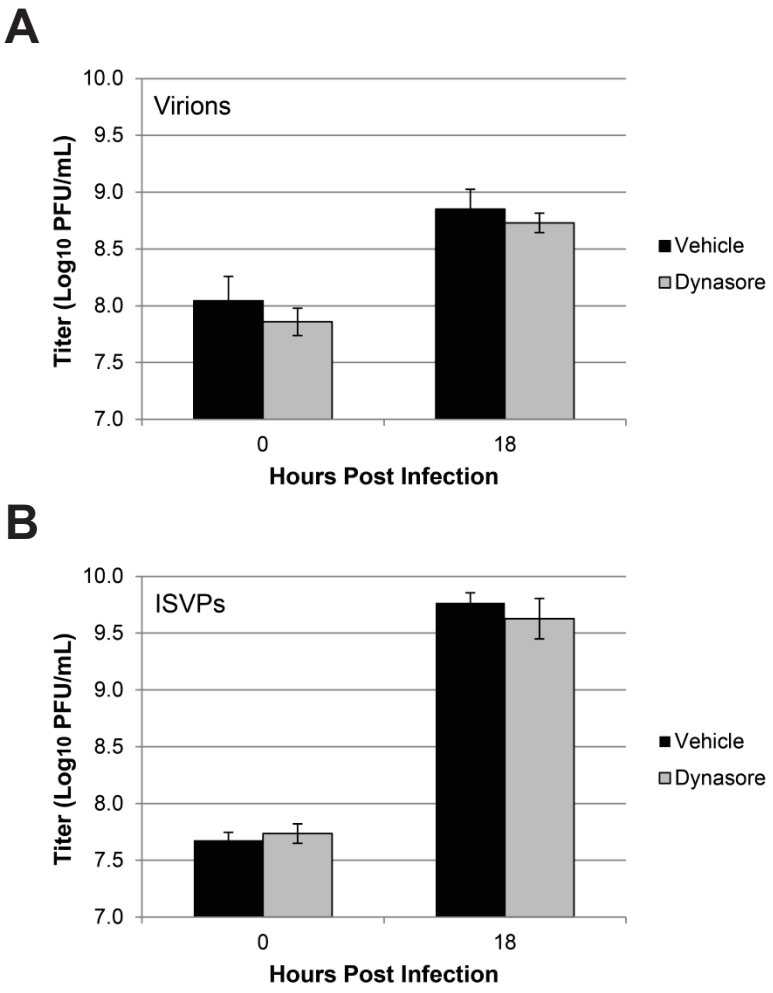
A
Virions
Titer (Log10 PFU/mL)
10.0
9.5
9.0
8.5
8.0
7.5
7.0
0
18
Hours Post Infection
Vehicle
Dynasore
B
ISVPs
Titer (Log10 PFU/mL)
10.0
9.5
9.0
8.5
8.0
7.5
7.0
0
18
Hours Post Infection
Vehicle
Dynasore

absorptive enterocytes are also capable of transcytosis (21, 87, 151). To determine if reovirus can be transcytosed by absorptive enterocytes, reovirus particles were adsorbed to the apical surface of polarized Caco-2 cultures for 1 hour at 4°C. Warm medium was added to the cultures, and they were incubated at 37°C for 30 minutes before being fixed, stained with anti-reovirus antiserum, and visualized by confocal microscopy. Shortly after adsorption with ISVPs, reovirus particles could be found from the apical plane to the basolateral plane of the cultures (Figure 5.4A). To determine if transcytosis delivers infectious particles to the basolateral surface of the epithelial cultures, we collected medium from the basolateral compartment of the transwells at various times postinfection, and determined the viral titer. As expected, no virus was recovered from the basolateral compartment immediately following adsorption, but infectious particles were recovered at 4, 8, 12 and 18 hpi (Figure 5.4B). To confirm that tight junctions remained intact in our cultures, we measured transepithelial resistance (TER) when the cultures were being established, and also after infection. The TER remained above 500Ω throughout the experiment (18 h) in the presence of reovirus particles (Figure 5.5), arguing that infection did not disrupt tight junctions. Together, these findings demonstrate that while reovirus can infect cells at the apical surface, infectious reovirus particles can also be transcytosed across polarized human intestinal epithelial cultures.

Reovirus transcytosis across polarized absorptive enterocytes is dynamin-dependent. Although our results indicate that the apical infection of

Figure 5.4. Caco-2 cells transcytose reovirus particles. A) Polarized Caco-2 cells were adsorbed with reovirus ISVPs at a concentration of 1 x 10^5 particles/cell at 4°C for 1 hour. Warm medium was added and the cultures were incubated at 37°C. At 30 min, cells were fixed and stained with Texas Red-conjugated phalloidin (red) and anti-reovirus antiserum (green). Uptake of reovirus particles was visualized by confocal microscopy. Scale bar represents 5 μM. B) Polarized Caco-2 cells were adsorbed with reovirus ISVPs as described above. At the indicated times following adsorption, transwell supports were removed and medium from the basolateral compartment was collected. Viral titers were determined by plaque assay on L929 cells.

Figure 5.4

A

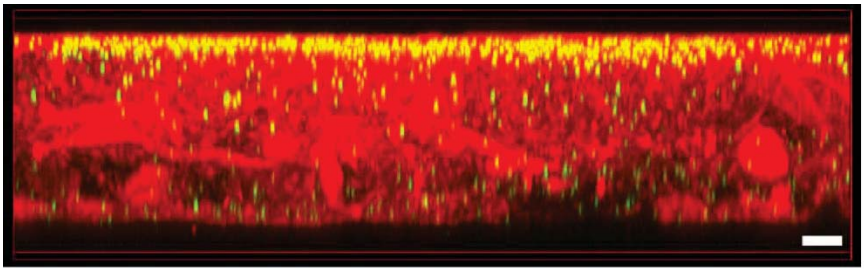

B

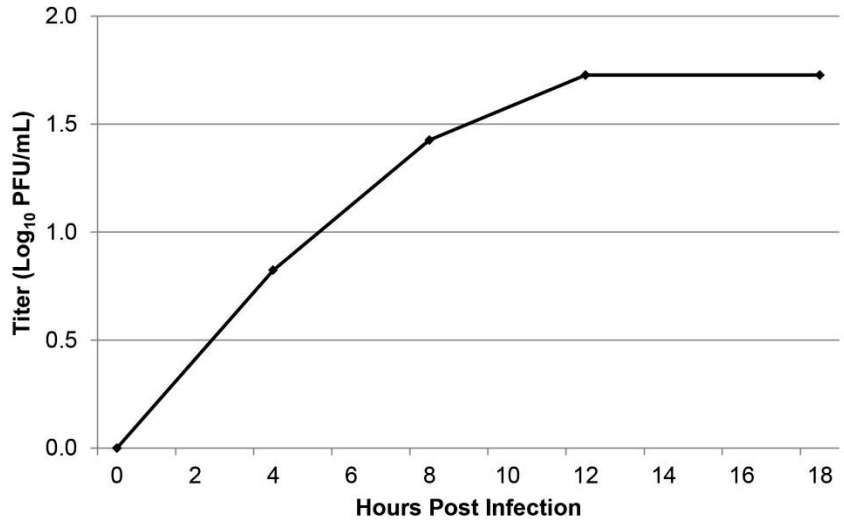
2.0
1.5
1.0
0.5
0.0
Titer (Log10 PFU/mL)
0
2
4
6
8
10
12
14
16
18
Hours Post Infection

Figure 5.5. Reovirus binding and infection do not disrupt tight junction integrity. Caco-2 cells were seeded on transwell supports at a density of 2 x 10^4 cells/well. At the indicated times after seeding, the TER was measured from two separate samples. After 21 days, the cultures were infected with reovirus ISVPs at a concentration of 1 x 10^5 particles/cell and TER measurements were taken from cultures harvested at 1 hpi (solid line) or 18 hpi (dashed line).

Figure 5.5

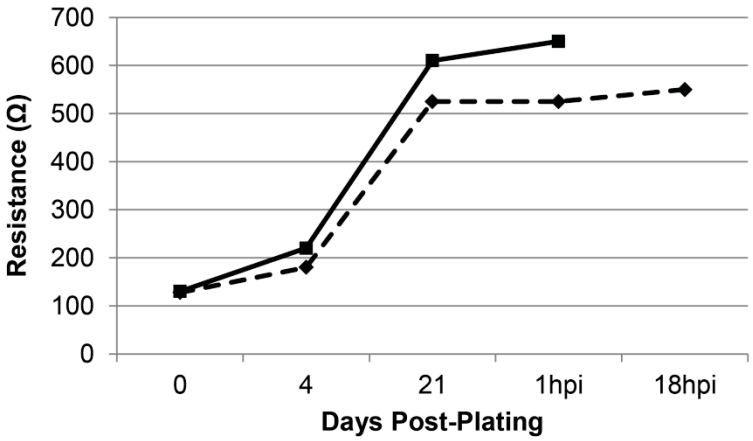
700
600
500
400
300
200
100
0
Resistance (Ω)
0
4
21
1hpi
18hpi
Days Post-Plating

polarized Caco-2 cells is dynamin-independent, dynamin is known to play an important role in transcytosis. We confirmed that our Caco-2 cultures were capable of dynamin-dependent transcytosis by analyzing the transport of HRP (22). In Caco-2 cells pretreated with dynasore, the basolateral transport of HRP was reduced by approximately 50% (Figure 5.6). This result is consistent with published work using dominant-negative dynamin (22). To determine if dynamin-dependent uptake is responsible for the transcytosis of reovirus particles in polarized cultures we pretreated polarized Caco-2 cells with 100 μM dynasore and adsorbed them with reovirus virions or ISVPs for 1 h at 4°C. Warm medium with or without inhibitor was added to the cultures and the cells were incubated at 37°C. At 1 hpi, the cultures were fixed and stained with antiserum specific for reovirus. In vehicle-treated samples, confocal imaging revealed a large percentage of reovirus particles at the basolateral surface of the transwell support. In contrast, in the dynasore-treated cultures, most particles remained localized at the apical membrane (Figure 5.7). Thus, while reovirus infection of polarized Caco-2 cultures is dynamin-independent, these data show that dynamin-dependent uptake delivers reovirus particles to the basolateral membrane of the cultures.

III. Discussion

Figure 5.6. Dynasore effectively blocks transcytosis in Caco-2 cells. Polarized Caco-2 cells were treated with vehicle (DMSO) or dynasore for 1 hour at 37°C. Fresh medium containing horseradish peroxidase (HRP) and either vehicle or dynasore was added to the cells and the cultures were incubated at 37°C. After 30 minutes, transwell supports were removed and the medium from the basolateral compartment was serially diluted. The amount of HRP in the basolateral chamber was calculated by adding the substrate 3,3',5,5'-tetramethylbezidine (TMB) and measuring absorbance at 450 nm.

Figure 5.6

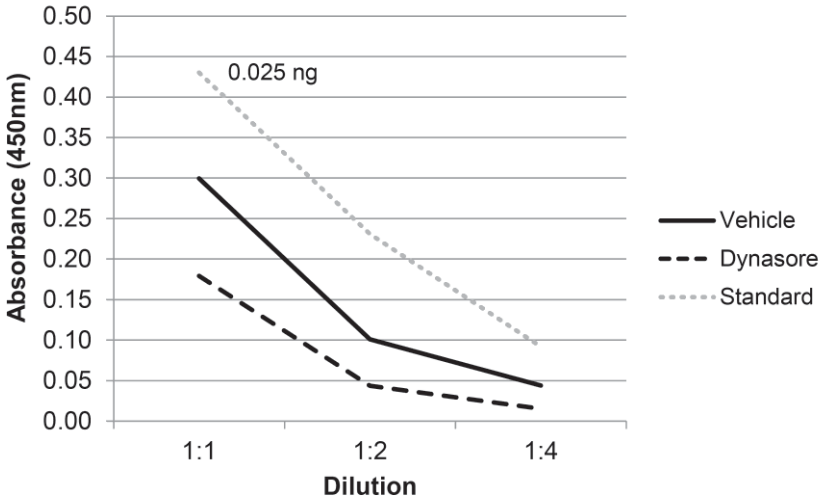
0.50
0.45
0.40
0.35
0.30
0.25
0.20
0.15
0.10
0.05
0.00
Absorbance (450nm)
0.025 ng
1:1
1:2
1:4
Dilution
Vehicle
Dynasore
Standard

Figure 5.7. Transcytosis of reovirus virions and ISVPs is dynamin-dependent. Polarized Caco-2 cells were treated as described above and then equilibrated at 4°C. Cultures were adsorbed with reovirus virions or ISVPs at a concentration of 1 x 10^5 particles/cell. After 1 h, warm medium with vehicle or inhibitor was added and the cultures were incubated at 37°C. At 1 hpi, cells were fixed and stained with Texas Red-conjugated phalloidin (red) and anti-reovirus antiserum (green). Transcytosis was visualized by confocal microscopy. Scale bars represent 10 μM.

Figure 5.7

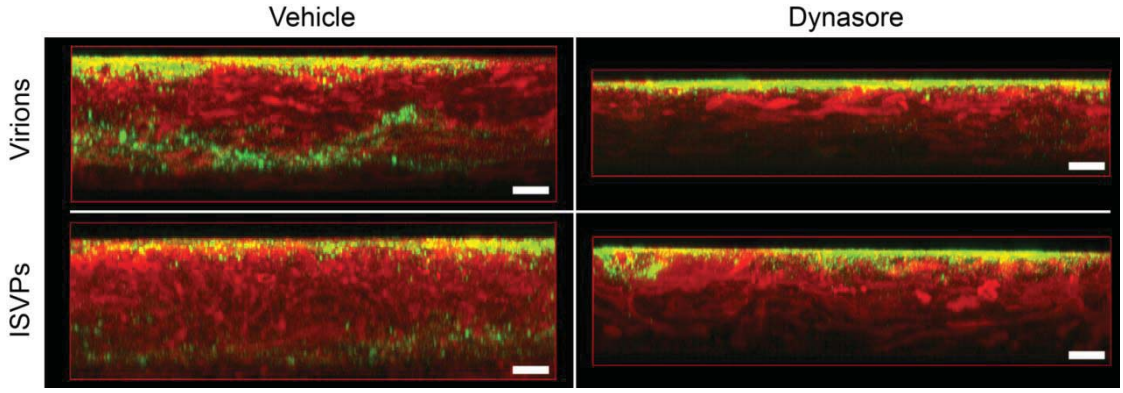

In this study, we have demonstrated that reovirus can infect polarized Caco-2 cells from the apical membrane independent of JAM-A. This finding extends prior work on reovirus interactions with intestinal epithelial cells which showed that although reovirus T1L is unable to bind to the apical surface of murine enterocytes, it can interact with the apical surface of human enterocytes (3, 155). Consistent with other reports (10), we found that treatment of non-polarized Caco-2 cells with an antibody specific for JAM-A inhibits infection. However, our results reveal that JAM-A blockade does not inhibit reovirus infection in polarized Caco-2 cells. In these cultures, we demonstrated that JAM-A localizes to sub-apical surfaces. Together, these findings suggest that human enterocytes express a receptor other than JAM-A on the apical surface that is not found on murine enterocytes and can promote T1L reovirus infection. Other studies in Caco-2 cells suggest that this receptor may be a glycoconjugate containing α2,3-linked sialic acid, as neuraminidase treatment has been reported to inhibit reovirus binding to the apical membrane (40). Prior reports using type 3 reovirus in a model of polarized airway epithelium showed that this strain of reovirus preferentially infects cells from the basolateral membrane, where JAM-A is thought to localize in polarized cells (40). In this respiratory model, removal of α2,3-linked sialic acid enhanced apical infection. In contrast, in our model of intestinal epithelium, reovirus T1L did not appear to efficiently infect the basolateral surface of Caco-2 cultures (W.L. Schulz and L.A. Schiff, unpublished observations). In addition, while JAM-A may be preferentially expressed at the

basolateral surface of polarized respiratory cells (40), our data show that it is distributed throughout the sub-apical membrane of polarized Caco-2 cells.

Penetration of the intestinal mucosa is necessary for reovirus to spread systemically from the intestinal tract. In the murine model of infection, evidence suggests that reovirus spreads by transcytosis through M cells (161). Ligands destined for transcytosis are taken up by one of several endocytic pathways, including clathrin-mediated and caveolar endocytosis (151). We have recently shown that reovirus can use both dynamin-dependent and –independent endocytic pathways to infect non-polarized cells (131). In this study, we have determined that dynamin is not required for apical infection of polarized Caco-2 cells, which suggests that one of the previously identified pathways, such as lipid raft-dependent endocytosis, is used for infection. In contrast, our data indicate that a dynamin-dependent pathway is required for transport of reovirus across the polarized Caco-2 cultures, and TER measurements argue that apical to basolateral transport is not due to passive diffusion of particles through intracellular junctions. These results are consistent with a model in which reovirus particles can undergo transcytosis through intestinal epithelial cells.

Our data show that reovirus can enter polarized and non-polarized cells through both dynamin-dependent and –independent endocytic pathways. However, in polarized enterocytes, particles internalized by dynamin-dependent endocytosis are trafficked to the basolateral surface, whereas particles that lead to infection use a dynamin-independent mechanism. These results underscore

the importance of using multiple cell lines in the study of reovirus entry and infection, as reovirus uses a different set of endocytic pathways to infect polarized cells. Further work is needed to address how reovirus enters primary cells and whether current models of infection accurately reflect reovirus entry *in vivo*.

CHAPTER 6

Major Conclusions and Outstanding Questions

When I started my thesis research, it was unknown whether uncoated reovirus particles entered cells by direct penetration of the plasma membrane or through endocytosis. Early studies supported a model in which reovirus could enter cells by directly penetrating the membrane. This was based on evidence which demonstrated that ISVPs cause hemolysis and membrane damage at high MOIs (25, 79). Additional studies also showed that clathrin-mediated endocytosis is dispensable for infection by these particles (34). However, high-resolution imaging revealed that ISVPs can be localized within endocytic vesicles, suggesting that endocytosis is important for infection (4, 143). In addition, ISVPs are transcytosed across the mucosa during intestinal infection, a process that requires endocytosis (4, 162). In the preceding chapters, I present evidence that shows ISVPs do use endocytosis as a mechanism for cell entry and, ultimately, productive infection. During these studies of reovirus entry, we also discovered that this process is far more complex than initially thought. Reovirus virions were previously known to use clathrin-mediated endocytosis for internalization. In this thesis, I demonstrate that they can also undergo caveolar and dynamin-independent endocytosis to enter cells. My work revealed that reovirus can use both of these pathways to enter a number of tissue culture cell lines; however, I showed that transformed rat embryo fibroblasts and polarized epithelial cells may

be infected through different mechanisms. These findings significantly advance our understanding of reovirus entry (Figure 6.1) and highlight the need for additional studies in primary and polarized cell lines, since entry pathways used to enter these cells may differ from those in traditional cell culture. More work is also needed to identify the molecular determinants that result in virions and ISVPs accessing different endocytic pathways for cell entry.

I. Reovirus ISVPs can use endocytosis to enter and infect host cells.

In Chapter 3 and (131), we showed that reovirus ISVPs can use endocytosis as a mechanism to enter cells and establish infection. We used two independent chemical inhibitors and dominant negative caveolin-1 to assess the role of caveolar endocytosis during reovirus entry and infection. These experiments demonstrated that ISVP internalization and growth are dependent on caveolar endocytosis. This is the first data that shows reovirus ISVPs use endocytosis to infect host cells. More efficient entry into transformed cells has been linked to reovirus oncolysis (2). Therefore, understanding how reovirus particles enter the cell is important for ongoing clinical trials of reovirus as a cancer therapy.

There are several reasons why endocytosis may be needed for viral infection. While the cytoplasm is typically thought of as fluid, it consists of a dense cytoskeletal matrix (53). Without molecular motors and trafficking proteins,

Figure 6.1. Revised model of reovirus entry. This figure illustrates the known pathways of reovirus entry. The shaded box represents prior literature that showed reovirus virions can take advantage of clathrin-mediated endocytosis. In this thesis, we have shown that reovirus ISVPs can use caveolar endocytosis during entry. We also demonstrated that reovirus virions can use multiple endocytic pathways to enter host cells.

Figure 6.1

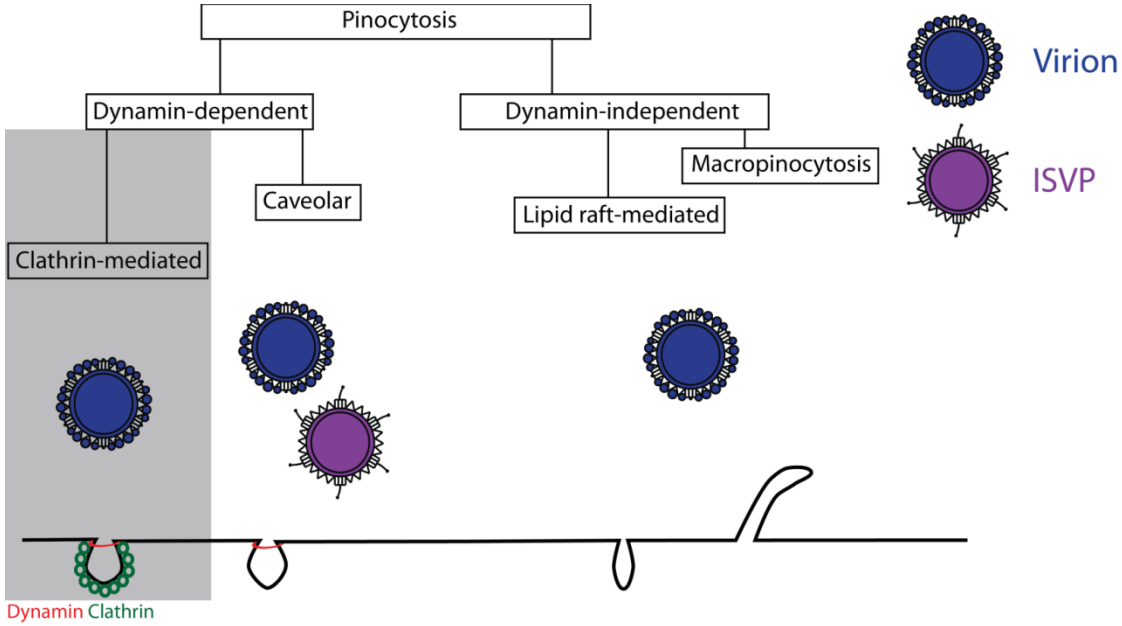
Pinocytosis
Dynamin-dependent
Dynamin-independent
Caveolar
Macropinocytosis
Lipid raft-mediated
Clathrin-mediated
Virion
ISVP
Dynamin Clathrin

it is unlikely that viral particles would localize to important intracellular locations where viral replication occurs, such as the perinuclear region. Localization to these regions is likely promoted by cellular trafficking machinery (53, 86). Reovirus virions are known to traffic through the endocytic pathway, where they are exposed to acid-dependent proteases (34, 81, 143). These proteases mediate the essential step of virion uncoating (49, 143). To efficiently infect cells in culture, virions must be transported through Rab5-positive early endosomes and Rab7-positive late endosomes (83). However, it remains unknown in which vesicle these particles are uncoated and from which vesicle they penetrate to the cytoplasm. While ISVPs have already lost the outermost capsid protein σ3 and have exposed the membrane penetration protein μ1, these particles are believed to require additional processing prior to membrane penetration and transcriptional activation (71, 129). This processing includes cleavage events that release μ1-related peptides that are thought to form pores within the membrane and other cleavage events that dissociate the capsid from the cellular receptor (168). Our work was the first to show that reovirus ISVPs undergo endocytosis during infection. We have not yet begun to characterize post-internalization steps needed for infection by ISVPs, but we are currently working to identify signaling motifs on the viral capsid that are important for intracellular trafficking.

While reovirus oncolysis was initially thought to be based on cellular Ras activation (76, 133), work from our laboratory and others has shown that viral uncoating and entry is critical for oncolysis (2). Tumor microenvironments are

often enriched in proteases (137, 159). Since these proteases may form ISVPs extracellularly, it is likely that ISVPs are the particle type entering transformed cells. Transformed cells are also known to upregulate or downregulate endocytic pathways (158). Therefore, learning how ISVPs enter cells is important for pairing reovirus therapy with the most susceptible tumors. In addition, many chemotherapeutic agents, such as the EGFR inhibitors gefitinib and cetuximab, inhibit the activity of some endocytic pathways within the cell (1). Because reovirus is being used as a combination therapy with radiation or chemotherapy, understanding the molecular details of reovirus entry is particularly important for ongoing clinical studies. We also found that different endocytic pathways may be involved in the infection of Ras transformed and non-transformed cells. Therefore, additional research with primary and clinically relevant cell lines will be important for learning which chemotherapeutic agents can be safely and effectively used with reovirus therapy in human subjects.

II. Reovirus virions use multiple endocytic pathways for entry and infection.

This work makes it clear that the entry of reovirus particles is far more complex than initially hypothesized. Early studies of reovirus entry found that reovirus virions can enter and infect cells through clathrin-mediated endocytosis. Surprisingly, I found that two other pathways, caveolar and lipid-raft dependent

endocytosis, are important for infection by reovirus virions (81). This shows that like several other viruses, including adenovirus (5, 35, 77), reovirus can take advantage of clathrin-dependent and –independent endocytosis. The ability to access such a diverse set of entry pathways has likely evolved as a mechanism to more efficiently infect a wider range host cells. A murine model of pathogenesis demonstrates that a number of organs, such as the nervous system and spleen, can be impacted by reovirus infection. In the context of oncolytic therapy, cell transformation can result in either upregulation or downregulation of endocytic pathways (158). During the infection of cells with dysregulated endocytic pathways, being able to use multiple pathways may improve the efficiency of viral entry.

My work showed that reovirus virions are sensitive to cholesterol depletion early in the infectious process. This block to infection is independent of dynamin, as the internalization of ligands that use dynamin-dependent endocytosis was unaffected by cholesterol depletion. This inhibition was specific to virions, as the growth of reovirus ISVPs was unaffected by cholesterol extraction. This finding suggests that virions, but not ISVPs, can undergo lipid raft-mediated endocytosis. Since virions require exposure to proteases to infect cells, this pathway likely delivers cargo to an acidic compartment within the cell. One alternative explanation is that cholesterol promotes the conversion of virions to ISVPs. However, we found that cholesterol did not affect the kinetics of reovirus uncoating by chymotrypsin *in vitro*, and that it did not directly mediate uncoating.

While we cannot rule out other early events, such as a requirement for cholesterol for the activation of clathrin-mediated endocytosis of reovirus particles, our results suggest that one of several cholesterol-dependent, but dynamin-independent pathways is important for reovirus infection. Several such pathways exist, such as macropinocytosis, which can be used during the entry of ebolavirus, influenza virus and several others, as well as a caveolin- and dynamin-independent pathway that is used by SV40 (31, 97, 112, 126).

As continued research reveals more about viral entry, it is becoming common to find that viruses take advantage of multiple pathways to enter cells. This is especially true in cultured cells, as viruses can adapt to use new receptors and endocytic pathways during passaging (119). In addition, it is likely that viruses capable of infecting a variety of cells need to access multiple endocytic pathways, as not all pathways are active in each cell type (31, 95). Since viral entry is a complex process, a better understanding of how viruses initiate this vital step of the infectious process is important for a better understanding of infection and the development of possible therapies for pathogenic viruses.

III. Reovirus can infect and be transcytosed from the apical membrane of polarized intestinal epithelial cells.

Since the natural route of reovirus infection in the host is through the intestinal tract, I was also interested in learning whether similar entry pathways were used to infect human intestinal cells. My work in Chapter 5 demonstrated that reovirus can infect polarized intestinal epithelial cells from the apical surface. While previous work showed that reovirus could attach to these cells (3), this was the first data showing that human enterocytes can also be infected from the apical membrane. Polarized enterocytes are known to express sialic acid and other carbohydrates on the apical membrane (3, 59). Prior studies showed that reovirus T1L can bind to a glycoconjugate containing α2,3-linked sialic acid on the apical surface of these cells (59). Since reovirus T1L is unable to bind to the apical surface of murine enterocytes (155), it is possible that reovirus binds to a carbohydrate receptor present on the apical surface of polarized human enterocytes that is not present or is inaccessible on murine cells. Because reovirus can infect human enterocytes from the apical membrane, these findings are relevant for ongoing trials of reovirus oncolysis. Current oncolytic therapy is administered intravenously (54), but intestinal adenocarcinoma may also be susceptible to oral administration since my work shows that these cells can be productively infected from the luminal surface of the intestinal tract.

I showed that reovirus can use multiple endocytic pathways to enter host cells. Polarized Caco-2 cells were no exception, as my work revealed that both dynamin-dependent and –independent mechanisms could be used for viral entry. However, the fate of particles entering through these pathways differed in

polarized epithelial cells. Unlike infection in L929 mouse fibroblasts, reovirus infection of Caco-2 cells did not rely on dynamin. This suggests that an alternate mechanism, such as dynamin-independent endocytosis or direct membrane penetration, is used for infection. Because of these differences in entry, it will be important to learn which endocytic pathways are used during the infection of primary cell lines, as combination drug therapies that affect these endocytic pathways may decrease the effectiveness of reovirus treatment.

Reovirus is known to spread from the intestinal lumen through specialized M cells in mouse models of infection (162). In this thesis, I have presented the first evidence that reovirus can also be transcytosed from the apical membrane of polarized human epithelial cells. My experiments showed that infectious reovirus particles added at the apical surface of a transwell culture could be recovered from the basolateral compartment by a dynamin-dependent process. Thus, while reovirus can enter polarized Caco-2 cells by dynamin-dependent and –independent pathways, internalization through these pathways results in different fates for reovirus particles. The eventual fate of reovirus particles may depend on interactions between reovirus and cellular receptors. Since reovirus could infect nonpolarized Caco-2 cells through a dynamin-dependent pathway, but did not use this pathway after polarization, binding to the receptor JAM-A may result in entry through clathrin-mediated endocytosis. In polarized cells that lack JAM-A at the apical membrane, other receptor interactions may target particles for transcytosis through dynamin-dependent pathways. Identification of

the molecular interactions that are important for trafficking could provide us with the ability to create a more efficient oncolytic therapy, as targeting viral particles to an endocytic pathway that results in infection would likely increase the effectiveness of reovirus treatment.

IV. Why do virions and ISVPs use different pathways to enter and infect host cells?

My work has shown that reovirus can access both dynamin-dependent and dynamin-independent pathways for cell entry. While virions can take advantage of both clathrin-mediated and caveolar endocytosis, ISVPs were only found to use caveolar endocytosis during infection. The molecular basis for this difference is not yet known. For many endocytic cargoes, the activation of cellular receptors leads to the internalization of both the receptor and ligand (65, 153). Other researchers have hypothesized that the conserved integrin binding motifs RGD (Figure 6.2A) and KGE (Figure 6.2B) may be responsible for the activation of β1 integrin and subsequent uptake of reovirus through clathrin-mediated endocytosis (34). However, this motif is present on the inner capsid protein λ2, which is found on both virions and ISVPs. Therefore, ISVPs would still be expected to activate β1 integrins since the λ2 protein is not removed during uncoating (129). Since ISVPs do not use clathrin-mediated endocytosis to enter cells, other signaling sequences are likely important for uptake. We identified an

Figure 6.2. Putative integrin binding sequences in reovirus capsid proteins. This figure shows a sequence alignment of reovirus type 1, type 2, and type 3 strains. (A) Sequence alignment of the inner capsid protein λ2 with the putative β1 integrin binding domain RGD highlighted. (B) Sequence alignment of the inner capsid protein λ2 with the putative β1 integrin binding domain KGE highlighted. (C) Sequence alignment of the outer capsid protein σ3 with the putative α4β1 binding domain highlighted. Type 1 and type 2 strains contain the four amino acid IDSS domain, while reovirus type 3 contains the three amino acid IDS domain.

Figure 6.2

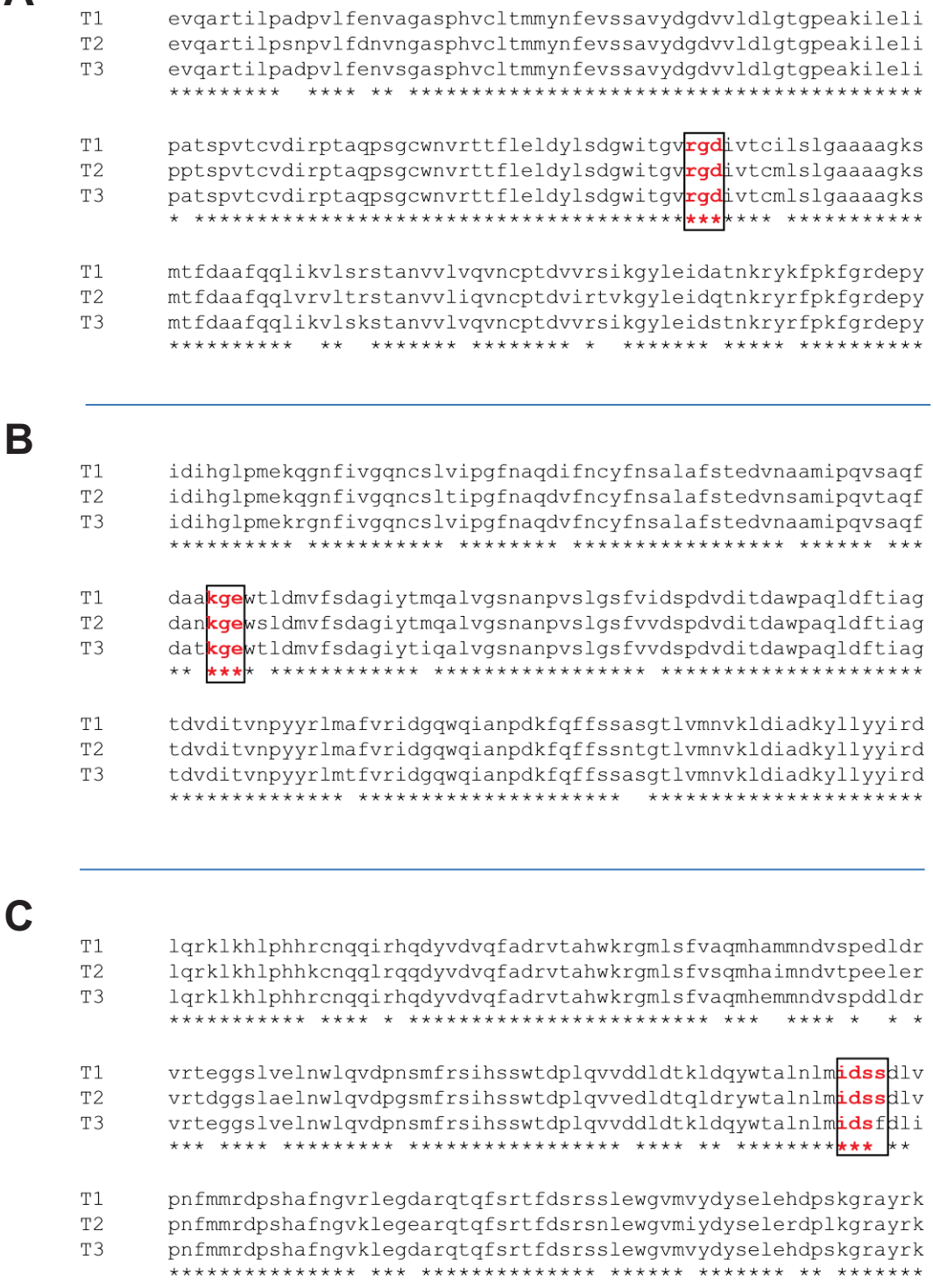
A
T1 evqartilpadpvlfenvagasphvcltmmynfevssavydgdvvldlgtgpeakileli
T2 evqartilpsnpvlfdnvngasphvcltmmynfevssavydgdvvldlgtgpeakileli
T3 evqartilpadpvlfenvsgasphvcltmmynfevssavydgdvvldlgtgpeakileli
T1 patspvtcvdirptaqpsgcwnvrttfleldylsdgwitgvrgdivtcilslgaaaagks
T2 pptspvtcvdirptaqpsgcwnvrttfleldylsdgwitgvrgdivtcmlslgaaaagks
T3 patspvtcvdirptaqpsgcwnvrttfleldylsdgwitgvrgdivtcmlslgaaaagks
T1 mtfdaafqqlikvlsrstanvvlvqvncptdvvrsikgyleidatnkrykfpkfgrdepy
T2 mtfdaafqqlvrvltrstanvvliqvncptdvirtvkgyleidqtnkryrfpkfgrdepy
T3 mtfdaafqqlikvlskstanvvlvqvncptdvvrsikgyleidstnkryrfpkfgrdepy
B
T1 idihglpmekqgnfivgqncslvipgfnaqdifncyfnsalafstedvnaamipqvsaqf
T2 idihglpmekqgnfivgqncsltipgfnaqdvfncyfnsalafstedvnsamipqvtaqf
T3 idihglpmekrgnfivgqncslvipgfnaqdvfncyfnsalafstedvnaamipqvsaqf
T1 daakgewtldmvfsdagiytmqalvgsnanpvslgsfvidspdvditdawpaqldftiag
T2 dankgewsldmvfsdagiytmqalvgsnanpvslgsfvvdspdvditdawpaqldftiag
T3 datkgewtldmvfsdagiytiqalvgsnanpvslgsfvvdspdvditdawpaqldftiag
T1 tdvditvnpyyrlmafvridgqwqianpdkfqffssasgtlvmnvkldiadkyllyyird
T2 tdvditvnpyyrlmafvridgqwqianpdkfqffssntgtlvmnvkldiadkyllyyird
T3 tdvditvnpyyrlmtfvridgqwqianpdkfqffssasgtlvmnvkldiadkyllyyird
C
T1 lqrklkhlphhrcnqqirhqdyvdvqfadrvtahwkrgmlsfvaqmhammndvspedldr
T2 lqrklkhlphhkcnqqlrqqdyvdvqfadrvtahwkrgmlsfvsqmhaimndvtpeeler
T3 lqrklkhlphhrcnqqirhqdyvdvqfadrvtahwkrgmlsfvaqmhemmndvspddldr
T1 vrteggslvelnwlqvdpnsmfrsihsswtdplqvvddldtkldqywtalnlmidssdlv
T2 vrtdggslaelnwlqvdpgsmfrsihsswtdplqvvedldtqldrywtalnlmidssdlv
T3 vrteggslvelnwlqvdpnsmfrsihsswtdplqvvddldtkldqywtalnlmidsfdli
T1 pnfmmrdpshafngvrlegdarqtqfsrtfdsrsslewgvmvydyselehdpskgrayrk
T2 pnfmmrdpshafngvklegearqtqfsrtfdsrsnlewgvmiydyselerdplkgrayrk
T3 pnfmmrdpshafngvklegdarqtqfsrtfdsrsslewgvmvydyselehdpskgrayrk

alternate integrin binding motif, IDS, that is known to interact with α4β1 integrin and is present on the outer capsid protein σ3 (67, 122). This sequence is conserved among reovirus strains (Figure 6.2C) and might explain why ISVPs are unable to access clathrin-mediated endocytosis, as σ3 removal would abolish signaling through β integrins. Ongoing work in our lab using the reovirus reverse genetics system aims to learn whether this sequence is important the activation of clathrin-mediated endocytosis. We are also assessing the role of other capsid sequences to determine if they play a role in the sorting of reovirus particles.

V. What other cellular genes are important for reovirus infection?

Our preliminary study to assess the feasibility of a genome-wide shRNA screen to identify host genes that promote reovirus infection was successful. While I did not complete a comprehensive screen of the entire genome as part of my thesis work, we identified several host genes that may be involved in reovirus infection and confirmed one of these through a follow-up study. The confirmed gene, RhoA, is known to function in clathrin-independent endocytosis (39). This supports our new finding that reovirus virions and ISVPs can use clathrin-independent endocytosis during infection. While no screen can positively identify every cellular protein that is important for viral replication, we had an approximately 0.3% hit rate in our study. This suggests that a comprehensive screen of the entire human genome, which contains approximately 21,000

protein-coding genes, could identify 63 virus-cell interactions. While this may seem like a modest success rate, increased coverage with each potential shRNA construct will likely increase the number of identified target genes. Future work using this approach will provide a number of novel host genes that are important for reovirus infection and oncolysis.

In conclusion, my work has revealed that reovirus ISVPs use endocytosis to infect host cells. In addition, I demonstrated that virions can use multiple endocytic pathways to infect cells and that the pathways used for infection differ in various cell types. While we do not yet know why virions can access more endocytic pathways than ISVPs, this thesis forms the foundation for ongoing studies of reovirus entry. This work is also important for clinical studies of reovirus oncolysis, as tumors with highly active endocytic pathways may be most susceptible to reovirus infection.

REFERENCES

1. **Abulrob, A., S. Giuseppin, M. F. Andrade, A. McDermid, M. Moreno, and D. Stanimirovic**. 2004. Interactions of EGFR and caveolin-1 in human glioblastoma cells: evidence that tyrosine phosphorylation regulates EGFR association with caveolae. Oncogene. **23**:6967–79.
2. **Alain, T., T. S. Kim, X. Lun, A. Liacini, L. A. Schiff, D. L. Senger, and P. A. Forsyth**. 2007. Proteolytic disassembly is a critical determinant for reovirus oncolysis. Mol. Ther. **15**:1512–21.
3. **Ambler, L., and M. Mackay**. 1991. Reovirus 1 and 3 bind and internalise at the apical surface of intestinal epithelial cells. Virology. **184**:162–9.
4. **Amerongen, H. M., G. A. Wilson, B. N. Fields, and M. R. Neutra**. 1994. Proteolytic processing of reovirus is required for adherence to intestinal M cells. J. Virol. **68**:8428–32.
5. **Amstutz, B., M. Gastaldelli, S. Kälin, N. Imelli, K. Boucke, E. Wandeler, J. Mercer, S. Hemmi, and U. F. Greber**. 2008. Subversion of CtBP1-controlled macropinocytosis by human adenovirus serotype 3. EMBO J. **27**:956–69.
6. **Aoki, T., R. Nomura, and T. Fujimoto**. 1999. Tyrosine phosphorylation of caveolin-1 in the endothelium. Exp. Cell. Res. **253**:629–36.
7. **Artursson, P.** 1990. Epithelial transport of drugs in cell culture. I: A model for studying the passive diffusion of drugs over intestinal absorptive (Caco-2) cells. J. Pharm. Sci. **79**:476–82.
8. **Barton, E. S., J. D. Chappell, J. L. Connolly, J. C. Forrest, and T. S. Dermody**. 2001. Reovirus receptors and apoptosis. Virology. **290**:173–80.
9. **Barton, E. S., J. L. Connolly, J. C. Forrest, J. D. Chappell, and T. S. Dermody**. 2001. Utilization of sialic acid as a coreceptor enhances reovirus attachment by multistep adhesion strengthening. J. Biol. Chem. **276**:2200–11.
10. **Barton, E. S., J. C. Forrest, J. L. Connolly, J. D. Chappell, Y. Liu, F. J. Schnell, A. Nusrat, C. A. Parkos, and T. S. Dermody**. 2001. Junction adhesion molecule is a receptor for reovirus. Cell. **104**:441–51.
11. **Bass, D. M., D. Bodkin, R. Dambrauskas, J. S. Trier, B. N. Fields, and J. L. Wolf**. 1990. Intraluminal proteolytic activation plays an important role in replication of type 1 reovirus in the intestines of neonatal mice. J. Virol. **64**:1830–3.
12. **Blechacz, B., and S. J. Russell**. 2008. Measles virus as an oncolytic vector platform. Curr. Gene Ther. **8**:162–75.
13. **Bodkin, D. K., M. L. Nibert, and B. N. Fields**. 1989. Proteolytic digestion of reovirus in the intestinal lumens of neonatal mice. J. Virol. **63**:4676–81.
14. **Boehme, K. W., J. M. Frierson, J. L. Konopka, T. Kobayashi, and T. S. Dermody**. 2011. The reovirus sigma1s protein is a determinant of hematogenous but not neural virus dissemination in mice. J. Virol. **85**:11781–90.

15. **Borsa, J., T. P. Copps, M. D. Sargent, D. G. Long, and J. D. Chapman**. 1973. New intermediate subviral particles in the in vitro uncoating of reovirus virions by chymotrypsin. J. Virol. **11**:552–64.
16. **Borsa, J., D. G. Long, M. D. Sargent, T. P. Copps, and J. D. Chapman**. 1974. Reovirus transcriptase activation in vitro: involvement of an endogenous uncoating activity in the second stage of the process. Intervirology. **4**:171–88.
17. **Borsa, J., M. D. Sargent, D. G. Long, and J. D. Chapman**. 1973. Extraordinary effects of specific monovalent cations on activation of reovirus transcriptase by chymotrypsin in vitro. J. Virol. **11**:207–17.
18. **Boucrot, E., S. Saffarian, R. Zhang, and T. Kirchhausen**. 2010. Roles of AP-2 in clathrin-mediated endocytosis. PLoS One. **5**:e10597.
19. **Broering, T. J., J. Kim, C. L. Miller, C. D. S. Piggott, J. B. Dinoso, M. L. Nibert, and J. S. L. Parker**. 2004. Reovirus nonstructural protein mu NS recruits viral core surface proteins and entering core particles to factory-like inclusions. J. Virol. **78**:1882–92.
20. **Börner, K., J. Hermle, C. Sommer, N. P. Brown, B. Knapp, B. Glass, J. Kunkel, G. Torralba, J. Reymann, N. Beil, J. Beneke, R. Pepperkok, R. Schneider, T. Ludwig, M. Hausmann, F. Hamprecht, H. Erfle, L. Kaderali, H.-G. Kräusslich, and M. J. Lehmann**. 2010. From experimental setup to bioinformatics: an RNAi screening platform to identify host factors involved in HIV-1 replication. Biotechnol. J. **5**:39–49.
21. **Cammisotto, P. G., M. Bendayan, A. Sané, M. Dominguez, C. Garofalo, and E. Levy**. 2010. Receptor-mediated transcytosis of leptin through human intestinal cells in vitro. Int. J. Cell Biol. **2010**:928169.
22. **Cao, H., J. Chen, M. Awoniyi, J. R. Henley, and M. a McNiven**. 2007. Dynamin 2 mediates fluid-phase micropinocytosis in epithelial cells. J. Cell Sci. **120**:4167–77.
23. **Carson, S. D., K.-S. Kim, S. J. Pirruccello, S. Tracy, and N. M. Chapman**. 2007. Endogenous low-level expression of the coxsackievirus and adenovirus receptor enables coxsackievirus B3 infection of RD cells. J. Gen. Virol. **88**:3031–8.
24. **Carter, G. C., L. Bernstone, D. Sangani, J. W. Bee, T. Harder, and W. James**. 2009. HIV entry in macrophages is dependent on intact lipid rafts. Virology. **386**:192–202.
25. **Chandran, K., D. L. Farsetta, and M. L. Nibert**. 2002. Strategy for nonenveloped virus entry: a hydrophobic conformer of the reovirus membrane penetration protein micro 1 mediates membrane disruption. J. Virol. **76**:9920–33.
26. **Chappell, J. D., J. L. Duong, B. W. Wright, and T. S. Dermody**. 2000. Identification of carbohydrate-binding domains in the attachment proteins of type 1 and type 3 reoviruses. J. Virol. **74**:8472–9.
27. **Chappell, J. D., V. L. Gunn, J. D. Wetzel, G. S. Baer, and T. S. Dermody**. 1997. Mutations in type 3 reovirus that determine binding to

sialic acid are contained in the fibrous tail domain of viral attachment protein sigma1. J. Virol. **71**:1834–41.
28. **Cody, J. J., and J. T. Douglas**. 2009. Armed replicating adenoviruses for cancer virotherapy. Cancer Gene Ther. **16**:473–88.
29. **Coffey, M. C., J. E. Strong, P. A. Forsyth, and P. W. Lee**. 1998. Reovirus therapy of tumors with activated Ras pathway. Science. **282**:1332–4.
30. **Coyne, C. B., K. S. Kim, and J. M. Bergelson**. 2007. Poliovirus entry into human brain microvascular cells requires receptor-induced activation of SHP-2. EMBO J. **26**:4016–28.
31. **Damm, E.-M., L. Pelkmans, J. Kartenbeck, A. Mezzacasa, T. Kurzchalia, and A. Helenius**. 2005. Clathrin- and caveolin-1-independent endocytosis: entry of simian virus 40 into cells devoid of caveolae. J. Cell. Biol. **168**:477–88.
32. **De Vries, E., D. M. Tscherne, M. J. Wienholts, V. Cobos-Jiménez, F. Scholte, A. García-Sastre, P. J. M. Rottier, and C. a M. de Haan**. 2011. Dissection of the influenza A virus endocytic routes reveals macropinocytosis as an alternative entry pathway. PLoS Pathog. **7**:e1001329.
33. **De Vries, E., D. M. Tscherne, M. J. Wienholts, V. Cobos-Jiménez, F. Scholte, A. García-Sastre, P. J. M. Rottier, and C. a M. de Haan**. 2011. Dissection of the influenza A virus endocytic routes reveals macropinocytosis as an alternative entry pathway. PLoS Pathog. **7**:e1001329.
34. **Dermody, T. S., M. S. Maginnis, J. C. Forrest, S. A. Kopecky-Bromberg, S. K. Dickeson, S. A. Santoro, M. M. Zutter, G. R. Nemerow, and J. M. Bergelson**. 2006. Beta1 integrin mediates internalization of mammalian reovirus. J. Virol. **80**:2760–2770.
35. **Diaz, F., D. Gravotta, A. Deora, R. Schreiner, J. Schoggins, E. Falck-Pedersen, and E. Rodriguez-Boulan**. 2009. Clathrin adaptor AP1B controls adenovirus infectivity of epithelial cells. Proc. Natl. Acad. Sci. USA. **106**:11143–8.
36. **Dix, C. J., I. F. Hassan, H. Y. Obray, R. Shah, and G. Wilson**. 1990. The transport of vitamin B12 through polarized monolayers of Caco-2 cells. Gastroenterology. **98**:1272–9.
37. **Doherty, G. J., and H. T. McMahon**. 2009. Mechanisms of endocytosis. Annu. Rev. Biochem. **78**:857–902.
38. **Ebert, D. H., J. Deussing, C. Peters, and T. S. Dermody**. 2002. Cathepsin L and cathepsin B mediate reovirus disassembly in murine fibroblast cells. J. Biol. Chem. **277**:24609–17.
39. **Ellis, S., and H. Mellor**. 2000. Regulation of endocytic traffic by rho family GTPases. Trends Cell Biol. **10**:85–8.
40. **Excoffon, K. J. D. A., K. M. Guglielmi, J. D. Wetzel, N. D. Gansemer, J. A. Campbell, T. S. Dermody, and J. Zabner**. 2009. Reovirus preferentially infects the basolateral surface and is released from the apical

surface of polarized human respiratory epithelial cells. J. Infect. Dis. **197**:1189–97.
41. **Fields, B. N., D. K. Bodkin, and M. L. Nibert**. 1989. Proteolytic digestion of reovirus in the intestinal lumens of neonatal mice. J. Virol. **63**:4676–81.
42. **Fish, K. N., S. L. Schmid, and H. Damke**. 2000. Evidence that dynamin-2 functions as a signal-transducing GTPase. J. Cell. Biol. **150**:145–54.
43. **Fogh, J., W. C. Wright, and J. D. Loveless**. 1977. Absence of HeLa cell contamination in 169 cell lines derived from human tumors. J. Natl. Cancer Inst. **58**:209–14.
44. **Fujioka, Y., M. Tsuda, T. Hattori, J. Sasaki, T. Sasaki, T. Miyazaki, and Y. Ohba**. 2011. The Ras-PI3K signaling pathway is involved in clathrin-independent endocytosis and the internalization of influenza viruses. PLoS One. **6**:e16324.
45. **Furlong, D. B., M. L. Nibert, and B. N. Fields**. 1988. Sigma 1 protein of mammalian reoviruses extends from the surfaces of viral particles. J. Virol. **62**:246–56.
46. **Gastaldelli, M., N. Imelli, K. Boucke, B. Amstutz, O. Meier, and U. F. Greber**. 2008. Infectious adenovirus type 2 transport through early but not late endosomes. Traffic. **9**:2265–78.
47. **Golden, J. W., J. A. Bahe, W. T. Lucas, M. L. Nibert, and L. A. Schiff**. 2004. Cathepsin S supports acid-independent infection by some reoviruses. J. Biol. Chem. **279**:8547–57.
48. **Golden, J. W., J. Linke, S. Schmechel, K. Thoemke, and L. A. Schiff**. 2002. Addition of exogenous protease facilitates reovirus infection in many restrictive cells. J. Virol. **76**:7430–43.
49. **Golden, J. W., and L. A. Schiff**. 2005. Neutrophil elastase, an acid-independent serine protease, facilitates reovirus uncoating and infection in U937 promonocyte cells. Virol. J. **2**:48.
50. **Grande-García, A., A. Echarri, J. de Rooij, N. B. Alderson, C. M. Waterman-Storer, J. M. Valdivielso, and M. a del Pozo**. 2007. Caveolin-1 regulates cell polarization and directional migration through Src kinase and Rho GTPases. J. Cell. Biol. **177**:683–94.
51. **Grove, J., and M. Marsh**. 2011. The cell biology of receptor-mediated virus entry. J. Cell. Biol. **195**:1071–82.
52. **Gruenberg, J., and F. G. van der Goot**. 2006. Mechanisms of pathogen entry through the endosomal compartments. Nat. Rev. Mol. Cell Biol. **7**:495–504.
53. **Gruenheid, S., and B. B. Finlay**. 2003. Microbial pathogenesis and cytoskeletal function. Nature. **422**:775–81.
54. **Harrington, K. J., C. L. White, K. Twigger, A. Melcher, M. Coffey, T. A. Yap, J. S. DeBono, L. Vidal, H. S. Pandha, and R. G. Vile**. 2008. A phase I study of intravenous oncolytic reovirus type 3 Dearing in patients with advanced cancer. Clin. Cancer Res. **14**:7127–37.

55. **Harrison, S. C.** 2008. Viral membrane fusion. Nat. Struct. Mol. Biol. **15**:690–8.
56. **Hayer, A., M. Stoeber, D. Ritz, S. Engel, H. H. Meyer, and A. Helenius**. 2010. Caveolin-1 is ubiquitinated and targeted to intralumenal vesicles in endolysosomes for degradation. J. Cell. Biol. **191**:615–29.
57. **Heaton, N. S., and G. Randall**. 2011. Multifaceted roles for lipids in viral infection. Trends Microbiol. **19**:368–75.
58. **Heinemann, L., G. R. Simpson, A. Boxall, T. Kottke, K. L. Relph, R. Vile, A. Melcher, R. Prestwich, K. J. Harrington, R. Morgan, and H. S. Pandha**. 2011. Synergistic effects of oncolytic reovirus and docetaxel chemotherapy in prostate cancer. BMC Cancer. **11**:221.
59. **Helander, A., K. J. Silvey, N. J. Mantis, A. B. Hutchings, K. Chandran, W. T. Lucas, M. L. Nibert, and M. R. Neutra**. 2003. The viral sigma1 protein and glycoconjugates containing alpha2-3-linked sialic acid are involved in type 1 reovirus adherence to M cell apical surfaces. J. Virol. **77**:7964–77.
60. **Helenius, a, J. Kartenbeck, K. Simons, and E. Fries**. 1980. On the entry of Semliki forest virus into BHK-21 cells. J. Cell. Biol. **84**:404–20.
61. **Henley, J. R., E. W. Krueger, B. J. Oswald, and M. A. McNiven**. 1998. Dynamin-mediated internalization of caveolae. J. Cell. Biol. **141**:85–99.
62. **Hewish, M. J., Y. Takada, and B. S. Coulson**. 2000. Integrins alpha2beta1 and alpha4beta1 can mediate SA11 rotavirus attachment and entry into cells. J. Virol. **74**:228–36.
63. **Hirasawa, K., S. G. Nishikawa, K. L. Norman, T. Alain, A. Kossakowska, and P. W. K. Lee**. 2002. Oncolytic reovirus against ovarian and colon cancer. Cancer Res. **62**:1696–701.
64. **Holm, G. H., E. Kirchner, T. Stehle, T. S. Dermody, and K. M. Guglielmi**. 2007. Reovirus binding determinants in junctional adhesion molecule-A. J Biol Chem. **282**:17930–40.
65. **Huang, F., A. Khvorova, W. Marshall, and A. Sorkin**. 2004. Analysis of clathrin-mediated endocytosis of epidermal growth factor receptor by RNA interference. J. Biol. Chem. **279**:16657–61.
66. **Huang, W. R., Y. C. Wang, P. I. Chi, L. Wang, C. Y. Wang, C. H. Lin, and H. J. Liu**. 2011. Cell entry of avian reovirus follows a caveolin-1-mediated and dynamin-2-dependent endocytic pathway that requires activation of p38 mitogen-activated protein kinase (MAPK) and Src signaling pathways as well as microtubules and small GTPase Rab5 protein. J. Biol. Chem. **286**:30780–94.
67. **Humphries, J. D., A. Byron, and M. J. Humphries**. 2006. Integrin ligands at a glance. J. Cell Sci. **119**:3901–3.
68. **Imelli, N., O. Meier, K. Boucke, S. Hemmi, and U. F. Greber**. 2004. Cholesterol is required for endocytosis and endosomal escape of adenovirus type 2. J. Virol. **78**:3089–98.

69. **Inoue, T., P. Moore, and B. Tsai**. 2011. How viruses and toxins disassemble to enter host cells. Annu. Rev. Microbiol. **65**:287–305.
70. **Ismail, I. A., K.-S. Kang, H. A. Lee, J.-W. Kim, and Y.-K. Sohn**. 2007. Genistein-induced neuronal apoptosis and G2/M cell cycle arrest is associated with MDC1 up-regulation and PLK1 down-regulation. Eur. J. Pharmacol. **575**:12–20.
71. **Ivanovic, T., M. L. Nibert, and M. A. Agosto**. 2006. Mammalian reovirus, a nonfusogenic nonenveloped virus, forms size-selective pores in a model membrane. Proc. Natl. Acad. Sci. USA. **103**:16496–501.
72. **Joklik, W. K.** 1972. Studies on the effect of chymotrypsin on reovirions. Virology. **49**:700–15.
73. **Kirkham, M., A. Fujita, R. Chadda, S. J. Nixon, T. V. Kurzchalia, D. K. Sharma, R. E. Pagano, J. F. Hancock, S. Mayor, and R. G. Parton**. 2005. Ultrastructural identification of uncoated caveolin-independent early endocytic vehicles. J. Cell. Biol. **168**:465–76.
74. **Kossmann, C. E., and G. E. Palade**. 1961. Blood Capillaries of the Heart and Other Organs. Circulation. **24**:368–384.
75. **Lee, P. W., E. C. Hayes, and W. K. Joklik**. 1981. Protein sigma 1 is the reovirus cell attachment protein. Virology. **108**:156–63.
76. **Lee, P. W., P. Sabinin, D. Tang, M. C. Coffey, and J. E. Strong**. 1998. The molecular basis of viral oncolysis: usurpation of the Ras signaling pathway by reovirus. EMBO J. **17**:3351–62.
77. **Leung, T. K. H., and M. Brown**. 2011. Block in entry of enteric adenovirus type 41 in HEK293 cells. Virus Res. **156**:54–63.
78. **Li, E., D. G. Stupack, S. L. Brown, R. Klemke, D. D. Schlaepfer, and G. R. Nemerow**. 2000. Association of p130CAS with phosphatidylinositol-3-OH kinase mediates adenovirus cell entry. J. Biol. Chem. **275**:14729–35.
79. **Lucia-Jandris, P., J. W. Hooper, and B. N. Fields**. 1993. Reovirus M2 gene is associated with chromium release from mouse L cells. J. Virol. **67**:5339–45.
80. **Macia, E., M. Ehrlich, R. Massol, E. Boucrot, C. Brunner, and T. Kirchhausen**. 2006. Dynasore, a cell-permeable inhibitor of dynamin. Dev. Cell. **10**:839–50.
81. **Maginnis, M. S., B. A. Mainou, A. Derdowski, E. M. Johnson, R. Zent, and T. S. Dermody**. 2008. NPXY motifs in the beta1 integrin cytoplasmic tail are required for functional reovirus entry. J. Virol. **82**:3181–91.
82. **Mainou, B. A., and T. S. Dermody**. 2011. Src kinase mediates productive endocytic sorting of reovirus during cell entry. J. Virol. **85**:3203–13.
83. **Mainou, B. A., and T. S. Dermody**. 2012. Transport to late endosomes is required for efficient reovirus infection. J. Virol. **86**:8346–58.
84. **Marcato, P., M. Shmulevitz, and P. W. Lee**. 2005. Connecting reovirus oncolysis and Ras signaling. Cell Cycle. **4**:556–9.

85. **Marsh, M., and R. Bron**. 1997. SFV infection in CHO cells: cell-type specific restrictions to productive virus entry at the cell surface. J. Cell Sci. **110**:95–103.
86. **Marsh, M., and A. Helenius**. 2006. Virus entry: open sesame. Cell. **124**:729–40.
87. **Martin-Latil, S., N. F. Gnädig, A. Mallet, M. Desdouits, F. Guivel-Benhassine, P. Jeannin, M.-C. Prevost, O. Schwartz, A. Gessain, S. Ozden, and P.-E. Ceccaldi**. 2012. Transcytosis of HTLV-1 across a tight human epithelial barrier and infection of subepithelial dendritic cells. Blood. **120**:572–80.
88. **Mason, S. D., and J. a Joyce**. 2011. Proteolytic networks in cancer. Trends Cell Biol. **21**:228–37.
89. **Matlin, K. S., H. Reggio, A. Helenius, and K. Simons**. 1981. Infectious entry pathway of influenza virus in a canine kidney cell line. J. Cell. Biol. **91**:601–13.
90. **Mayor, S., and R. E. Pagano**. 2007. Pathways of clathrin-independent endocytosis. Nat. Rev. Mol. Cell Biol. **8**:603–12.
91. **McMahon, H. T., and E. Boucrot**. 2011. Molecular mechanism and physiological functions of clathrin-mediated endocytosis. Nat. Rev. Mol. Cell Biol. **12**:517–33.
92. **McNiven, M. A., H. Cao, K. R. Pitts, and Y. Yoon**. 2000. The dynamin family of mechanoenzymes: pinching in new places. Trends Biochem Sci. **25**:115–20.
93. **Medina-Kauwe, L. K.** 2007. “Alternative” endocytic mechanisms exploited by pathogens: new avenues for therapeutic delivery? Adv. Drug Deliv. Rev. **59**:798–809.
94. **Meier, O., K. Boucke, S. V. Hammer, S. Keller, R. P. Stidwill, S. Hemmi, and U. F. Greber**. 2002. Adenovirus triggers macropinocytosis and endosomal leakage together with its clathrin-mediated uptake. J. Cell. Biol. **158**:1119–31.
95. **Meier, O., and U. F. Greber**. 2004. Adenovirus endocytosis. J. Gene Med. **6 Suppl 1**:S152–63.
96. **Mercer, J., and A. Helenius**. 2008. Vaccinia virus uses macropinocytosis and apoptotic mimicry to enter host cells. Science. **320**:531–5.
97. **Mercer, J., and A. Helenius**. 2009. Virus entry by macropinocytosis. Nat. Cell Biol. **11**:510–20.
98. **Mettlen, M., T. Pucadyil, R. Ramachandran, and S. L. Schmid**. 2009. Dissecting dynamin’s role in clathrin-mediated endocytosis. Biochem. Soc. Trans. **37**:1022–6.
99. **Middleton, J. K., M. A. Agosto, T. F. Severson, J. Yin, and M. L. Nibert**. 2007. Thermostabilizing mutations in reovirus outer-capsid protein mu1 selected by heat inactivation of infectious subvirion particles. Virology. **361**:412–25.

100. **Miller, C. L., M. M. Arnold, T. J. Broering, C. E. Hastings, and M. L. Nibert**. 2010. Localization of mammalian orthoreovirus proteins to cytoplasmic factory-like structures via nonoverlapping regions of microNS. J. Virol. **84**:867–82.
101. **Miller, C. L., T. J. Broering, J. S. L. Parker, M. M. Arnold, and M. L. Nibert**. 2003. Reovirus sigma NS protein localizes to inclusions through an association requiring the mu NS amino terminus. J. Virol. **77**:4566–76.
102. **Mirre, C., L. Monlauzeur, M. Garcia, M. H. Delgrossi, and A. Le Bivic**. 1996. Detergent-resistant membrane microdomains from Caco-2 cells do not contain caveolin. Am. J. Physiol. **271**:C887–94.
103. **Norkin, L. C., H. A. Anderson, S. A. Wolfrom, and A. Oppenheim**. 2002. Caveolar endocytosis of simian virus 40 is followed by brefeldin A-sensitive transport to the endoplasmic reticulum, where the virus disassembles. J. Virol. **76**:5156–5166.
104. **Norman, K. L., M. C. Coffey, K. Hirasawa, D. J. Demetrick, S. G. Nishikawa, L. M. DiFrancesco, J. E. Strong, and P. W. K. Lee**. 2002. Reovirus oncolysis of human breast cancer. Hum. Gene Ther. **13**:641–52.
105. **Ostrom, R. S., and X. Liu**. 2007. Detergent and detergent-free methods to define lipid rafts and caveolae. Methods Mol. Biol. **400**:459–68.
106. **Ouyang, G., L. Yao, K. Ruan, G. Song, Y. Mao, and S. Bao**. 2009. Genistein induces G2/M cell cycle arrest and apoptosis of human ovarian cancer cells via activation of DNA damage checkpoint pathways. Cell Biol. Int. **33**:1237–44.
107. **Parton, R. G., B. Joggerst, and K. Simons**. 1994. Regulated internalization of caveolae. J. Cell. Biol. **127**:1199–215.
108. **Parton, R. G., and M. T. Howes**. 2010. Revisiting caveolin trafficking: the end of the caveosome. J. Cell. Biol. **191**:439–41.
109. **Parton, R. G., and K. Simons**. 2007. The multiple faces of caveolae. Nat. Rev. Mol. Cell Biol. **8**:185–94.
110. **Patel, K. P., C. B. Coyne, and J. M. Bergelson**. 2009. Dynamin- and lipid raft-dependent entry of decay-accelerating factor (DAF)-binding and non-DAF-binding coxsackieviruses into nonpolarized cells. J. Virol. **83**:11064–77.
111. **Patton, R. G.** 1996. Caveolae and caveolins. Curr. Opin. Cell Biol. **8**:542–8.
112. **Pelkmans, L., J. Kartenbeck, and A. Helenius**. 2001. Caveolar endocytosis of simian virus 40 reveals a new two-step vesicular-transport pathway to the ER. Nat. Cell Biol. **3**:473–483.
113. **Permanyer, M., E. Ballana, and J. a Esté**. 2010. Endocytosis of HIV: anything goes. Trends Microbiol. **18**:543–51.
114. **Petrelli, F., K. Borgonovo, M. Cabiddu, and S. Barni**. 2012. Efficacy of EGFR tyrosine kinase inhibitors in patients with EGFR-mutated non-small-cell lung cancer: a meta-analysis of 13 randomized trials. Clin. Lung Cancer. **13**:107–14.

115. **Pietiäinen, V. M., V. Marjomäki, J. Heino, and T. Hyypiä**. 2005. Viral entry, lipid rafts and caveosomes. Ann. Med. **37**:394–403.
116. **Prusty, B. K., A. Karlas, T. F. Meyer, and T. Rudel**. 2011. Genome-wide RNAi screen for viral replication in mammalian cell culture. Methods Mol. Biol. **721**:383–95.
117. **Ramos, S.** 2007. Effects of dietary flavonoids on apoptotic pathways related to cancer chemoprevention. J. Nutr. Biochem. **18**:427–42.
118. **Reed, R. A., J. Mattai, and G. G. Shipley**. 1987. Interaction of cholera toxin with ganglioside GM1 receptors in supported lipid monolayers. Biochemistry. **26**:824–32.
119. **Reischl, A., M. Reithmayer, G. Winsauer, R. Moser, I. Gösler, and D. Blaas**. 2001. Viral evolution toward change in receptor usage: adaptation of a major group human rhinovirus to grow in ICAM-1-negative cells. J. Virol. **75**:9312–9.
120. **Rodal, S. K., G. Skretting, O. Garred, F. Vilhardt, B. van Deurs, and K. Sandvig**. 1999. Extraction of cholesterol with methyl-beta-cyclodextrin perturbs formation of clathrin-coated endocytic vesicles. Mol. Biol. Cell. **10**:961–74.
121. **Roy, A. M., J. S. Parker, C. R. Parrish, and G. R. Whittaker**. 2000. Early stages of influenza virus entry into Mv-1 lung cells: involvement of dynamin. Virology. **267**:17–28.
122. **Ruoslahti, E.** 1996. RGD and other recognition sequences for integrins. Annu. Rev. Cell Dev. Biol. **12**:697–715.
123. **Rust, M. J., M. Lakadamyali, F. Zhang, and X. Zhuang**. 2004. Assembly of endocytic machinery around individual influenza viruses during viral entry. Nat. Struct. Mol. Biol. **11**:567–73.
124. **Sabharanjak, S., P. Sharma, R. G. Parton, and S. Mayor**. 2002. GPI-anchored proteins are delivered to recycling endosomes via a distinct cdc42-regulated, clathrin-independent pinocytic pathway. Dev. Cell. **2**:411–23.
125. **Sabin, A. B.** 1959. Reoviruses. A new group of respiratory and enteric viruses formerly classified as ECHO type 10 is described. Science. **130**:1387–9.
126. **Saeed, M. F., A. a Kolokoltsov, T. Albrecht, and R. a Davey**. 2010. Cellular entry of ebola virus involves uptake by a macropinocytosis-like mechanism and subsequent trafficking through early and late endosomes. PLoS Pathog. **6**:e1001110.
127. **Safran, M., I. Dalah, J. Alexander, N. Rosen, T. Iny Stein, M. Shmoish, N. Nativ, I. Bahir, T. Doniger, H. Krug, A. Sirota-Madi, T. Olender, Y. Golan, G. Stelzer, A. Harel, and D. Lancet**. 2010. GeneCards Version 3: the human gene integrator. Database : the journal of biological databases and curation. **2010**:baq020.

128. **Sandvig, K., M. L. Torgersen, H. A. Raa, and B. van Deurs**. 2008. Clathrin-independent endocytosis: from nonexisting to an extreme degree of complexity. Histochem. Cell Biol. **129**:267–76.
129. **Schiff, L. A., M. L. Nibert, and K. L. Tyler**. 2007. Orthoreoviruses and Their Replication. Fields Virology.
130. **Schmitt, K., and G. D. Fewell**. 2006. Vector-based RNAi approaches for stable, inducible and genome-wide screens. Drug Discov. Today. **11**:975–82.
131. **Schulz, W. L., A. K. Haj, and L. A. Schiff**. 2012. Reovirus Uses Multiple Endocytic Pathways for Cell Entry. J. Virol.
132. **Seachrist, J. L., and S. S. G. Ferguson**. 2003. Regulation of G protein-coupled receptor endocytosis and trafficking by Rab GTPases. Life Sci. **74**:225–35.
133. **Shmulevitz, M., P. Marcato, and P. W. K. Lee**. 2005. Unshackling the links between reovirus oncolysis, Ras signaling, translational control and cancer. Oncogene. **24**:7720–8.
134. **Sieczkarski, S. B., and G. R. Whittaker**. 2002. Dissecting virus entry via endocytosis. J. Gen. Virol. **83**:1535–45.
135. **Sieczkarski, S. B., and G. R. Whittaker**. 2002. Influenza virus can enter and infect cells in the absence of clathrin-mediated endocytosis. J. Virol. **76**:10455–64.
136. **Singh, R. D., V. Puri, J. T. Valiyaveettil, D. L. Marks, R. Bittman, and R. E. Pagano**. 2003. Selective Caveolin-1 – dependent Endocytosis of Glycosphingolipids. Mol. Biol. Cell. **14**:3254–3265.
137. **Sloane, B. F., S. Yan, I. Podgorski, B. E. Linebaugh, M. L. Cher, J. Mai, D. Cavallo-Medved, M. Sameni, J. Dosescu, and K. Moin**. 2005. Cathepsin B and tumor proteolysis: contribution of the tumor microenvironment. Semin. Cancer Biol. **15**:149–57.
138. **Smith, J. A., S. C. Schmechel, B. R. G. Williams, R. H. Silverman, and L. A. Schiff**. 2005. Involvement of the interferon-regulated antiviral proteins PKR and RNase L in reovirus-induced shutoff of cellular translation. J. Virol. **79**:2240–50.
139. **Spendlove, R. S., M. E. McClain, and E. H. Lennette**. 1970. Enhancement of reovirus infectivity by extracellular removal or alteration of the virus capsid by proteolytic enzymes. J. Gen. Virol. **8**:83–94.
140. **Stamatovic, S. M., N. Sladojevic, R. F. Keep, and A. V. Andjelkovic**. 2012. Relocalization of junctional adhesion molecule-A during inflammatory stimulation of brain endothelial cells. Mol. Cell Biol.
141. **Strong, J. E., and P. W. Lee**. 1996. The v-erbB oncogene confers enhanced cellular susceptibility to reovirus infection. J. Virol. **70**:612–616.
142. **Strong, J. E., M. C. Coffey, D. Tang, P. Sabinin, and P. W. Lee**. 1998. The molecular basis of viral oncolysis: usurpation of the Ras signaling pathway by reovirus. EMBO J. **17**:3351–62.

143. **Sturzenbecker, L. J., M. Nibert, D. Furlong, and B. N. Fields**. 1987. Intracellular digestion of reovirus particles requires a low pH and is an essential step in the viral infectious cycle. J. Virol. **61**:2351–61.
144. **Sturzenbecker, L. J., M. Nibert, D. Furlong, and B. N. Fields**. 1987. Intracellular digestion of reovirus particles requires a low pH and is an essential step in the viral infectious cycle. J. Virol. **61**:2351–61.
145. **Tai, J. H., J. V. Williams, K. M. Edwards, P. F. Wright, J. E. Crowe, and T. S. Dermody**. 2005. Prevalence of reovirus-specific antibodies in young children in Nashville, Tennessee. J. Infect. Dis. **191**:1221–4.
146. **Thirukkumaran, C. M., M. J. Nodwell, K. Hirasawa, Z.-Q. Shi, R. Diaz, J. Luider, R. N. Johnston, P. a Forsyth, A. M. Magliocco, P. Lee, S. Nishikawa, B. Donnelly, M. Coffey, K. Trpkov, K. Fonseca, J. Spurrell, and D. G. Morris**. 2010. Oncolytic viral therapy for prostate cancer: efficacy of reovirus as a biological therapeutic. Cancer Res. **70**:2435–44.
147. **Thirukkumaran, C., and D. G. Morris**. 2009. Oncolytic viral therapy using reovirus. Methods Mol. Biol. **542**:607–34.
148. **Thompson, H. M., and M. a McNiven**. 2006. Discovery of a new “dynasore”. Nat. Chem. Biol. **2**:355–6.
149. **Thorley, J. a, J. a McKeating, and J. Z. Rappoport**. 2010. Mechanisms of viral entry: sneaking in the front door. Protoplasma.
150. **Tsai, B.** 2007. Penetration of nonenveloped viruses into the cytoplasm. Annu. Rev. Cell Dev. Biol. **23**:23–43.
151. **Tuma, P. L., and A. L. Hubbard**. 2003. Transcytosis: crossing cellular barriers. Physiol. Rev. **83**:871–932.
152. **Tyler, K. L., M. K. Squier, S. E. Rodgers, B. E. Schneider, S. M. Oberhaus, T. A. Grdina, J. J. Cohen, and T. S. Dermody**. 1995. Differences in the capacity of reovirus strains to induce apoptosis are determined by the viral attachment protein sigma 1. J. Virol. **69**:6972–9.
153. **Upla, P., V. Marjomäki, P. Kankaanpää, J. Ivaska, T. Hyypiä, F. G. Van Der Goot, and J. Heino**. 2004. Clustering induces a lateral redistribution of alpha 2 beta 1 integrin from membrane rafts to caveolae and subsequent protein kinase C-dependent internalization. Mol. Biol. Cell. **15**:625–36.
154. **Vile, R., D. Ando, and D. Kirn**. 2002. The oncolytic virotherapy treatment platform for cancer: unique biological and biosafety points to consider. Cancer Gene Ther. **9**:1062–7.
155. **Weiner, D. B., K. Girard, W. V. Williams, T. McPhillips, and D. H. Rubin**. 1988. Reovirus type 1 and type 3 differ in their binding to isolated intestinal epithelial cells. Microb Pathog. **5**:29–40.
156. **Wickham, T. J., P. Mathias, D. A. Cheresh, and G. R. Nemerow**. 1993. Integrins alpha v beta 3 and alpha v beta 5 promote adenovirus internalization but not virus attachment. Cell. **73**:309–19.
157. **Wilcox, M. E., W. Yang, D. Senger, N. B. Rewcastle, D. G. Morris, P. M. Brasher, Z. Q. Shi, R. N. Johnston, S. Nishikawa, P. W. Lee, and P. A.**

Forsyth. 2001. Reovirus as an oncolytic agent against experimental human malignant gliomas. J. Natl. Cancer Inst. **93**:903–12.
158. **Williams, T. M., and M. P. Lisanti**. 2005. Caveolin-1 in oncogenic transformation, cancer, and metastasis. Am. J. Physiol. Cell Physiol. **288**:C494–506.
159. **Wojton, J., and B. Kaur**. 2011. Impact of tumor microenvironment on oncolytic viral therapy. Cytokine Growth Factor Rev. **21**:127–34.
160. **Wolf, J. L., R. Dambrauskas, A. H. Sharpe, and J. S. Trier**. 1987. Adherence to and penetration of the intestinal epithelium by reovirus type 1 in neonatal mice. Gastroenterology. **92**:82–91.
161. **Wolf, J. L., R. S. Kauffman, R. Finberg, R. Dambrauskas, B. N. Fields, and J. S. Trier**. 1983. Determinants of reovirus interaction with the intestinal M cells and absorptive cells of murine intestine. Gastroenterology. **85**:291–300.
162. **Wolf, J. L., D. H. Rubin, R. Finberg, R. S. Kauffman, a H. Sharpe, J. S. Trier, and B. N. Fields**. 1981. Intestinal M cells: a pathway for entry of reovirus into the host. Science. **212**:471–2.
163. **Yamada, E.** 1955. The fine structure of the gall bladder epithelium of the mouse. J. Biophys. Biochem. Cytol.. **1**:445–58.
164. **Yang, Y., Y. Yixuan, S.-K. Lim, L. S. Kiat, L.-Y. Choong, C. L. Yee, H. Lee, L. Huiyin, Y. Chen, C. Yunhao, P.-K. Chong, C. P. Kuan, H. Ashktorab, A. Hassan, T. T. Wang, W. T. Ting, M. Salto-Tellez, S. Manuel, K.-G. Yeoh, Y. K. Guan, Y.-P. Lim, and L. Y. Pin**. 2010. Cathepsin S mediates gastric cancer cell migration and invasion via a putative network of metastasis-associated proteins. J. Proteome Res. **9**:4767–78.
165. **Yao, Q., J. Chen, H. Cao, J. D. Orth, J. M. McCaffery, R.-V. Stan, and M. a McNiven**. 2005. Caveolin-1 interacts directly with dynamin-2. J. Mol. Biol. **348**:491–501.
166. **Yu, M., S. Suluraju, G. Crameri, J. Rosli, H. S. Tan, K. Voon, L.-F. Wang, K. B. Chua, and J. A. McEachern**. 2008. Identification and Characterization of a New Orthoreovirus from Patients with Acute Respiratory Infections. PLoS ONE. **3**:e3803.
167. **Zeh, H. J., and D. L. Bartlett**. 2002. Development of a replication-selective, oncolytic poxvirus for the treatment of human cancers. Cancer Gene Ther. **9**:1001–12.
168. **Zhang, L., S. C. Harrison, T. Ivanovic, M. L. Nibert, M. A. Agosto, and K. Chandran**. 2008. Peptides released from reovirus outer capsid form membrane pores that recruit virus particles. EMBO J. **27**:1289–98.
169. **Zhang, L., M. a Agosto, T. Ivanovic, D. S. King, M. L. Nibert, and S. C. Harrison**. 2009. Requirements for the formation of membrane pores by the reovirus myristoylated micro1N peptide. J. Virol. **83**:7004–14.